Gastroenterology

Immune Cell and Stromal Signature Associated with Progression-free Survival of Patients with Resected Pancreatic Ductal Adenocarcinoma

--Manuscript Draft--

Manuscript Number:	GASTRO-D-17-02455R1
Full Title:	Immune Cell and Stromal Signature Associated with Progression-free Survival of Patients with Resected Pancreatic Ductal Adenocarcinoma
Article Type:	Basic - Pancreas
Section/Category:	Translational
Corresponding Author:	Julia Mayerle, M.D. Klinikum der Universitat Munchen München, GERMANY
Corresponding Author Secondary Information:	
Corresponding Author's Institution:	Klinikum der Universitat Munchen
Corresponding Author's Secondary Institution:	
First Author:	Ujjwal Mukund Mahajan, PhD
First Author Secondary Information:	
Order of Authors:	Ujjwal Mukund Mahajan, PhD
	Enno Langhoff, MD
	Elisabetta Goni, MD
	Eithne Costello, PhD
	William Greenhalf, PhD
	Christopher Halloran, MD
	Steffen Ormanns, MD
	Stephan Kruger, MD
	Stefan Boeck, MD
	Silvia Ribback, MD
	Georg Beyer, MD
	Frank Dombroswki, MD
	Frank-Ulrich Weiss, PhD
	John P. Neoptolemos, MD
	Jens Werner, MD
	Jan G D'Haese, MD
	Alexandr Bazhin, Ph.D.
	Julian Peterhansl, MD (appearing)
	Svenja Pichlmeier, MD (appearing)
	Markus Buechler, MD
	Jeorg Kleeff, MD
	Paula Ghaneh, MD

	Matthias Sendler, PhD
	Daniel H Palmer, MD
	Thomas Kohlmann, PhD
	Roland Rad, MD
	Ivonne Regel, Ph.D.
	Markus M Lerch, MD
	Julia Mayerle, M.D.
Order of Authors Secondary Information:	
Abstract:	Background & Aims: Changes to the microenvironment of pancreatic ductal adenocarcinomas (PDACs) have been associated with poor outcomes of patients. We studied the associations between composition of the pancreatic stroma (fibrogenic, inert, dormant, or fibrolytic stroma) and infiltration by inflammatory cells and times of progression-free survival (PFS) of patients with PDACs after resection. Methods: We obtained 1824 tissue microarray specimens from 385 patients included in the European Study Group for Pancreatic Cancer trial 1 and 3 and performed immunohistochemistry to detect alpha smooth muscle actin, type 1 collagen, CD3, CD4, CD8, CD68, CD206, and neutrophils. Tumors that expressed high and low levels of these markers were compared with patient outcomes using Kaplan-Meier curves and multivariable recursive partitioning for discrete-time survival tree analysis. Prognostic index was delineated by a multivariable Cox-proportional-hazards-model of immune cell and stromal markers and PFS. Findings were validated using 279 tissue microarray specimens from 93 patients in a separate cohort. Results: Levels of CD3, CD4, CD8, CD68, and CD206 were independently associated with tumor recurrence. Recursive partitioning for discrete-time survival tree analysis identified a high level of CD3 as the strongest independent predictor for longer PFS. Tumors with levels of CD3 and high levels of CD206 associated with a median PFS time of 16.6 months and a median prognostic index of –0.32 (95% CI, –0.35 to –0.31), whereas tumors with low level of CD3 cell and low level of CD8 and high level of CD68 associated with a median PFS time of 7.9 month and a prognostic index of 0.32 (95% CI, 0.050–0.32)—we called these patterns histologic signatures. Stroma composition, when unassociated with inflammatory cell markers, did not associate significantly with PFS. In the validation cohort, the histologic signature resulted in an error matrix accuracy of predicted response of 0.75 (95% CI, 0.64–0.83; accuracy P<.001). Conclusions: In an analysis of PDAC tissue microarray specimens, we identified and validated a histologic signature, based on leukocyte and stromal factors, that associates with PFS times of patients with resected PDACs. Immune cells might affect the composition of the pancreatic stroma to affect progression of PDAC. These findings provide new insights into the immune response to PDAC. Key words: ESPAC, pancreatic cancer, histologic analysis, prognostic factor

KLINIKUM DER UNIVERSITÄT MÜNCHEN

CAMPUS GROSSHADERN

MEDIZINISCHE KLINIK UND POLIKLINIK II
DIREKTORIN: PROF. DR. JULIA MAYERLE

Klinikum der Universität München · Med. Klinik und Poliklinik II ·
Prof. Dr. med. J. Mayerle · Marchioninistr. 15 · 81377 München

To

Prof. Dr. Richard Peek,
Editor-in-Chief

Prof. Dr. Ashok K Saluja
Section Editor Pancreas
Gastroenterology

Prof. Dr. med. Julia Mayerle

Telefon +49 (0)89 4400 - 72391
Telefax +49 (0)89 4400 - 78887
Direktion.Med2@
med.uni-muenchen.de

www.klinikum.uni-muenchen.de

Postanschrift:
Marchioninistr. 15
81377 München

Ihr Zeichen:	Unser Zeichen:	München, den 19.07.2018
	Prof. Mayerle/bs	

Submission of revision to Gastroenterology: Immune Cell and Stromal Signature Associated with Progression-free Survival of Patients with Resected Pancreatic Ductal Adenocarcinoma by Mahajan and co-workers.

Dear Professor Saluja, dear Ashok

Dear Professor Peek,

Thank you for allowing us to submit a revision of our recent manuscript on a “Immune Cell and Stromal Signature Associated with Progression-free Survival of Patients with Resected Pancreatic Ductal Adenocarcinoma”. We have now conducted a number of experiments to address your and the reviewers concerns and are able to show that in an independent validation cohort regardless of the staining technology applied the signature derived from the ESPAC-TPlus cohort is reliable and robust. We are excited about our findings and hope that you will be equally excited. Below you can find our point to point response. We hope that the revised version of our manuscript will now be acceptable for publication in Gastroenterology.

Best,

Julia and Markus

Dear Professor Saluja, dear Ashok

Dear Professor Peek,

Thank you for allowing us to submit a revision of our recent manuscript on a “Prognostic histological signature based on interaction of immune cell infiltration with stromal composition for resected pancreatic ductal adenocarcinoma. We have now conducted a number of experiments to address your and the reviewers concerns and are able to show that in an independent validation cohort regardless of the staining technology applied the signature derived from the ESPAC-TPlus cohort is reliable and robust. We are excited about our findings and hope that you will be equally excited. Below you can find our point to point response. We hope that the revised version of our manuscript will now be acceptable for publication in Gastroenterology.

Best,

Julia and Markus

Response to comments from the editor:

Your manuscript was reviewed by two experts in the field and the Board of Editors. While all of us think that your study will make an important contribution, some additional data will strengthen your study.

We are particularly interested in data validating your low vs high assignment on IHC by comparing it with traditional FACS analysis of a few of the immunological subsets.

We would like to thank the editor for raising this question. To compare the results obtained by immunohistochemistry of TMA to traditional FACS analysis, we isolated intratumoral cells (ITCs) from 10 resected PDAC samples (provided by the Biobank of the Department of General, Visceral and Transplantation Surgery, Ludwig-Maximilians University (LMU), Munich, Germany under the administration of the Human Tissue and Cell Research (HTCR) Foundation, ethical approval number 025-12). To extend the analysis and compare all possible modalities to FACS analysis and classical immunohistochemistry, we used a three-tier comparison. This includes comparison of FACS immune markers with classical immunohistochemistry of tissue-blocks (TMA), immunocytochemistry on cytoblocks prepared from isolated intratumoral cells (ITCs) and immunocytochemistry on cytospins prepared from ITCs. We stained each of these samples for CD3, CD4, CD8, CD68 and CD206 expression. We quantified the staining for comparison with FACS data as percentage of positive cells as well as the number of cells per mm^2 as described in the materials and methods section. We stratified the immunohistochemistry results into a low and high expression cohort using cut-offs reported in **suppl table S1**. As internal control we used FACS analysis of peripheral blood derived monocytes (PBMCs).

We performed multiple correlation analyses and incorporated the correlation matrix of different immunostainings as scatter plots for distribution stratified for low and high expression as shown in **suppl fig.S4**.

We observed a strong correlation between immunohistochemistry on tissue-blocks when compared with traditional FACS (solid black square in correlogram in **suppl fig.S4**).

Furthermore, we found a strong correlation between the percentage of CD3 cells in tissue-blocks and the percentage of $CD45^+CD3^+$ cells (R=0.64, p=0.04). We found a similarly robust correlation for CD8 (R=0.72, P=0.01), CD68 (R=0.73, P=0.01) and CD206 (R=0.87, P=0.001) when compared with immunohistochemistry on tissue-blocks and traditional FACS analysis. Overall, we found a highly significant strength of agreement between immunohistochemistry staining of immune markers in tissue blocks and FACS analysis of ITCs.

To note, we did not find any correlation between immunohistochemistry on tissue-blocks and traditional FACS analysis performed on PBMCs (dotted black square in correlogram in **suppl fig.S4** suggesting that the local tumor immune response is not reflected systemically on the level of surface markers on immune cells.

*We have included these analyses in the materials and methods section of the main manuscript on page number 8 and a figure as **suppl fig.S4.***

Also, data from multiplex immunoassays, given that these are now validated and provide the opportunity for quantification and permit co-localization of markers (e.g. Lisa Coussens Cell April 2017), will be very helpful and reinforce your conclusions.

We thank the editor for his suggestion. To confirm our finding by multiplex immunostaining and hereby study tumor heterogeneity, we introduced an independent validation cohort consisting of 93 patients (CONSORT diagram in **suppl fig.S9**). We performed serial immunostainings of CD3, CD4, CD8, CD68, CD206, MPO, α-SMA and collagen, followed by multiplex immunostaining analysis. The flow of multiplexing analysis and quantification is shown in **suppl fig.S11**.

Representative multiplex immunostainings of a PDAC TMA and a tonsil (control) are shown in **suppl fig.S10A**. We performed image cytometric analysis from multiplex immunostainings. On comparison of the number of $CD3^+$ cells/mm^2 on immunohistochemistry with the percentages of $CD45^+CD3^+$ cells by image cytometry, we found a positive correlation with R=0.79, P<0.001 (**suppl fig.S10B**). Subsequently, we found a positive correlation between the number of $CD4^+$ cells/mm^2 and the percentage of $CD45^+CD3^+CD4^+$ cells (R=0.73, P<0.001). We observed similar positive correlations for CD8 (R=0.31, P=0.02), CD68 (R=0.40, P<0.001), CD206 (R=0.80, P<0.001) and MPO (R=0.24, p=0.02). We also compared percentages of $\alpha\text{-SMA}^+$ cells with α-SMA H-score and found a positive correlation (R=0.59, P<0.001, **suppl fig.S10B**).

After establishing the correlation between single staining with multiplex immunostaining in our independent validation cohort, we aimed to validate the prognostic signature delineated from the identification study performed on the ESPAC-Tplus samples. We performed survival analyses for high and low expression of CD3, CD4, CD8, CD68, CD206, MPO and stromal composition and observed a similar prognostic association with PFS, as in the ESPAC cohort (**suppl fig.S10C**). Results from the validation cohort confirmed our finding that an absence of infiltrating T-lymphocytes is associated with decreased PFS. However, contrary to the ESPAC cohort, we did not find a significant association between high and low CD68 counts and PFS in the validation cohort.

We validated the prognostic histological signature from the identification cohort using the validation cohort (see consort diagram **suppl fig.S9**, n=93). To achieve this, we predicted the response of the prognostic histological signature derived from the ESPAC cohort. The readout of predicted response was terminal nodal localization (categorization into prognostic subgroup by

IHC signature) and predicted median progression free survival of subjects of the validation cohort with respect to prognostic signature subgroup. We plotted an alluvial plot depicting prediction accuracy of the response (predicted median progression free survival time per subgroup) in comparison to actual response (actual median progression free survival time per subgroup) (see **fig.3D**, we revised figure 3 and now panel D shows the alluvial plot). Left side of the alluvial plot depicts predicted response per subgroup and the right panel depicts actual response per subgroup. The blue bar connecting left to the right graph represents perfect match while the red ribbon shows a mismatch in the response. The thickness of the bar or ribbon is representative of the number of subjects. Our prediction analysis revealed Cohen's Kappa as 0.69 with a Harrell's C-index of 0.60. Cohen's kappa is a measure of concordance and values in the range of 0.64-0.80 depict good concordance. The C-index is a measure of quality fit for binary outcomes in a logistic regression model and indicates the probability of a randomly selected patient experiencing an event burdened with a higher risk score than a patient who had not experienced the event. A value of greater than 0.5 represents good predictability of the model.

We substantiated our conclusion, by plotting Kaplan-Meier curves of predicted responses and actual responses (**suppl fig.S10D**). We observed an accuracy of prediction in the validation cohort using the prognostic signature with 0.75 (95%CI: 0.64-0.83, accuracy P<0.001). We found a positive correlation between predicted response and actual response R=0.62 and P<0.001. From our data we draw the conclusion that our prognostic model has good reproducibility and robustness.

*We have included these data in the main manuscript on page number 16 and as figure in panel D of **figure 3** and **suppl fig.S10.***

Furthermore, after validation of the prognostic signature using conventional morphometric analysis we tested whether the prognostic signature is still robust if we employ cytometry of the multiplex immunostaining. In cytometry results are expressed as percentage of positive cells as in conventional FACS analysis and thus cut-offs for dichotomization cannot directly be translated from one quantification method (Multiplex immunostaining on a single TMA but analysis of each staining cycle as individual staining versus merging all the stainings of a TMA in one image and analyzing it by image cytometry) to the other. We dichotomized $CD45^+CD3^+$cells, $CD45^+CD3^+CD4^+$ cells, $CD45^+CD3^+CD8^+$ cells, $CD45^+CD68^+$ cells, $CD45^+CD206^+$ cells and $CD45^+MPO^+$ cells into high and low percentages using the cut-off described below **(table R1).**

Table R1: Cut-off for low/high expression determined by cut-off finder for the immune markers identified by image cytometric analysis

Sr. No	Marker	Low expression	High expression
1	$CD45^+$ cells$^\$$	≤ 45.28	> 45.28
2	$CD45^+CD3^+$ cells$^\$$	≤ 5.23	> 5.23
3	$CD45^+CD3^+CD4^+$ cells$^\$$	≤ 37.13	> 37.13
4	$CD45^+CD3^+CD8^+$ cells$^\$$	≤ 6.47	> 6.47
5	$CD45^+CD68^+$ cells$^\$$	≤ 16.88	> 16.88
6	$CD45^+CD206^+$ cells$^\$$	≤ 38.62	> 38.62
7	$CD45^+MPO^+$ cells$^\$$	≤ 11.29	> 11.29
8	$ASMA^+$ cells$^\$$	≤ 47.64	> 47.64

$^\$$ Percentage of positive cells analyzed by Image cytometric analysis.

Predicting the response and nodal localisation/patients' subgroup, using above immune markers derived from the image cytometric analysis, we observed a strong concordance between predicted response and actual response (Alluvial plot, **fig. R1**). We determined Cohen's Kappa with 0.67 with a Harrell's C-index of 0.56 confirming the robustness of the prognostic histological signature even using a different way of image processing and analysis.

Figure R1

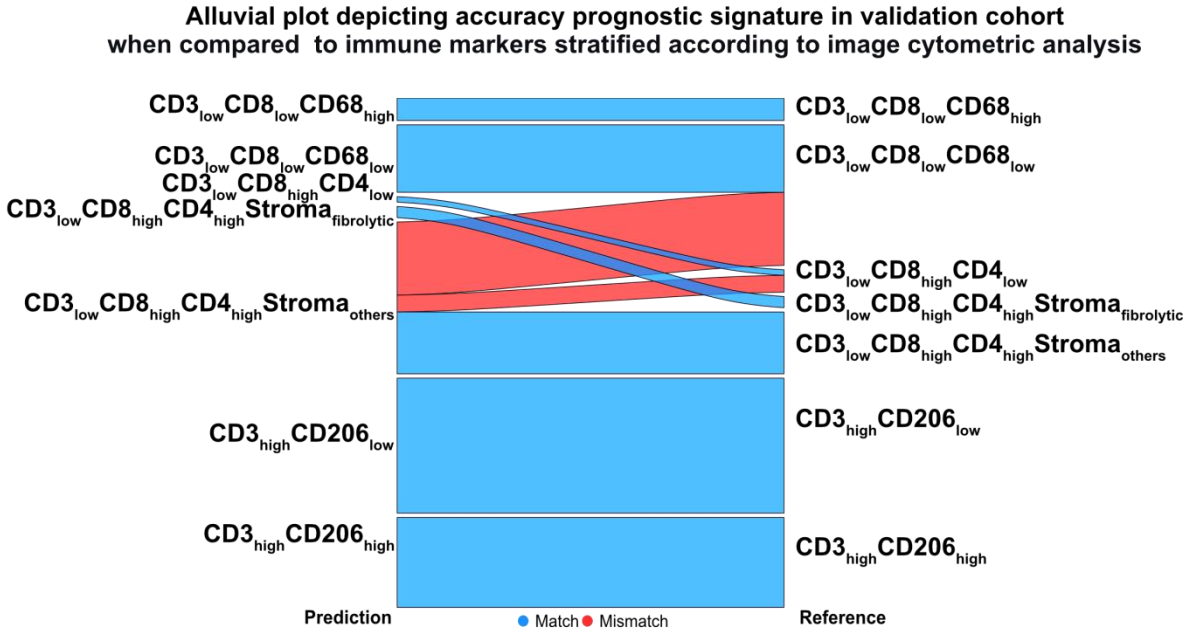

Figure R1: Multiplex immunostaining followed by image cytometric analysis in validation cohort. Alluvial plot depicting prediction accuracy of response (predicted m(pfst) per node) in comparison with actual response (actual m(pfst) per node) in validation cohort for the markers stratified according to image cytometric analysis. Left side of the alluvial plot depicts predicted response per node and right depicts actual response per node. Blue area connecting left to the right graph represent perfect match while red area represent mismatch in the response. The thickness of the color areas depicts the number of subjects.

Kaplan-Meier curves for predicted response and actual response using the signature from image cytometric analysis showed an accuracy of 0.81 (95%CI: 0.71-0.89, accuracy P<0.001) **fig. R2**). Comparison of the C-index from immunohistochemistry with image cytometry showed marginal superiority and quality of single immunohistochemistry counts.

Figure R2

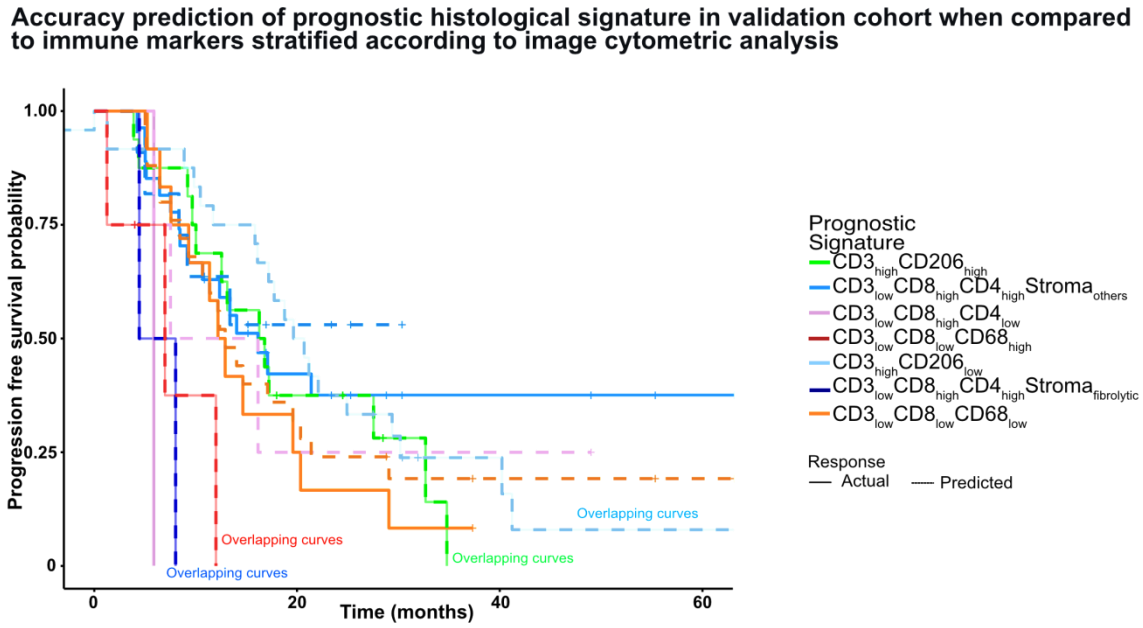

Figure R2: Accuracy of prediction of the prognostic histological signature in the validation cohort on comparison to immune markers stratified according to image cytometry. Kaplan-Meier curve representing actual response obtained from immune markers stratified according to image cytometric analysis and predicted response derived from the prognostic histological signature generated from the ESPAC-Tplus cohort. Dotted lines depict the curves for predicted response whereas solid lines represent curves for actual response. The accuracy of prediction in the validation cohort using prognostic histological signature is given with 0.81 (95%CI: 0.71-0.89, accuracy P<0.001). P<0.05 is considered as significant.

These results confirm that a prognostic signature is a powerful and robust tool in resected PDAC patients with good reproducibility, predictability and reliability. Furthermore, it confirmed that, irrespective of single immunohistochemistry on the consecutive sections or immunohistochemistry on a single section by multiplexing the prognostic histological signature has good reproducibility and robustness. These results indicate that tumor-infiltrating leukocytes and their response to stroma modulations are interdependent variables.

We have not included the comparison of conventional image analysis and multiplexing cytometry in the manuscript as we believe that it does not directly impact on our story line and distracts the reader from our main findings. However, we found the data of great interest and wanted to share them with you. We hope that we have sufficiently addressed your concerns and we are grateful for your suggestions.

Reviewer 1:

This is a detailed histological study using resected PDAC samples from a retrospective cohort of patients, performed by a highly experienced and expert research team. Importantly, the focus in this study on characterising immune cell infiltration in PDAC stroma adds important knowledge to the field, while building upon previous literature related to stromal composition in terms of collagen and activated fibroblast/pancreatic stellate cells. The authors report identification of

specific leukocyte + stromal composition signatures that correlate with clinical outcome in terms of progression free survival.

While the reported findings have the potential (if confirmed in validation studies) to identify patients who would do well or poorly with adjuvant treatment, it would be helpful if the following issues were addressed:

1. Study subjects include a combination of patients actually treated with Gemcitabine or 5FU. It would be useful to indicate whether there were any differences in PFS per se between these two patient groups, to ensure that this would not confound the study results.

We would like to apologize to the reviewer for not having been clearer in the manuscript regarding the treatment groups. The conclusion of the ESPAC3 trial was that, compared to the use of fluorouracil plus folinic acid, gemcitabine did not result in improved overall survival or improved progression free survival in patients with resected pancreatic cancer. 5FU treatment is not superior to Gemcitabine treatment in the adjuvant setting of pancreatic cancer treatment.

To entirely rule out your concerns we have now added data on the LIFETEST procedure for pairwise comparison of survival with different immune markers. In general, there was no statistical significant correlation between treatment arm and immune markers **(suppl table S7)**. Also, pairwise comparison of survival factors to stroma composition did not reveal any statistical significant correlation **(suppl table S8)**. Thus, we ruled out the influence of the treatment group on the signature.

We have incorporated this results in the main manuscript on page number 14.

Also was PFS defined as local (pancreatic) recurrence or the identification of malignant foci elsewhere? This issue may have relevance to the proposed pathogenetic role of type 2 macrophages for example in pancreatic cancer progression.

We thank the reviewer for raising this concern. In the ESPAC-1 and the ESPAC-3 trial, from which the ESPAC-Tplus TMAs are derived, progression-free survival was measured from the date of resection to the date of death from any cause or date of local tumor recurrence or metastases as documented by contrast enhanced CT. Patients remaining alive and without progression were censored at the date last seen alive[1,2]. In the ESPAC-3 trial, 63% of the patients developed local recurrence, metastases or both, 87% of which died[1]. On an individual patient level, we can't discriminate from the trial data recorded who developed local recurrences or metastasis and patients' numbers are too low in each subgroup to do meaningful statistics. We will try to answer your very relevant question on the role of M2 macrophages and their role of metastasis formation in a separate project.

2. What was the inter-observer concordance between the two independent investigator scores for the various parameters tested?

We would like to thank reviewer for his/her suggestion. We evaluated inter-observer concordance at two levels. We tested inter-rater reliability for H-score and observed an inter-concordance coefficient (ICC), which is a measure of concordance for continuous variables, for picrosirius red/ fast green staining with 0.84 (95%CI: 0.82-0.85) **(suppl fig. S2A)**. When we analyzed the inter-rater concordance for α-SMA H-Score, we found an ICC of 0.92 (95%CI:

0.92-0.93) **(suppl fig. S2B)**. ICC in the range of 0.75-1.00 is associated with excellent inter-rater concordance[3].

Furthermore, we analyzed the inter-rater concordance for dichotomous high and low expression of picrosirius red/fast green and α-SMA. We determined Cohen's Kappa, as a measure for inter-rater concordance for categorical variables for picrosirius red/fast green with 0.75 (95%CI: 0.72-0-77) and for α-SMA with 0.79 (95%CI: 0.77-0.81) (**suppl fig. S2C-D)**. Cohen's kappa in the range of 0.61-0.80 denotes good concordance[4]. Thus, overall we observed a good to excellent strength of agreement and inter-rater concordance.

We have included these concordance data in the main manuscript on page number 7 and as figure in **suppl fig.S2.**

3. While acknowledging the expertise of the pathologists involved in this study, it would be useful to include some details as to how intermediate staining was differentiated from low or high staining. While Supplementary Fig 4 provides examples of low and high expression, examples of 'intermediate' expression are missing.

We would like to thank the reviewer for bringing this concern to our attention. We have modified the figure and added intermediate expression denoted as "borderline expression" in **suppl fig.1** for illustrating purposes**.**

We amended suppl figure 4 which is now incorporated as **suppl fig.S3.**

4. The fibrolytic subtype of stroma (high alphaSMA high expression with low collagen expression) may indicate that the collagen secreted by activated fibroblasts is being actively degraded. In this context it may be of interest to assess the expression of matrix metalloproteinases/TIMPs in these samples.

In order to answer the question above, we performed MMP7 immunohistochemistry staining in the validation cohort (n=93) and compared the staining intensity (H-Score) with respect to the stroma composition. We did not find any significant associations between MMP7 expression and type of stroma composition though the fibrolytic stroma type showed a trend to higher MMP7 expression. In order to validate our data, we used the expression dataset (GSE71729) from Moffitt *et al.*[5] and performed differential expression analysis in PDAC compared to normal pancreas. Selecting significantly altered genes with $p<0.05$, and stratification for the stroma subtypes based on expression of *ACTA2* (α-SMA) and *COL1A1* (collagen), the heatmap revealed differential expression of different collagen genes, matrix metalloproteases (MMPs) and the tissue inhibitors of metalloproteinases (TIMPs). However, we did not observe significant changes in MMP7 expression corresponding to stroma subtypes. MMP7 expression is always accompanied by dysregulated TIMP1 expression and is required for MMP7 activity[6]. We detected upregulated TIMP1 expression in the fibrolytic stroma compartment group.

It has been reported that pancreatic stellate cells are able to secrete different MMPs and their activities regulate the degradation as well as the synthesis of extracellular matrix proteins[7] .In order to substantiate these claim, we performed multiplexing followed by image cytometric analysis. We found a significant increase in $MMP7^+$ cells in the fibrolytic stroma compartment. Furthermore, we found a significant increment in $MMP7^+$ cells in $\alpha\text{-}SMA^+$ gated cells. Thus, our

results support the hypothesis that higher MMP7 expression in fibrolytic stroma are associated with collagen degradation.

We have included these data for review purposes only as we think, though very interesting indeed, it detracts the reader from our initial story line and the manuscript is already to lengthy with regard to the author guidelines of Gastroenterology. We hope that you can agree on this.

Figure R3

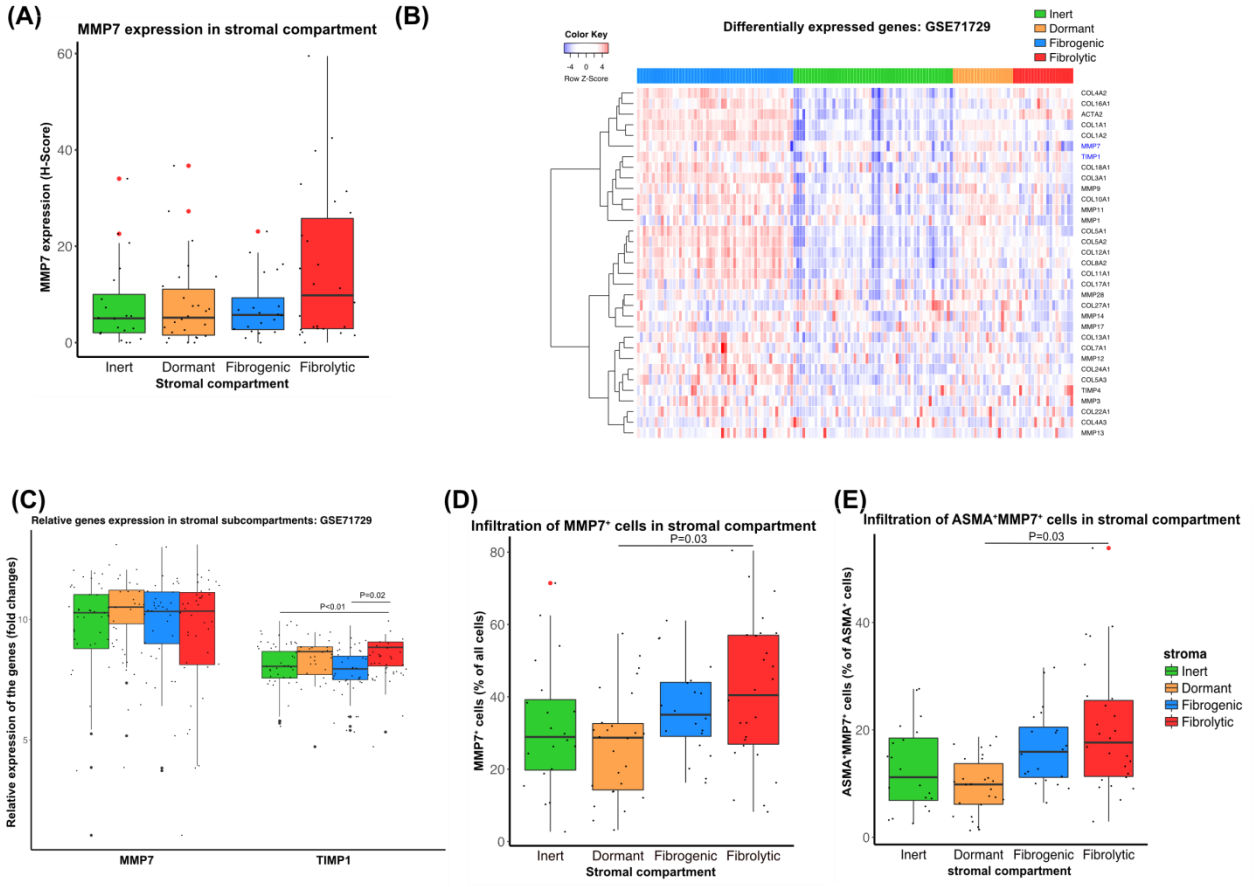

Figure R3: High MMP7 expression in fibrolytic stroma compartment patients. (a) Boxplot showing MMP7 expression in the validation cohort stratified according to the stroma subtype . **(b)** Heatmap showing differentially expressed matrix metalloproteases (MMPs) and tissue inhibitors of matrix metalloproteases (TIMPs) genes from GSE71729 expression dataset. **(c)** Boxplot illustrating expression of MMP7 and TIMP1 genes in different stromal compartment. **(d)** Boxplot revealing percent of MMP7⁺ cells in different stroma subtypes inform the validation cohort analyzed by image cytometry following multiplexing. **(e)** Boxplot showing percent of MMP7⁺ cells in α-SMA⁺ gated cells in different stroma subtypes in the validation cohort. *p<0.05 considered statistically significant.

Reviewer 2:

The authors investigated immune microenvironment and stromal composition in resectable pancreatic cancer from the ESPAC-1 and 3 cohorts. They showed the evidence of a prognostic signature incorporating leukocytic subpopulations and stromal composition to stratify PDAC patients with respect to PFS. They provide prognostic tree for PFS and classified the PDAC patients into seven subtypes based on expression of CD3, CD4, CD8, CD68, CD206, and

stromal composition. Patients with CD3highCD206high signature had the best PFS whereas patients with CD3lowCD8lowCD68high signature showed the worst PFS. They concluded that their prognostic signature can provide important prognostic information for PDAC patients with further validation study. This is an interesting study but there are several concerns that need attention:

1. This article provides a discrete-time survival tree for PFS using immune and stromal signature. It seems unclear why these two factors were chosen whereas there were much more powerful factors such as lymphatic node invasion and postoperative CA19-9 for predicting PDAC prognosis in this study. Furthermore, there is no other comparative index in this manuscript to compare the performance of stratification into homogenous prognostic subgroups to show the superiority of their signature.

We thank the reviewer for the concern and suggestion. He raises a very valuable point. We initially selected immune markers and stroma subtypes that demonstrated a statistically significant effect on progression free survival based on a multivariate analysis adjusted for independent prognostic variables such as the ones mentioned by the reviewer. (**table 4, suppl table 9)**.

We have now performed nonparametric testing for competing risks using random forest iterations analysis for categorical variables such as stage, resection margin, postOpCA19.9 (dichotomized based on median), lymph node invasion and local invasion and used it as a reference signature. We determined that only postOpCA19.9 and Lymph node invasion significantly influence PFS, however with a lower strength of VIMPs (**suppl fig.S8A**). Based on these results, we performed multivariate recursive partitioning for discrete-time survival tree for PFS, which lead to the three-terminal nodal prognostic signature. The relative error of the signature was 0.07 (x-error 0.01) (**suppl fig.S8A**). When we compared our histological signature to the reference signature for the prediction, using ROC survival analysis, we observed an AUC of the histological signature of 0.71(concordance: 0.60 ± 0.01) compared to 0.63 (concordance: 0.63 ± 0.01) for the reference signature **suppl fig.S8A**). This lead us to conclude that the histological signature performed better if compared to the reference signature suggested by the reviewer.

*We have included this data in the main manuscript on page number 16 and as figure in **suppl fig.S8.***

2. The authors concluded that their prognostic signature can provide important information for patients after PDAC resection with the implication of therapeutic stratification and postoperative management. However, in this study, pairwise comparisons of variations of immune cell subpopulation and stromal composition with respect to the therapeutic arm did not show any statistically significant association with PFS or OS, which limits the novelty and enthusiasm for this work.

We would like to apologize to the reviewer for not having been clearer in our conclusion. We entirely agree we developed a prognostic signature which is currently not predictive. We took your concern seriously and have amended our discussion.

We amended our conclusion and now it reads on page 21 as:

When thinking about adjuvant immunomodulatory therapy such as using M2-macrophage inhibitors or JAK inhibitors such signatures could become the basis for stratification.

3. In page 10 line 7, 8 and line 22, "hazard ratio of 0.78 (95%CI 1.02- 1.58, p=0.03)" and "0.69 (95%CI 1.10-1.88)"seems strange because these HRs are not in their 95%CI. This must be addressed.

We thank the reviewer for bringing this to our notice. It was a typographical error.

We have corrected it and now it read as "hazard ratio of 0.78 (95%CI 0.63- 0.98, p=0.03)" and "0.69 (95%CI 0.52-0.90)".

4. ESPAC is the study for resectable pancreatic head cancer but the table demonstrates there were 20 distal pancreatectomy cases. It is difficult to imagine the situation where the distal pancreatectomy was performed for pancreatic head cancer with respect to anatomy.

We would like to thank the reviewer for this concern. In the ESPAC trial, patients were eligible to participate in the trial if they had undergone complete macroscopic (R_0 or R_1) resection for ductal adenocarcinoma of the pancreas with histological confirmation and with no evidence of malignant ascites, peritoneal metastasis, or spread to the liver or other distant abdominal or extra-abdominal organs. The type and extent of resection was determined using an established international classification[1]. In summary, the localization of the primary was not an exclusion criteria as long it was resectable and no systemic spread was detected at time of diagnosis. The original publication is cited as reference 1 for detailed information on the study protocol.

5. In table 3, the multivariate analysis was performed using selected variables. It seems unclear why authors chose only immune and stromal status whereas lymph node invasion, resection margin, and post-operative serum CA19-9 have high impact to PFS in univariate analysis.

We would like to thank the reviewer for bringing this to our attention and from a clinician perspective his/her concern is very relevant. We preformed multivariate analysis to obtain a Cox proportional hazard model with variables consisting of stroma composition CD3, CD4, CD8, CD68, CD206 expression, lymph node invasion, resection margin and tumor stage (**suppl table S9**). We determined an AIC (Akaike information criterion) for this model with 2851.15 in comparison to the AIC for a model involving only stroma and immune markers of 2792.91. Thus, we conclude that based on Akaike information criterion (AIC), having lower AIC, the model described in **table 4** is superior to the model described in **suppl table S9**.

Furthermore, after adjusting for independent variables, the model including lymph node invasion, resection margin and tumor stage did not demonstrate a statistically significant impact on progression free survival.

*We have included this data in main manuscript on page number 15 and as **suppl table S9.***

6. It might be better that Figure 1D is treated as a table.

We thank the reviewer for his/her suggestion.

*We have amended Figure 1 and made a table which is now incorporated as **table 2**.*

7. For OS multivariate analysis, the different way of selecting variables from PFS analysis was employed. The explanation for it might be required.

We would like to apologize to the reviewer for not having provided this explanation. The variable selection in multivariate recursive partitioning for discrete-time survival tree for the overall survival model is based on random forest iterations and is an unbiased selection. Also, the multivariate recursive partitioning for discrete-time survival tree model is based on prognostic strength of individual biomarkers taken into consideration (**table 4 and suppl table S3**). As the prognostic strength is different for PFS and OS, we determined a different model for OS.

We incorporated the description in legends of **suppl fig.S7.**

Minor comments:
1. In Supplementary Table S2, the spelling of "fibrogenic" in second column and first row should be fixed.

We thank the reviewer for pointing out this typographical error.

We have amended the table which is now ***suppl table S4****.*

2. In Supplementary Table S5, the spelling of "fibrogenic" in second column and first row should be fixed.

We thank reviewer for pointing this typographical error.

We have amended the table which is now ***suppl table S5****.*

3. In Supplementary Figure 3B, "m(pfst)" in node 11 should be changed as m(st).
We thank the reviewer for bringing this to our notice.

We have corrected it and now it reads as m(st).

References:

1. Neoptolemos JP, Stocken DD, Bassi C, et al. Adjuvant chemotherapy with fluorouracil plus folinic acid vs gemcitabine following pancreatic cancer resection: a randomized controlled trial. JAMA 2010;304:1073–1081.
2. Neoptolemos JP, Stocken DD, Friess H, et al. A Randomized Trial of Chemoradiotherapy and Chemotherapy after Resection of Pancreatic Cancer. N Engl J Med 2004;350:1200–1210.
3. Cicchetti DV. Guidelines, criteria, and rules of thumb for evaluating normed and standardized assessment instruments in psychology. Psychol Assess 1994;6:284–290.
4. Landis JR, Koch GG. The measurement of observer agreement for categorical data. Biometrics 1977;33:159–174.
5. Moffitt RA, Marayati R, Flate EL, et al. Virtual microdissection identifies distinct tumor- and stroma-specific subtypes of pancreatic ductal adenocarcinoma. Nat Genet 2015;47:1168–1178.
6. Bramhall SR, Neoptolemos JP, Stamp GW, et al. Imbalance of expression of matrix metalloproteinases (MMPs) and tissue inhibitors of the matrix metalloproteinases (TIMPs) in human pancreatic carcinoma. J Pathol 1997;182:347–355.
7. Phillips JA, Vacanti CA, Bonassar LJ. Fibroblasts regulate contractile force independent of MMP activity in 3D-collagen. Biochem Biophys Res Commun 2003;312:725–732.

Graphical Abstract

Patients resected for PDAC and receiving adjuvant chemotherapy (ESPAC-Tplus trial)

Immuno-histochemistry

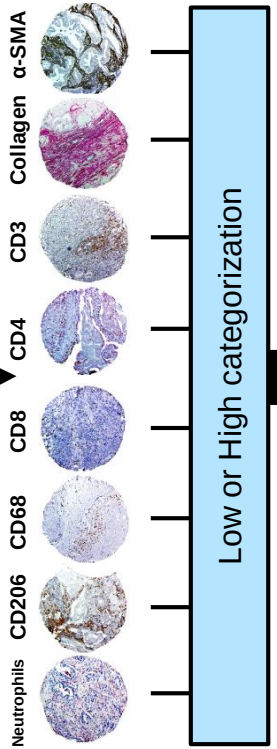

Low or High categorization

Prognostic histological signature

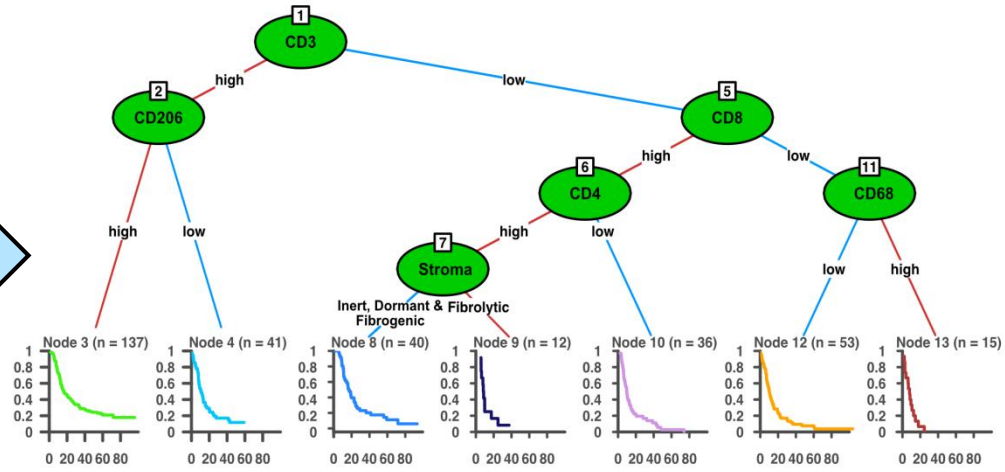

Progression free survival

Gastroenterology

Immune Cell and Stromal Signature Associated with Progression-free Survival of Patients with Resected Pancreatic Ductal Adenocarcinoma

U. M. Mahajan[1,2], E. Langhoff[2], E. Goni[1], E. Costello[3], W. Greenhalf[3], C. Halloran[3], S. Ormanns[4], S. Kruger[5], S. Boeck[5], S. Ribback[6], G. Beyer[1,2], F. Dombroswki[6], F.-U. Weiss[2], J. P. Neoptolemos[3,7], J. Werner[8], J. G. D'Haese[8], A. Bazhin[8], J. Peterhansl[1], S. Pichlmeier[1], M. W. Büchler[7], J. Kleeff[9], P. Ganeh[3], M. Sendler[2], D. H. Palmer[3,10], T. Kohlmann[11], R. Rad[12], I. Regel[1], M.M. Lerch[2], J. Mayerle[1,2]

[1]Department of Medicine II, University Hospital, LMU Munich, Germany
[2]Department of Medicine A, University Medicine Greifswald, Greifswald, Germany
[3]Institute of Translational Medicine, University of Liverpool, Liverpool, UK
[4]Institute of Pathology, Faculty of Medicine, LMU Munich, Munich, Germany
[5]Department of Medicine III, University Hospital, LMU-Munich, Germany
[6]Department of Pathology, University Medicine Greifswald, Greifswald, Germany
[7]Department of General, Visceral and Transplantation Surgery, University of Heidelberg, Heidelberg, Germany
[8]Department of General, Visceral, and Transplant Surgery, Ludwig-Maximilians-University Munich, Munich, Germany
[9]Department of Visceral, Vascular and Endocrine Surgery, Martin-Luther University Halle-Wittenberg, Halle, Germany
[10]Clatterbridge Cancer Centre NHS Foundation Trust, Wirral, UK
[11]Department of Community Medicine, University Medicine Greifswald, Greifswald, Germany
[12]Center for Translational Cancer Research (TranslaTUM), Technische Universität München, Munich, Germany

Word count: 6442

Funding: This work was supported by the Deutsche Krebshilfe/ Dr. Mildred-Scheel-Stiftung (109102) and the European Union (EU-FP-7: EPC-TM and EU-FP7-REGPOT-2010-1), PePPP center of excellence MV ESF/14-BM-A55-0045/16; ESF MV V-630-S-150-2012/132/133); CRU Cancer UK and the LCTU Liverpool.

Author contributions: JM, UMM, EL, EG, JP, SP, IR, RR, MML were involved in the acquisition of the data, analysis, and interpretation of the data and drafting of the manuscript. TK provided expert statistical help. SR, FD served as expert pathologists. JPN, BG, EC, CH, SO, SK, SB, JW, JDH, AB, JK, PG, MS, DP provided technical expertise and samples for the analysis. FUW, GB, MWB, provided relevant intellectual input. UMM, MML and JM: Study concept and design, drafting of the manuscript, obtained funding, study supervision. All participants finally approved the manuscript.

Acknowledgement: The authors would like to thank especially David A. Tuveson and the members of the ESPAC-T Plus steering committee study as well as all participants and centers of the ESPAC study including the patients enrolled in this trial. Without their help, we would not have been able to perform these experiments. Authors would like to thank Simon Gahr and Michaela Svihla for their technical support.

Conflict of interests: The authors disclose no conflicts.

Glossary

Term	Explanation
Immunohistochemistry (IHC):	immunostaining on the sections obtained from formalin fixed paraffin embedded tissue-blocks or tissue microarrays.
Multiplex immunostaining	consecutive multiple immunostaining followed by destaining on sections obtained from paraffin embedded histoblocks or tissue microarrays (TMA).
Intratumoral cells (ITC)	isolated cells from the digestion of PDAC resection specimen.
Image cytometry	colocalization analysis and quantification of immune markers after multiplex immunostaining.
Cytoblocks	immunostaining on the sections obtained from paraffin embedded isolated intratumoral cells.
Cytospins	immunostaining on slides obtained from cytospining of isolated intratumoral cells.
Actual response	actual median progression free survival of patients recruited in the validation cohort with respect to the immune marker subcohort.
Predicted response	predicted median progression free survival of patients recruited in the validation cohort with respect to the immune marker subcohort derived from ESPAC-Tplus cohort.
VIMP	Variable of importance (VIMP) depicting the weightage of the categorical variable in random forest iterations.
Terminal node	binary split criteria in a decision tree using random forest iterations are called node. Terminal nodes are prognostic subcohorts derived from the recursive partitioning for discrete time survival tree analysis.

Address of correspondence:
Julia Mayerle, MD
Medizinische Klinik und Poliklinik II
Klinikum der LMU München-Campus Grosshadern
Marchioninistr. 15
81377 Munich, Germany
Tel +49 (0) 89 4400-72390
Fax +49 (0) 89 4400-78887
Email: julia.mayerle@med.uni-muenchen.de

Abstract:

Background & Aims: Changes to the microenvironment of pancreatic ductal adenocarcinomas (PDACs) have been associated with poor outcomes of patients. We studied the associations between composition of the pancreatic stroma (fibrogenic, inert, dormant, or fibrolytic stroma) and infiltration by inflammatory cells and times of progression-free survival (PFS) of patients with PDACs after resection.

Methods: We obtained 1824 tissue microarray specimens from 385 patients included in the European Study Group for Pancreatic Cancer trial 1 and 3 and performed immunohistochemistry to detect alpha smooth muscle actin, type 1 collagen, CD3, CD4, CD8, CD68, CD206, and neutrophils. Tumors that expressed high and low levels of these markers were compared with patient outcomes using Kaplan-Meier curves and multivariable recursive partitioning for discrete-time survival tree analysis. Prognostic index was delineated by a multivariable Cox-proportional-hazards-model of immune cell and stromal markers and PFS.

Findings were validated using 279 tissue microarray specimens from 93 patients in a separate cohort.

Results: Levels of CD3, CD4, CD8, CD68, and CD206 were independently associated with tumor recurrence. Recursive partitioning for discrete-time survival tree analysis identified a high level of CD3 as the strongest independent predictor for longer PFS. Tumors with levels of CD3 and high levels of CD206 associated with a median PFS time of 16.6 months and a median prognostic index of –0.32 (95% CI, –0.35 to –0.31), whereas tumors with low level of CD3 cell and low level of CD8 and high level of CD68 associated with a median PFS time of 7.9 month and a prognostic index of 0.32 (95% CI, 0.050–0.32)—we called these patterns histologic signatures.

Stroma composition, when unassociated with inflammatory cell markers, did not associate significantly with PFS. In the validation cohort, the histologic signature resulted in an error matrix accuracy of predicted response of 0.75 (95% CI, 0.64–0.83; accuracy P<.001).

Conclusions: In an analysis of PDAC tissue microarray specimens, we identified and validated a histologic signature, based on leukocyte and stromal factors, that associates with PFS times of patients with resected PDACs. Immune cells might affect the composition of the pancreatic stroma to affect progression of PDAC. These findings provide new insights into the immune response to PDAC.

Key words: ESPAC, pancreatic cancer, histologic analysis, prognostic factor

Introduction:

Pancreatic ductal adenocarcinoma (PDAC) is one of the most aggressive malignancies and burdened with a 5-year survival rate of around 6%[1,2]. Multiple factors are considered to be responsible for this dismal prognosis but essentially involve two problems: late diagnosis and profound treatment resistance - combined with lack of personalized treatment options[3,4]. PDAC is known for its desmoplastic stroma reaction comprised of activated myofibroblasts, leukocytes and extracellular matrix[5]. PDAC desmoplasia is thought to confer biological aggressiveness[6], however, recent evidence from animal models demonstrated that an absence of desmoplasia resulted in an even more undifferentiated and aggressive tumor phenotype[5,7,8], suggesting that stroma composition influences cancer biology in a more complex manner. Preliminary data suggest a correlation between poorer clinical outcome and the composition and quantity of tumor infiltrating immune cells as well as tumor associated myofibroblasts, resulting in a weaker adaptive immune response in PDAC[9,10]. Not surprisingly several attempts have been made to evaluate the prognostic significance of tumor-infiltrating leukocytes in a variety of human non-pancreatic cancers at the level of genomics, transcriptomics and histology[11]. Here, prognostic significance of a prominent overall leukocyte infiltration has been shown to be associated with increased survival[11]. However, to understand the complexity and plasticity of stroma formation in pancreatic cancer and its associated leukocytes, a combination of approaches with supervised predictors of disease progression is required to determine prognostic signatures. Such an approach could reveal signatures for risk stratification and will be hypothesis-generating with regard to underlying biological mechanisms and potential targets[12].

In order to generate a prognostic landscape of infiltrating immune cells and stromal composition across pancreatic cancer we investigated T-lymphocytes (CD3, CD4/CD8), tumor associated macrophages, alternatively activated macrophages and neutrophils along with their associated stromal composition and compared those to progression free survival data of the patients.

Promising prognostic biomarkers did not achieve clinical significance and some explanation are the use of retrospectively collected uncontrolled material with too small a sample size, non-standardized assays and inappropriate or misleading statistical analyses. To overcome these limitations and to minimize the bias we not only followed the REMARK guidelines[4] but used data and tissue from a prospective randomized controlled trial (ESPAC-Tplus) on adjuvant treatment of pancreatic cancer conducted by the European Study group for Pancreatic Cancer. We delineated a prognostic signature based on organ-based leukocyte subpopulations and stromal composition which identifies cancer subtypes and predicts progression free survival.

Materials and Methods:

Study Design

The translational ESPAC-T studies received ethical committee approval for characterization of tumor markers for chemotherapy from the Liverpool (Adult) Research Ethics Committee (07/H1005/87). Use of Good Clinical Practice standard operating procedures[13] ensures a full audit trail and prevents access to outcome data by pathologists and laboratory researchers. After resection for pancreatic ductal adenocarcinoma, patients in the ESPAC-3 study were randomized to receive either 5FU/folinic acid or gemcitabine. ESPAC-3 was analyzed on an intention to treat basis, but for the ESPAC-T study patients, arms were selected for inclusion only if treatment was actually received. This study was conducted and reported in accordance with the REMARK criteria[4,14].

Tissue Microarray Manufacture for identification and validation cohort

The arrays from ESPAC-Tplus were reported previously[4]. TMAs for the independent validation cohort (n=93) were derived from a prospective cohort recruited at the university of Munich carried out according to the recommendations of the local ethics committee of the Medical Faculty of the University of Munich, Germany. TMA generation was reported previously[15].

Single and multiplex immunostaining and quantification of TMA cores

Detailed information of the single and multiplex immunostaining and antibodies are provided in the **supplemental materials and methods** section. Immunohistochemistry using DAB complex conjugation techniques (Vector Laboratories Ltd., Peterborough, UK) were performed as described earlier[16]. Chloracetate esterase staining for detection of neutrophils infiltration was performed using Naphthol AS-D chloracetate (specific esterase) kit (Sigma-Aldrich) as per manufacturer's instruction. Specific collagen staining was performed on each core using Picrosirius Red-Fast Green staining solution (0.1% Direct Red 80 and 0.1% Fast Green FCF in aqueous picric acid). Multiplex immunostaining for the validation cohort was

performed as described previously with some modifications[17]. Details of multiplex immunostaining and quantification are provided in **supplementary materials and methods**.

All the staining cores were scored by two investigators independently blinded to treatment group when scoring, as well as blinded to patient outcomes throughout the study. Quantification was undertaken for α-SMA according to the intensity of staining in the tumor core ranked from 0 to 3 (0= no staining, 1= low staining, 2= intermediate staining and 3= high staining) and the percentage of area stained was calculated using an algorithm developed for NIH ImageJ software **(suppl fig.S1A)**. H-Scores were calculated for each core by multiplying intensity score by the percentage of core staining and a median H-Score calculated for all cores from each patient. Collagen quantification was performed by Picrosirius Red (Collagen) and Fast Green (rest of the tissue) according to the intensity of staining in the tumor core ranked from 0 to 3 (0= no staining, 1= low staining, 2= intermediate staining and 3= high staining) and the percentage of area stained was calculated using an algorithm developed for the NIH software ImageJ. H-Scores were calculated for each core by multiplying the intensity score by the percentage of core staining and a median H-Score calculated for all cores from each patient individually for Picrosirius Red and Fast Green. Final H-score for collagen staining was calculated as a ratio of Picrosirius Red to that of Fast Green. Inter-rater reliability for the H-score and the observed inter-concordance coefficient (ICC) for picrosirius red/ fast green staining was 0.84 (95%CI: 0.82-0.85) and for α-SMA 0.92 (95%CI: 0.92-0.93) **(suppl fig. S2A-B)**. The leukocyte infiltration was determined as number of cells/mm^2 (**suppl fig. S3**) using an algorithm developed for NIH software ImageJ (**suppl fig. S1B**). The cut-off for each marker was calculated using cut-off finder with the incorporation of the Log-rank method described earlier[18]. All the cut-offs used for classification of markers to dichotomize low and high expression are described in the **suppl table S1**, with representative images in **suppl fig.S3**. Stromal composition by means of expression of α-SMA/collagen was divided as described previously as dormant (low α-SMA/high collagen expression), inert (low α-SMA/low collagen expression), fibrogenic (high

α-SMA/high collagen expression) and fibrolytic (high α-SMA/low collagen expression) stroma[10,19].

IHC staining evaluation in comparison to flow cytometry

From 10 PDAC patients, freshly resected tumor tissue was processed for paraffin tissue-block embedding and primary cell isolation. Moreover, EDTA blood was provided for assessment of peripheral blood derived monocytes cells (PBMCs); the detailed isolation procedure is given in the **supplemental material and method** section. The PDAC tissue samples were double-coded and corresponding data were provided by the Biobank of the Department of General, Visceral and Transplantation Surgery, University Hospital, LMU Munich, Germany, under the administration of the Human Tissue and Cell Research (HTCR) Foundation. The framework of HTCR Foundation[20], which includes obtaining written informed consent from all donors, has been approved by the ethics commission (approval number 025-12) of the Faculty of Medicine, LMU Munich, Germany as well as by the Bavarian State Medical Association, Germany (approval number 11142). The leukocyte cell population from tumor tissue and blood samples was analyzed by flow cytometry (fluorescence-activated cell sorting, FACS). The intratumoral leukocytes determined by FACS revealed a strong positive correlation to immunohistochemical staining on tissue-blocks (solid black square in the correlogram in **suppl fig.S4**).

Statistical Analysis

For all analyses, the sample size was limited to appropriate cases with full data; no imputation was performed to estimate missing clinical information. Survival from the date of resection was analyzed by the method of Kaplan-Meier; differences between groups were assessed using the Mantel-Cox log rank test. Survival was either to death from cancer (overall survival time, OS) or to recurrence as assessed by computer tomography or ultrasound or through histology/cytology (progression free survival time, PFS). Multivariate Cox regression analyses were used to adjust for the progression free survival effect by all important prognostic variables on a complete case basis. Covariates were included in the

multivariable model using forward stepwise regression approach based on the Akaike Information Criterion if they had an unadjusted log-rank significance of P<0.25. When more than two survival cohorts were compared, the log-rank test was used to assess global differences in survival. Box-and-whisker plots show median, quartiles, and range of continuous data to demonstrate the variability of data and the degree of normality. All analyses were carried out using R 2.1.0 (http://cran.r-project.org/src/base/R-2/R-2.1.0.tar.gz) and R-studio 1.0.153 (https://github.com/rstudio/rstudio/tarball/v1.0.153). A two-sided significance of P<0.05 was used throughout. Detailed methodology is described in **supplementary materials and methods**.

Results

Patients and tissue samples

Tissue microarrays (TMA) from 403 patients resected for pancreatic ductal adenocarcinoma (for detail see CONSORT diagram in **figure 1A**) were employed. As expected and previously reported, there was no significant difference with regard to treatment with gemcitabine or 5-flourouracil/folinic acid for progression free survival (PFS) or overall survival (OS) within the trial and our cohort[21]. Furthermore, treatment regimens did not impact on PFS with regard to specific prognostic signatures delineated within this manuscript **(**see **suppl table S7-S8)**. Demographics, surgery and pathology features of the patients included are summarized in **table 1**. Within the present study, we mainly focus on PFS as primary outcome as we controlled for the effect of adjuvant chemotherapy by randomization.

Composition of leukocyte infiltrate and its prognostics association

To systematically map compositional differences of different leukocyte subsets in the tumor microenvironment and their influence on PFS, we performed immunohistochemical analysis of CD3, CD4, CD8, CD68, CD206 and chloracetate esterase in TMAs and quantified leukocyte subpopulations **(figure 1B)**.

The density of tumor infiltrating T-lymphocytes has been proposed as an independent predictor of outcome in solid tumors[22–24]. In line with these observations, we performed survival analyses for high and low levels of CD3 expression and observed a significant association of high CD3 expression with significantly increased PFS; median PFS 14.32 months (95%CI 12.74-17.28) compared to low CD3 expression; median PFS 11.03 months (95%CI 9.69-12.45), resulting in a hazard ratio of 0.65 (95%CI 0.53-0.80, p<0.0001) **(figure 1C, table 2)**. To investigate the associations of CD4+ T-cells with PFS we performed Kaplan-Meier survival analyses for dichotomized CD4 low and high counts, which only marginally influenced PFS (median PFS 12.81 (95%CI 11.72-14.91) for high CD4 expression vs 10.87 (95%CI 9.23-14.91) for low CD4 expression, p=0.03) **(table 2).** The importance of tumor infiltrating lymphocytes, particularly antitumor cytotoxic T-cell (CD8 positive), has been

underlined by their prognostic associations in several human cancers[25]**.** We sought to determine the influence of cytotoxic T-cell infiltration on PFS. Kaplan-Meier survival analysis revealed a trend towards higher cytotoxic T-cell counts in the tumor with favorable PFS resulting in a hazard ratio of 0.78 (95%CI 0.63-0.98, p=0.03) **(table 2)** which supports previous studies[25]. In short, absence of infiltrating T-lymphocytes is associated with decreased PFS.

Next, we evaluated the density of infiltrating CD68 expressing tumor associated macrophages (TAMs) and performed Kaplan-Meier survival analysis with regard to CD68 expression and observed higher counts of TAMs (CD68) associated with improved PFS; median PFS of 13.30 months (95%CI 11.92-16.39) compared to patients with low infiltration median PFS 11.72 months (95%CI 9.52-13.76)) giving a hazard ratio of 0.78 (95%CI 0.62-0.98, p=0.02) **(table 2)**.

There is evidence suggesting TAMs are reprogrammed from polarized activated macrophages (ΦM1) to alternatively activated macrophages (ΦM2) shifting the immunoregulatory response and affecting microenvironment[26]. We quantified the staining of alternatively activated macrophages (ΦM2, CD206+), and dichotomized distribution of CD206 counts. It revealed a significant association of high CD206 count with a median PFS of 13.76 months (95%CI 11.99-15.63) compared to a median PFS of 10.28 months (95%CI 8.60-12.74) in the low CD206 count group, giving a hazard ratio of 0.69 (95%CI 0.52-0.90) **(table 2)**. Our dataset revealed that differential tumor infiltration of ΦM1 with a concomitant increase in ΦM2 correlates to an increase in PFS.

Circulating leukocytes, such as neutrophils are known to contribute to the tumor microenvironment[11]. Several lines of evidence indicate that a high density of neutrophils promotes tumor growth and metastasis[27]. Density of neutrophil infiltration on PFS or OS did not show a significant correlation **(table 2)**.

Identification of different subtypes of stromal composition

The key to understanding the role of the stroma is its composition. We investigated the expression pattern of α-SMA and collagen in resected PDAC with respect to PFS. Unexpectedly, α-SMA as well as collagen expression alone were not associated with extensive stroma formation or PFS **(suppl fig.5A-B)**. Thus, we categorized the stroma on the basis of differential expression of α-SMA and collagen I as previously established by Erkan and colleagues[10] as fibrogenic (high α-SMA/high collagen expression), inert (low α-SMA/low collagen expression), dormant (low α-SMA/high collagen expression) and fibrolytic stroma (high α-SMA/low collagen expression) **(figure 2A,** representative images**)**. The overall median PFS of the cohort was 12.71 months (95% CI 11.63-14.19) with a median PFS for inert stroma of 13.76 months (95%CI 10.87-16.65), with dormant stroma of 12.69 months (95% CI 9.69-16.06), with fibrogenic stroma of 14.09 months (95% CI 11.99-20.10) and with fibrolytic stroma of 11.05 months (95%CI 8.87-12.74), χ^2=7.09, p=0.06 **(figure 2B)**. The difference between fibrolytic in comparison to fibrogenic stroma was significant with a hazard ratio of 1.48 (95%CI 1.08-2.01, p=0.01) **(suppl fig.S5C; OS: suppl. Fig.S6)**. Taken together, these results indicate that categorization of stromal composition considering differential α-SMA and collagen expression correlates to PFS.

The impact of the stromal compartment on T-lymphocytes migration orchestrates the hierarchy of interactions between immune cells and tumor cells[28]. This suggests that the tumor microenvironment regulates the immune response and vice versa. In order to identify the connection between stromal subtype and immune infiltration, we performed comparative correlation analyses. It revealed dominant clusters each for a T_H1 driven immune response characterised by abundant CD3, CD4, CD206 expression and for pro-inflammatory modulators such as CD8, CD68 and neutrophils in respect to fibrogenic and dormant stroma. Inert and fibrolytic stroma showed the two dominant clusters for CD4, CD206, CD3, CD8, CD68 and neutrophils **(figure 2C)**.

To ascertain the influence of immune infitration in modulating stromal composition, we analyzed distribution of immune infitrates in different stromal subtypes and found differential distribution of immune cells infitrates with respect to stromal subtypes **(figure 2D)**. Fibrolytic stroma has more abundant CD206+ ΦM2 with reduced CD8+ T-cells and CD68+ ΦM1 suggesting an immunosuppressive tumor microenvironment while fibrogenic stroma associated with increased PFS was more abundant for CD8 T-cells and CD68 positive macrophages **(figure 2D).**

We analyzed the influence of low and high expression of immune infiltrates on PFS with respect to stromal subtypes **(table 3)**. We found that CD3 dichotomization predicts differential PFS in fibrogenic and fibrolytic stratified patients, whereas CD4 dichotomization predicts differential PFS in fibrogenic stroma. CD68 dichotomization predicts differential PFS in inert stratified patients whereas CD206 dichotomization predict differential PFS in dormant stratified patients. Taken together, subtypes of stroma not only differ in α-SMA and collagen-I expression but show a distinctly different pattern of leukocytes subpopulation depending on stroma subtype which then predicts PFS.

Contingency testing of immune infiltrate and stromal subtypes with other clinical and tumor characteristics **(suppl. Table S2)** did not reveal any statistically significant associations.

Contribution of infiltrating leukocytes in defining stromal composition

To complement our immune cell marker-centered survival analysis, we compiled combinatorial prognostic associations for immune infiltrates ($CD3^+$ T-cells, $CD4^+$ T-cells, cytotoxic T-cells, ΦM1, ΦM2, and neutrophils). We performed a univariate analysis with PFS as endpoint and observed considerable variations between infiltrating immune cell subpopulations and survival **(table 4)**. Univariate analysis of the independent variables: lymph node invasion, resection margin status, local invasion, maximum tumor diameter and post-operative CA19.9, showed significant associations with PFS in the complete cohort **(table 4)**. Univariate analysis and multivariable analysis with overall survival factors showed similar results **(suppl. table S3)**.

Pairwise comparisons of variations of immune cell subpopulations with respect to stromal composition did not show significant associations with PFS or OS **(suppl. table S4).** A positive resection margin increased the risk of local recurrence. Pairwise comparison of resection margin and immune infiltrates to investigate the influence on PFS or OS was performed. We found a significant association of high expression of immune cells in negative resection margin stratified patients **(suppl. table S5-6)**. Pairwise PFS as well as OS survival comparisons of variations of immune cell subpopulation and stromal composition with respect to the therapeutic arm did not show any statistically significant association with PFS or OS **(suppl. table S7-S8)**.

A composite prognostic signature for predicting progression free survival in PDAC

Low expression of T-lymphocytes and tumor-associated macrophages are associated with worse prognosis and our data on fibrolytic stroma suggest that activated fibroblasts are at least partially involved in the poor outcome of these patients. We thus hypothesized that the differential expression pattern of high leukocyte subpopulations may characterize a favorable stroma composition. Analyses presented above were all dependent on tumor stratification and the set-up of predefined groups. In order to evaluate this, we performed a non-parametric approach for competing risks using random survival forests and used it for selecting progression-specific variables and for estimating the cumulative incidence function. Progression-specific variables of importance (VIMP) and minimal depth variable selection were used to identify variables specific for all events. We found that, except for neutrophils count, all variables (CD3, CD4, CD8, CD68, CD206 and stroma) significantly influenced PFS. CD3 expression has the maximum influence on PFS with a VIMP of 2.63 and a minimum depth of 1.15 followed by CD8 and CD206 **(figure 3A)**.

To establish a prognostic signature combining leukocyte infiltration and stroma composition, we developed an algorithm evaluating the presence and prognostic strength of a signature in resected pancreatic cancer. Recursive-partitioning for discrete-time survival-tree-analysis using PFS as predictive endpoint delineated a regression tree according to prognostic

variables that classified patients into homogeneous subsets by PFS **(figure 3B)**. We detected seven terminal nodes (subcohorts) characterizing a prognostic signature. The predicted prognostic signature for patients harboring $CD3_{high}CD206_{high}$ signature was associated with a median PFS time of 16.60 (95%CI 13.80-23.80) compared to patients harboring $CD3_{low}CD8_{low}CD68_{high}$ showing the worst PFS of 6.27 months (7.95 months (95%CI 3.91-14.56). Our analyses support a complex, multi-marker signature model of stromal compartments in PDAC, which may explain why single predefined marker analyses have yielded mixed results.

We extended the analysis by separately testing the association between the prognostic signature and clinical outcome in a multivariable Cox proportional hazards model integrating variables for random forest analysis **(table 4)**. After adjustment for infiltrating immune cell subpopulations, multivariable analysis confirmed CD3, CD8 and CD206 expression status as significantly associated with PFS (CD3, p=0.005, CD8, p=0.02 and CD206, p=0.004). We compared this multivariate analysis obtained from a Cox proportional hazard model with a multivariate analysis again using the Cox proportional hazard model including stromal composition, CD3, CD4, CD8, CD68 and CD206 expression, along with known relevant risk factors such as lymph node invasion, resection margin and tumor stage (**suppl table S9**). Based on Akaike's information criterion (AIC) described in **table 4,** a model only taking into account stroma composition and immune infiltrate had a higher predictive strength than a model including clinical parameters as described in **suppl table S9**. Furthermore, after adjusting for independent variables the model including clinical parameters did not predict progression free survival. We integrated the prognostic signature incorporating immune infiltrates and stromal composition delineating a relative prognostic index from a multivariable Cox-proportional-hazards-model of prognostic factors and PFS. The waterfall plot of our relative prognostic indices of terminal nodes (patients' subgroups) depicts the relevance of this approach. Of note, the prognostic index for patients harboring $CD3_{high}CD206_{high}$ signature depicts a higher probability of prolonged PFS than patients harboring a $CD3_{low}CD8_{low}CD68_{high}$ signature **(figure 3C, overall survival: suppl fig S7)**. Nonparametric

testing for competing risks using random forest iterations analysis for risk factors such as stage, resection margin, postOpCA19.9 (dichotomized based on median), lymph node invasion and local invasion used as a reference signature. Immune marker-based signature (AUC=0.71) fared better compared to reference signature (AUC=0.63) **(suppl fig.S8)**.

Independent validation of the prognostic signature derived from the ESPAC-Tplus cohort

To validate our prognostic histological signature, we used an independent cohort consisting of 93 patients (CONSORT diagram in **suppl fig.S9**). We performed immunostaining of CD3, CD4, CD8, CD68, CD206, MPO, α-SMA and collagen, followed by multiplex immunostaining analysis. The demographics of patients are shown in **suppl. table S10**. The median overall survival (OS) and progression free survival (PFS) of the validation cohort was 33.53 months (95%CI: 27.39-39.87) and 16.79 (95%CI: 12.55-20.35), respectively. As depicted in **suppl fig.S10C** our results on individual markers and their correlation from the identification cohort are replicated in the validation cohort except for the CD68 count and its correlation to PFS (**suppl fig.S10C**). Results of univariate and multivariate analysis of prognostic factors in the validation cohort are shown in **suppl table S11-12** and again validate our data from the identification study. When we tested the prognostic histological signature in the validation cohort the predicted response as defined by nodal localization as well as the accuracy of the predicted median progression free survival (predicted m(pfst) per subcohort) in comparison with the actual response (actual m(pfst) per subcohort) was in good concordance and good predictability as depicted by the alluvial plot (**figure 3D**). The prediction analysis revealed a Cohen's Kappa with 0.69 and Harrell's C-index with 0.60. In conclusion, the signature showed good reproducibility and robustness in the validation cohort.

We substantiated our finding by plotting Kaplan-Meier curves of predicted response and actual response of the validation cohort (**suppl fig.S10D**). We determined an accuracy of 0.75 (95%CI: 0.64-0.83, accuracy P<0.001). We detected a positive correlation between predicted response and actual response with R=0.62 and P<0.001. In conclusion, the

validation cohort confirmed the prognostic value of the biomarker signature established in the ESPAC cohort (identification cohort).

Discussion:

In this article, we demonstrate that the immune microenvironment in PDAC cancer can be of prognostic value for PFS after resection. Moreover, we provide evidence of a prognostic signature incorporating leukocytes subpopulations and stromal composition to stratify patients in respect to PFS. Subtypes of stroma not only differ in a-SMA and collagen I expression but show a distinctly different pattern of leukocyte subpopulation depending on stroma subtypes. As the prognostic signatures presented here can predict PFS, we envision discovery of predictive biomarkers for the response to immunotherapies in the future.

The role of the adaptive immune response in controlling growth and recurrence of human cancers has been controversial[29]. It is now generally accepted that a number of solid tumors are capable of inactivating an anti-tumorigenic immune response. Once tumor immune surveillance is overcome, the composition of the immune infiltrate changes and a pro-tumorigenic leukocyte profile emerges. T-cells can be both tumor suppressing and tumor promoting depending on their downstream target-cells[27]. We characterized the tumor-infiltrating leukocytes and found that once human PDAC becomes clinically detectable and thus resected, the adaptive immune response mediated by $CD3^+$ and $CD4^+$ cells effects tumor recurrence. Intratumoral T-cells could modify tumor-stroma or tumor-cells in ways that attenuate the metastatic potential of PDAC[29,31]. We found a positive correlation between the presence of markers for T_{H1} polarized memory T-cells ($CD3^+$ and $CD4^+$) and prolonged PFS. We argue that the trafficking properties and long-lasting anti-tumor capacity of memory T-cells play a central role in the control of tumor recurrence.

The ultimate goal of cancer immunotherapy is to induce high affinity cytotoxic T-cells without causing autoimmunity[32]. The accumulation of cytotoxic $CD8^+$ T-cells correlates well with survival of patients with different types of cancer as well as PDAC[33–35,25,36]. We confirmed these findings in our cohorts.

Tumor-associated macrophages ($CD68^+$ cells) are the most prevalent population of the tumor-infiltrating mononuclear cells. In addition, TAMs have also been suggested to promote

immune tolerance, at least in part by modulating the phenotype of tumor-infiltrating CD8+ T-cells with $CD8^+$ cell populations in the microenvironment being dependent on TAMs[37]. We show a significant and positive correlation between infiltration of $CD68^+$ TAMs and increased PFS supporting previous mechanistic studies[38]. Moreover, TAMs proved to be independent predictive markers for recurrence after resection of PDAC. In addition, we detected significant differences in high CD206 expression in predicting increased PFS.

Plasticity is a hallmark of TAMs, as they can acquire both pro-tumorigenic and anti-tumorigenic phenotypes. Alternatively, polarized ΦM_2 are believed to be major contributors to the immunosuppressive environment of the tumor. Contrary to these findings, we observed that high infiltration of ΦM_2 increased PFS in the identification cohort but could not validate this finding. Only tumors with high infiltration of ΦM_2 can obtain a prognostic advantage in response to chemotherapy whereas this effect is lost in sparsely infiltrated tumors[39,40].

A fibro-inflammatory stromal reaction influences PDAC initiation, progression, and relapse[41]. Stroma is believed to enhance stiffness, elevate hydrostatic pressure and contribute to cancer hypoperfusion and hypoxia[42,43]. However, depletion of stroma in experimental models resulted in a biologically more active and aggressive PDAC phenotype[5,8]. The function of the desmoplastic stroma is likely dynamic during cancer progression and its heterogeneous cellular and acellular constituents change in relation to the prognostic landscapes of cancers[8,41]. The expression of α-smooth muscle actin (α-SMA) in PSCs marks the transdifferentiation of the quiescent PSCs to an activated phenotype. The putative role of activated PSCs is to secrete various cytokines, chemokines and growth factors and thereby contribute to the inflammatory milieu stimulating cancer cell proliferation and migration. There are several studies depicting differential expression of α-SMA and collagen I, as a tumor-promoter or -suppressor depending on stromal turn-over serving as an independent prognostic marker[5,8,10]. Our data support the previous finding that poor-prognosis stroma subtypes are characterized by the differential expression of α-SMA and collagen-I[19] which led us to speculate that distinct stromal subtypes might be responsible for aggressiveness and associated with differential infiltration of immune cells. Having classified stromal composition

based on α-SMA and collagen I expression as inert, dormant, fibrogenic and fibrolytic stroma, we applied these subtypes to our cohort. We detected fibrolytic stroma indicating worse prognosis, thus confirming the previously published data[10].

The presence of tumor infiltrating leukocytes (TILs) within the tumor microenvironment is considered to be an indication of the host immune response to the tumor and reflects the dynamic process of cancer immunoediting[23]. There is evidence suggesting an interplay between cancer associated fibroblasts and immune cells in cancer development with a striking imbalance between pro-tumorigenic and anti-tumorigenic leukocyte subpopulations[32,44]. In the present study, we present a complex pattern of differential expression profiling of leukocyte subpopulations with an orthogonal behavior with respect to stromal subtypes for most TIL subtypes; being positively correlated with each other irrespective of stromal composition.

Some tumors acquire the ability to sabotage the inflammatory response and exploit them to promote tumorigenesis. For this reason, the leukocyte infiltrate in the microenvironment and stromal composition may be a consequence of an inflammatory response that favors either dissemination of tumor cells or is immunosuppressive[33]. The independent prognostic potential of individual markers such as CD3, CD8, CD68 and CD206 which are confounders of stromal composition is thus limited. Therefore, we developed prognostic signatures to predict recurrence incorporating these confounding markers.

In patients undergoing surgical resection of PDAC, prognosis and management are currently entirely based on tumor grading, nodal status and post-operative serum CA19-9 levels[21,45] despite considerable variability in outcome. Accordingly, prognostic classifiers that readily implement heterogeneity and type of tumor composition are needed to foster decision making and patients' stratification. Here, implementing recursive-partitioning of discrete-PFS-trees, we classified patients into 7 subtypes based on expression of CD3, CD4, CD8, CD68, CD206 and stromal composition. On the basis of this classification, we found statistically significant associations of these signatures in predicting recurrence. Of note, since all the

prognostic markers incorporated in the signatures had independent prognostic potential, no interaction was found between different signatures. Patients harboring $CD3_{high}CD206_{high}$ signature have the best post-operative PFS whereas patients with $CD3_{low}CD8_{low}CD68_{high}$ signature showed the worst PFS. Moreover, these signatures minimize false negative cases obtained by employing single prognostic markers. Our findings support previous mechanistic data and demonstrate the ability of prognostic signatures to predict clinical outcome. The independent validation confirmed the performance of a prognostic histological signature and showed strong reproducibility and robustness of the signature.

Despite several important observations, our study has limitations which include the retrospective design and inability to examine the predictive potential of our prognostic signature in correlation with treatment responses. While an effort was made to control for multiple comparisons for marker stratifications in low and high expression group, pairwise comparisons with p-values that are close to the 0.05 significance level should be interpreted with caution. We acknowledge that other molecular events within the prognostic signature could have an additional profound impact on prognosis and adjuvant chemotherapy does have an impact on recurrence rates.

In conclusion, we defined a prognostic signature incorporating prognostic landscapes of tumor infiltrating leukocytes and stromal composition that can identify distinct subtypes with respect to recurrence within a cohort of resected PDAC patients and independently validated these signature. These data represent the largest and most comprehensive analysis to date for prognostic signatures for tumor infiltrating leukocytes and stromal composition and their prognostic effects. When thinking about adjuvant immunomodulatory therapy such as using M2-macrophage inhibitors or JAK inhibitors such signatures could become the basis for stratification.

References:

1. Maitra A, Leach SD. Disputed Paternity: The Uncertain Ancestry of Pancreatic Ductal Neoplasia. Cancer Cell 2012;22:701–703.
2. Moffitt RA, Marayati R, Flate EL, et al. Virtual microdissection identifies distinct tumor- and stroma-specific subtypes of pancreatic ductal adenocarcinoma. Nat Genet 2015;47:1168–1178.
3. Louvet C, Philip PA. Accomplishments in 2007 in the treatment of metastatic pancreatic cancer. Gastrointest Cancer Res GCR 2008;2:S37-41.
4. Greenhalf W, Ghaneh P, Neoptolemos JP, et al. Pancreatic Cancer hENT1 Expression and Survival From Gemcitabine in Patients From the ESPAC-3 Trial. JNCI J Natl Cancer Inst 2014;106:djt347–djt347.
5. Rhim AD, Oberstein PE, Thomas DH, et al. Stromal elements act to restrain, rather than support, pancreatic ductal adenocarcinoma. Cancer Cell 2014;25:735–747.
6. Olive KP, Jacobetz MA, Davidson CJ, et al. Inhibition of Hedgehog signaling enhances delivery of chemotherapy in a mouse model of pancreatic cancer. Science 2009;324:1457–1461.
7. Gore J, Korc M. Pancreatic Cancer Stroma: Friend or Foe? Cancer Cell 2014;25:711–712.
8. Özdemir BC, Pentcheva-Hoang T, Carstens JL, et al. Depletion of carcinoma-associated fibroblasts and fibrosis induces immunosuppression and accelerates pancreas cancer with reduced survival. Cancer Cell 2014;25:719–734.
9. Tjomsland V, Niklasson L, Sandström P, et al. The Desmoplastic Stroma Plays an Essential Role in the Accumulation and Modulation of Infiltrated Immune Cells in Pancreatic Adenocarcinoma. Clin Dev Immunol 2011;2011:1–12.
10. Erkan M, Michalski CW, Rieder S, et al. The Activated Stroma Index Is a Novel and Independent Prognostic Marker in Pancreatic Ductal Adenocarcinoma. Clin Gastroenterol Hepatol 2008;6:1155–1161.
11. **Gentles AJ, Newman AM,** Liu CL, et al. The prognostic landscape of genes and infiltrating immune cells across human cancers. Nat Med 2015;21:938–945.
12. Chang HY, Nuyten DSA, Sneddon JB, et al. From The Cover: Robustness, scalability, and integration of a wound-response gene expression signature in predicting breast cancer survival. Proc Natl Acad Sci 2005;102:3738–3743.
13. Sarzotti-Kelsoe M, Cox J, Cleland N, et al. Evaluation and Recommendations on Good Clinical Laboratory Practice Guidelines for Phase I–III Clinical Trials. PLoS Med 2009;6:e1000067.
14. McShane LM, Altman DG, Sauerbrei W, et al. REporting recommendations for tumour MARKer prognostic studies (REMARK). Br J Cancer 2005;93:387–391.
15. Ormanns S, Assmann G, Reu S, et al. ALK expression is absent in pancreatic ductal adenocarcinoma. J Cancer Res Clin Oncol 2014;140:1625–1628.
16. Mahajan UM, Teller S, Sendler M, et al. Tumour-specific delivery of siRNA-coupled superparamagnetic iron oxide nanoparticles, targeted against PLK1, stops progression of pancreatic cancer. Gut 2016.
17. Tsujikawa T, Kumar S, Borkar RN, et al. Quantitative Multiplex Immunohistochemistry Reveals Myeloid-Inflamed Tumor-Immune Complexity Associated with Poor Prognosis. Cell Rep 2017;19:203–217.

18. Budczies J, Klauschen F, Sinn BV, et al. Cutoff Finder: A Comprehensive and Straightforward Web Application Enabling Rapid Biomarker Cutoff Optimization Diest P van, ed. PLoS ONE 2012;7:e51862.
19. Erkan M, Hausmann S, Michalski CW, et al. The role of stroma in pancreatic cancer: diagnostic and therapeutic implications. Nat Rev Gastroenterol Hepatol 2012;9:454–467.
20. **Thasler WE, Weiss TS,** Schillhorn K, et al. Charitable State-Controlled Foundation Human Tissue and Cell Research: Ethic and Legal Aspects in the Supply of Surgically Removed Human Tissue For Research in the Academic and Commercial Sector in Germany. Cell Tissue Bank 2003;4:49–56.
21. Neoptolemos JP, Stocken DD, Bassi C, et al. Adjuvant chemotherapy with fluorouracil plus folinic acid vs gemcitabine following pancreatic cancer resection: a randomized controlled trial. JAMA 2010;304:1073–1081.
22. Laghi L, Bianchi P, Miranda E, et al. CD3+ cells at the invasive margin of deeply invading (pT3-T4) colorectal cancer and risk of post-surgical metastasis: a longitudinal study. Lancet Oncol 2009;10:877–884.
23. Sato E, Olson SH, Ahn J, et al. Intraepithelial CD8+ tumor-infiltrating lymphocytes and a high CD8+/regulatory T cell ratio are associated with favorable prognosis in ovarian cancer. Proc Natl Acad Sci 2005;102:18538–18543.
24. Dieu-Nosjean M-C, Antoine M, Danel C, et al. Long-term survival for patients with non-small-cell lung cancer with intratumoral lymphoid structures. J Clin Oncol Off J Am Soc Clin Oncol 2008;26:4410–4417.
25. Ene–Obong A, Clear AJ, Watt J, et al. Activated Pancreatic Stellate Cells Sequester CD8+ T Cells to Reduce Their Infiltration of the Juxtatumoral Compartment of Pancreatic Ductal Adenocarcinoma. Gastroenterology 2013;145:1121–1132.
26. Mantovani A, Allavena P, Sica A, et al. Cancer-related inflammation. Nature 2008;454:436–444.
27. Yamanaka T, Matsumoto S, Teramukai S, et al. The Baseline Ratio of Neutrophils to Lymphocytes Is Associated with Patient Prognosis in Advanced Gastric Cancer. Oncology 2007;73:215–220.
28. Watt J, Kocher HM. The desmoplastic stroma of pancreatic cancer is a barrier to immune cell infiltration. OncoImmunology 2013;2:e26788.
29. Galon J, Costes A, Cabo-Sanchez F, et al. Type, Density, and Location of Immune Cells Within Human Colorectal Tumors Predict Clinical Outcome. Science 2006;313:1960–1964.
30. Bazhin AV, Shevchenko I, Umansky V, et al. Two immune faces of pancreatic adenocarcinoma: possible implication for immunotherapy. Cancer Immunol Immunother 2014;63:59–65.
31. Curiel TJ, Coukos G, Zou L, et al. Specific recruitment of regulatory T cells in ovarian carcinoma fosters immune privilege and predicts reduced survival. Nat Med 2004;10:942–949.
32. Feig C, Gopinathan A, Neesse A, et al. The Pancreas Cancer Microenvironment. Clin Cancer Res 2012;18:4266–4276.
33. Pagès F, Berger A, Camus M, et al. Effector Memory T Cells, Early Metastasis, and Survival in Colorectal Cancer. N Engl J Med 2005;353:2654–2666.
34. Salama P, Phillips M, Grieu F, et al. Tumor-Infiltrating FOXP3 $^{+}$ T Regulatory Cells Show Strong Prognostic Significance in Colorectal Cancer. J Clin Oncol 2009;27:186–192.

35. **Carstens JL, Correa de Sampaio P,** Yang D, et al. Spatial computation of intratumoral T cells correlates with survival of patients with pancreatic cancer. Nat Commun 2017;8:15095.

36. Ryschich E, Nötzel T, Hinz U, et al. Control of T-cell-mediated immune response by HLA class I in human pancreatic carcinoma. Clin Cancer Res Off J Am Assoc Cancer Res 2005;11:498–504.

37. Beatty GL, Winograd R, Evans RA, et al. Exclusion of T Cells From Pancreatic Carcinomas in Mice Is Regulated by Ly6Clow F4/80+ Extratumoral Macrophages. Gastroenterology 2015;149:201–210.

38. DeNardo DG, Brennan DJ, Rexhepaj E, et al. Leukocyte Complexity Predicts Breast Cancer Survival and Functionally Regulates Response to Chemotherapy. Cancer Discov 2011;1:54–67.

39. Di Caro G, Cortese N, Castino GF, et al. Dual prognostic significance of tumour-associated macrophages in human pancreatic adenocarcinoma treated or untreated with chemotherapy. Gut 2016;65:1710–1720.

40. Kurahara H, Shinchi H, Mataki Y, et al. Significance of M2-Polarized Tumor-Associated Macrophage in Pancreatic Cancer. J Surg Res 2011;167:e211–e219.

41. Sherman MH, Yu RT, Tseng TW, et al. Stromal cues regulate the pancreatic cancer epigenome and metabolome. Proc Natl Acad Sci 2017;114:1129–1134.

42. Provenzano PP, Cuevas C, Chang AE, et al. Enzymatic targeting of the stroma ablates physical barriers to treatment of pancreatic ductal adenocarcinoma. Cancer Cell 2012;21:418–429.

43. Jacobetz MA, Chan DS, Neesse A, et al. Hyaluronan impairs vascular function and drug delivery in a mouse model of pancreatic cancer. Gut 2013;62:112–120.

44. Erez N, Truitt M, Olson P, et al. Cancer-Associated Fibroblasts Are Activated in Incipient Neoplasia to Orchestrate Tumor-Promoting Inflammation in an NF-kappaB-Dependent Manner. Cancer Cell 2010;17:135–147.

45. Geer RJ, Brennan MF. Prognostic indicators for survival after resection of pancreatic adenocarcinoma. Am J Surg 1993;165:68–73.

Author names in bold designate shared co-first authorship

Figure legends:

Figure 1: Low expression levels of tumor infiltrate leukocytes correlate with poor progression free survival across resected PDAC. (A) CONSORT diagram. 5FU/FA = 5-fluorouracil/folinic acid; FFPE = formalin-fixed paraffin-embedded; PDAC = pancreatic ductal adenocarcinoma; TMA = tissue microarray. **(B)** Representative image showing analysis of immune infiltration (number of cells/mm^2) using an algorithm developed for NIH ImageJ software. **(C)** The Kaplan-Meier survival analysis shows that patients with low CD3 expression are burdened with as decreased progression free survival time in comparison to high CD3 expression.

Figure 2: Contribution of multifaceted stromal composition in defining progression free survival. (A) Representative images of α-SMA and collagen-I staining characterizing fibrogenic, inert, dormant and fibrolytic stroma. **(B)** Kaplan-Meier survival analysis of patients with resected PDAC in respect to stroma subtype with median survival for inert stroma (light green) as 13.76 (95%CI 10.94-16.65), dormant stroma (orange) as 12.81 (95% CI 9.88-16.06), fibrogenic stroma (light blue) as 14.09 (95% CI 11.99-20.10) and fibrolytic stroma (red) as 11.03 (95%CI 8.87-12.74). **(C)** Correlation matrixes demonstrating results of the correlation analyses followed by unsupervised hierarchical clustering between leukocyte subpopulations and corresponding stromal composition. **(D)** Box and whisker plot comparing the differential distribution of leukocyte subpopulations in different stromal composition with p-values from Kruskal-Wallis testing with Dunn post-hoc.

Figure 3: Inferred leukocyte subtype frequencies associated with prognostic association in determining progression free survival corresponding to stromal composition. (A) Random forest iterations determine “variable of importance (VIMP)” and minimal depth of the prognostic variables in determining progression free survival. Longer VIMP bars with shorter minimal depth bars indicate a higher effect of the variable. Area shaded in grey depicts the prognostic window for the prognostic variables. **(B)** Multivariate recursive partitioning for discrete-time survival tree for progression free survival depicting

prognostic signatures amalgating two or more markers with median progression free survival varying between 7.95 months to 16.60 months with a relative error of prediction given with 0.08 (X-error -0.02). **(C)** Waterfall plot of each prognostic signature as delineated from the terminal nodes illustrating the relative prognostic index of each signature calculated using Cox multivariate proportional hazards. **(D)** Alluvial plot depicting prediction accuracy of response (predicted m(pfst) per subcohort) in comparison with actual response (actual m(pfst) per subcohort) in the validation cohort. Left side of the alluvial plot depicts predicted response per node and right depict actual response per node of the validation cohort. Blue area connecting left to the right graph represent perfect match while red area represent mismatch in the response. The thickness of the color areas depicts the number of subjects. $P<0.05$ is considered as significant.

Table 1: Demographic, surgery and pathology features of the patients scored for multifaceted stromal composition.

Demographics		Total
Characteristics		
		N=385
Age Median (IQR) years		64 (32-83)
Sex	**Female**	160
	Male	225
WHO Performance score	**0**	128
	1	210
	2	47
Diabetes		**N=368**
	No	291
	IDDM	46
	NIDDM	31
Smoking		**N=345**
	Never	149
	Past	135
	Present	61
Post-Op. CA 19-9 Median (IQR) KU/l		**N=290**
		27 (0-27016)
Surgery to Randomisation Median (IQR) days		49 (4-92)
Surgery		**N=373**
	Whipples resection	193
	Pylorus preserving	147
	Distal pancreatectomy	20
	Total pancreatectomy	13
Extent of resection		**N=366**
	Standard	274
	Radical	53
	Extended Radical	39
Maximum tumor diameter. mm median (IQR)		**N=377**
		30 (3-350)
Differentiation status		**N=378**
	Well	30
	Moderate	246
	Poor	102
Lymph Node Invasion	**Negative**	84
	Positive	301
Resection Margin	**Negative**	215
	Positive	170
Local Invasion		**N=372**
	No	199
	Yes	173
Tumor Stage		**N=380**
	I	26
	II	100
	III	243
	IV	11
CD3		**N=385**
	Low	186
	High	199
CD4		**N=342**
	Low	56
	High	286
CD8		**N=365**
	Low	151
	High	214
CD68		**N=383**
	Low	175
	High	208
CD206		**N=350**
	Low	81
	High	269
Neutrophils		**N=359**
	Low	180
	High	179
Stroma		**N=384**

Demographics		Total
Characteristics		
	Fibrolytic	102
	Inert	96
	Dormant	96
	Fibrogenic	90
Therapeutic Arm		**N=385**
	5FU	190
	Gemcitabine	195

Table 2: Tabular representation of the Kaplan-Meier survival analysis depicting influence of high and low expression of immune infiltrate markers, CD3, CD4, CD8, CD68, CD206 and neutrophils in predicting PFS and OS.

Immune markers	stratification	Progression free survival			Overall survival		
		m(pfst)	χ^2	*p*	m(st)	χ^2	*p*
CD3	Low	11.03 (95%CI: 9.69-12.45)	15.20	**<0.001**	20.13 (95%CI: 16.39-22.60)	9.60	**0.001**
	High	14.32 (95%CI: 12.74-17.28)			25.95 (95%CI: 22.53-29.17)		
CD4	Low	10.87 (95%CI: 9.23-14.19)	4.50	**0.03**	21.94 (95%CI: 14.98-27.40)	2.30	0.12
	High	12.81 (95%CI: 11.72-14.91)			24.34 (95%CI: 20.89-26.44)		
CD8	Low	12.05 (95%CI: 10.11-13.83)	4.30	**0.03**	21.22 (95%CI: 16.26-27.49)	3.30	0.07
	High	13.10 (95%CI: 11.72-15.93)			24.34 (95%CI: 20.63-27.49)		
CD68	Low	11.72 (95%CI: 9.36-13.60)	5.00	**0.02**	20.40 (95%CI: 16.62-24.11)	4.50	0.03
	High	13.30 (95%CI: 111.92-16.39)			25.52 (95%CI: 21.78-28.78)		
CD206	Low	10.28 (95%CI: 8.60-12.74)	7.40	**0.006**	16.91 (95%CI: 13.89-22.24)	11.50	**<0.001**
	High	13.76 (95%CI: 11.99-15.63)			25.95 (95%CI: 22.43-28.78)		
Neutophils	Low	13.60 (95%CI: 11.99-15.34)	0.01	0.87	25.13 (95%CI: 21.22-28.02)	0.50	**0.49**
	High	11.95 (95%CI: 10.54-15.04)			22.04 (95%CI: 16.82-25.69)		

Table 3: Influence of immune infiltration with respect to stromal composition

Immune markers	Stroma type	Stratification	Progression free survival m(pfst) - 95%CI	$\chi 2$	p
CD3	Fibrogenic	Low High	11.26 (6.63-17.80) 20.10 (12.81-24.73)	6.50	**0.01**
	Inert	Low High	12.45 (9.98-15.93) 16.65 (9.79-26.67)	3.30	0.07
	Dormant	Low High	10.64 (8.77-16.06) 14.32 (12.74-17.28)	2.60	1.1
	Fibrolytic	Low High	9.52 (7.58-12.05) 12.38 (8.87-14.32)	4.10	**0.04**
CD4	Fibrogenic	Low High	10.71 (6.30-14.09) 19.08 (12.81-24.73)	7.50	**0.006**
	Inert	Low High	17.64 (7.88-38.80) 12.5 (10.11-16.65)	0.20	0.63
	Dormant	Low High	9.88 (6.17-20.30) 14.34 (9.95-19.12)	3.50	0.06
	Fibrolytic	Low High	11.03 (8.34-13.83) 10.84 (8.87-14.32)	0.01	0.87
CD8	Fibrogenic	Low High	17.80 (6.63-23.35) 13.33 (11.72-20.36)	0.10	0.76
	Inert	Low High	11.63 (8.44-16.65) 16.32 (11.13-29.14)	2.00	0.15
	Dormant	Low High	11.30 (7.81-15.04) 13.14 (9.95-20.30)	1.00	0.31
	Fibrolytic	Low High	11.00 (8.27-13.83) 11.05 (8.41-15.34)	0.80	0.37
CD68	Fibrogenic	Low High	18.79 (7.12-21.97) 14.09 (11.79-21.61)	0.10	0.74
	Inert	Low High	11.07 (9.19-15.40) 17.64 (11.63-26.25)	4.60	**0.03**
	Dormant	Low High	10.94 (7.91-15.63) 13.76 (9.88-20.23)	0.40	0.50
	Fibrolytic	Low High	11.03 (8.27-14.19) 10.56 (7.95-12.74)	0.30	0.57
CD206	Fibrogenic	Low High	11.00 (7.98-17.80) 19.71 (12.81-24.73)	3.60	0.05
	Inert	Low High	15.93 (4.30-22.93) 13.02 (10.11-16.65)	0.10	0.74
	Dormant	Low High	9.59 (6.01-12.41) 15.63 (10.64-22.89)	11.60	**0.0006**
	Fibrolytic	Low High	8.96 (4.66-15.63) 11.17 (8.73-13.83)	0.10	0.80
Neutrophils	Fibrogenic	Low High	19.28 (12.45-23.35) 12.81 (9.49-21.61)	0.60	0.45
	Inert	Low High	14.76 (10.51-20.40) 13.09 (9.16-20.36)	0.99	0.884
	Dormant	Low High	11.92 (8.60-15.63) 13.04 (9.69-22.89)	0.99	0.31
	Fibrolytic	Low High	11.61 (8.27-14.25) 10.18 (7.95-15.34)	0.99	0.84

Table 4: Univariate analysis of progression free survival factors.

Characteristic		Univariate analysis	Multivariate analysis
Age		0.99 (0.98 to 1.01) χ^2=1.29 (P=0.25)	
Sex	Female	1(Referent)	
	Male	0.88 (0.71 to 1.09) χ^2=1.36 (P=0.24)	
Smoking	Never	1(Referent)	
	Past	1.08 (0.84 to 1.38) χ^2=2.67 (P=0.51)	
	Present	1.29 (0.94 to 1.77) χ^2=2.00 (P=0.10)	
Lymph Node Invasion	Negative	1(Referent)	
	Positive	1.95 (1.47 to 2.58) χ^2=21.84 **(P<0.0001)**	
Resection Margin	Negative	1(Referent)	
	Positive	1.59 (1.28 to 1.97) χ^2=18.21 **(P<0.0001)**	
Local Invasion	No	1(Referent)	
	Yes	1.30 (1.05 to 1.61) χ^2=5.91 **(P=0.01)**	
Tumor Stage	I	1(Referent)	
	II	1.56 (0.92 to 2.62) χ^2=13.10 (P=0.09)	
	III	2.08 (1.27 to 3.42) χ^2=3.00 **(P=0.003)**	
	IV	1.31 (0.58 to 2.94) χ^2=0.004 (P=0.51)	
Post-operative CA19.9		1.00 (1.00 to 1.01) χ^2=13.49 **(P=0.0002)**	
Maximum tumor size		1.00 (0.99 to 1.00) χ^2=2.09 (P=0.14)	
Differentiation status	well	1(Referent)	
	moderate	0.91 (0.61 to 1.34) χ^2=1.85 (P=0.63)	
	poor	1.07 (0.70 to 1.63) χ^2=2.00 (P=0.73)	
WHO Performance score	0	1(Referent)	
	1	1.12 (0.88 to 1.42) χ^2=1.02 (P=0.31)	
	2	1.06 (0.75 to 1.53) χ^2=2.00 (P=0.69)	
CD3	Low	1(Referent)	1(Referent)
	High	0.65 (0.52 to 0.80) χ^2=14.96 **(P=0.0001)**	0.69 (0.54 to 0.89) z-stat=-2.79 **(P=0.005)**
CD4	Low	1(Referent)	1(Referent)
	High	0.72 (0.54 to 0.97) χ^2=4.49 **(P=0.03)**	0.78 (0.56 to 1.08) z-stat=-1.46 (P=0.14)
CD8	Low	1(Referent)	1(Referent)
	High	0.78 (0.63 to 0.98) χ^2=4.25 **(P=0.03)**	0.72 (0.55 to 0.95) z-stat=-2.27 **(P=0.02)**
CD68	Low	1(Referent)	1(Referent)
	High	0.78 (0.62 to 0.97) χ^2=4.93 **(P=0.02)**	0.83 (0.64 to 1.08) z-stat=-1.37 (P=0.16)
CD206	Low	1(Referent)	1(Referent)
	High	0.69 (0.52 to 0.90) χ^2=7.36 **(P=0.006)**	0.64 (0.47 to 0.87) z-stat=-2.87 **(P=0.004)**
Neutrophils	Low	1(Referent)	
	High	0.98 (0.78 to 1.22) χ^2=0.03 (P=0.87)	
Stroma	Fibrolytic	1(Referent)	1(Referent)
	Inert	0.76 (0.56 to 1.03) χ^2=7.10 (P=0.08)	0.75 (0.55 to 1.06) z-stat=-1.63 (P=0.10)
	Dormant	0.77 (0.57 to 1.04) χ^2=3.00 (P=0.09)	0.85 (0.61 to 1.19) z-stat=-0.92 (P=0.35)
	Fibrogenic	0.66 (0.48 to 0.90) χ^2=0.06 **(P=0.01)**	0.73 (0.52 to 1.02) z-stat=-1.80 (P=0.07)
Concordance			**0.61 ± 0.01**

Figure 1

A

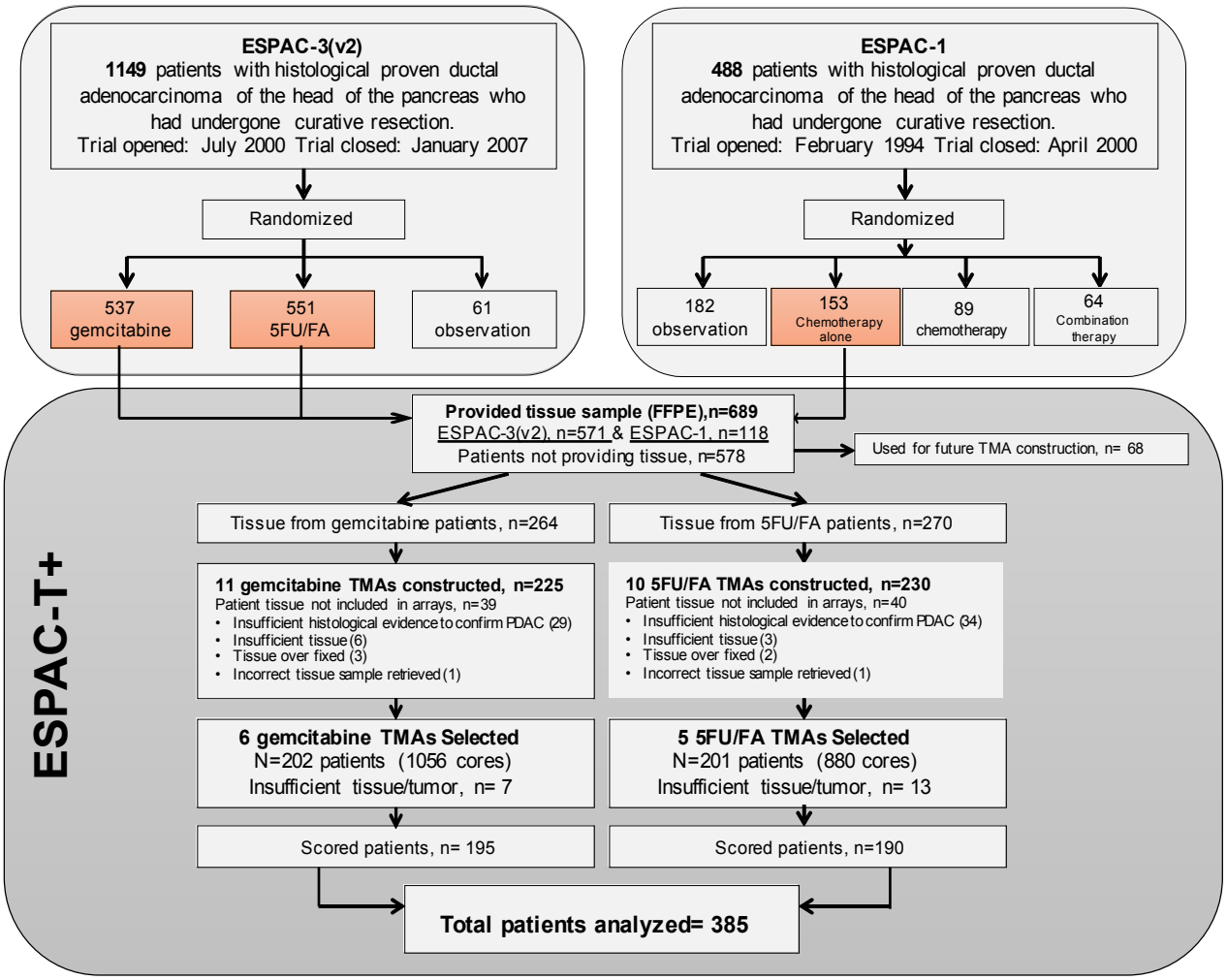
ESPAC-3(v2)
1149 patients with histological proven ductal adenocarcinoma of the head of the pancreas who had undergone curative resection.
Trial opened: July 2000 Trial closed: January 2007
Randomized
537 gemcitabine
551 5FU/FA
61 observation
ESPAC-1
488 patients with histological proven ductal adenocarcinoma of the head of the pancreas who had undergone curative resection.
Trial opened: February 1994 Trial closed: April 2000
Randomized
182 observation
153 Chemotherapy alone
89 chemotherapy
64 Combination therapy
ESPAC-T+
Provided tissue sample (FFPE),n=689
ESPAC-3(v2), n=571 & ESPAC-1, n=118
Patients not providing tissue, n=578
Used for future TMA construction, n= 68
Tissue from gemcitabine patients, n=264
Tissue from 5FU/FA patients, n=270
11 gemcitabine TMAs constructed, n=225
Patient tissue not included in arrays, n=39
Insufficient histological evidence to confirm PDAC (29)
Insufficient tissue (6)
Tissue over fixed (3)
Incorrect tissue sample retrieved (1)
10 5FU/FA TMAs constructed, n=230
Patient tissue not included in arrays, n=40
Insufficient histological evidence to confirm PDAC (34)
Insufficient tissue (3)
Tissue over fixed (2)
Incorrect tissue sample retrieved (1)
6 gemcitabine TMAs Selected
N=202 patients (1056 cores)
Insufficient tissue/tumor, n= 7
5 5FU/FA TMAs Selected
N=201 patients (880 cores)
Insufficient tissue/tumor, n= 13
Scored patients, n= 195
Scored patients, n=190
Total patients analyzed= 385

B

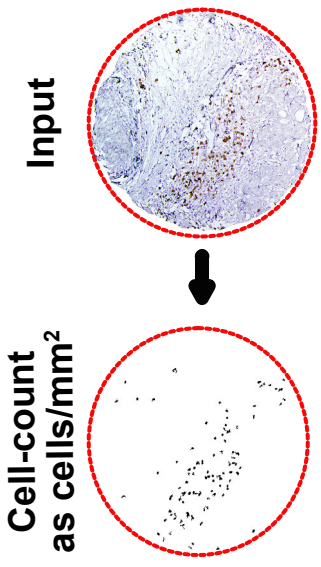
Input
Cell-count as cells/mm²

C

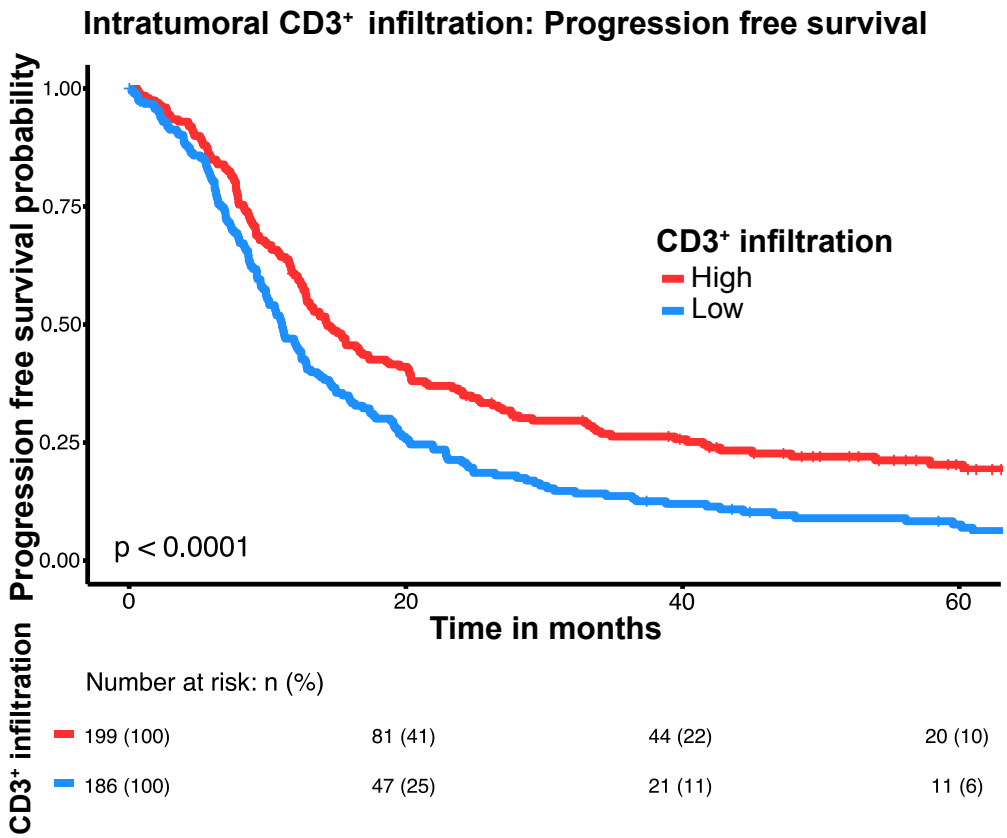
Intratumoral CD3⁺ infiltration: Progression free survival
Progression free survival probability
1.00
0.75
0.50
0.25
0.00
CD3⁺ infiltration
High
Low
p < 0.0001
0
20
40
60
Time in months
Number at risk: n (%)
CD3⁺ infiltration
199 (100)
81 (41)
44 (22)
20 (10)
186 (100)
47 (25)
21 (11)
11 (6)

Figure 2

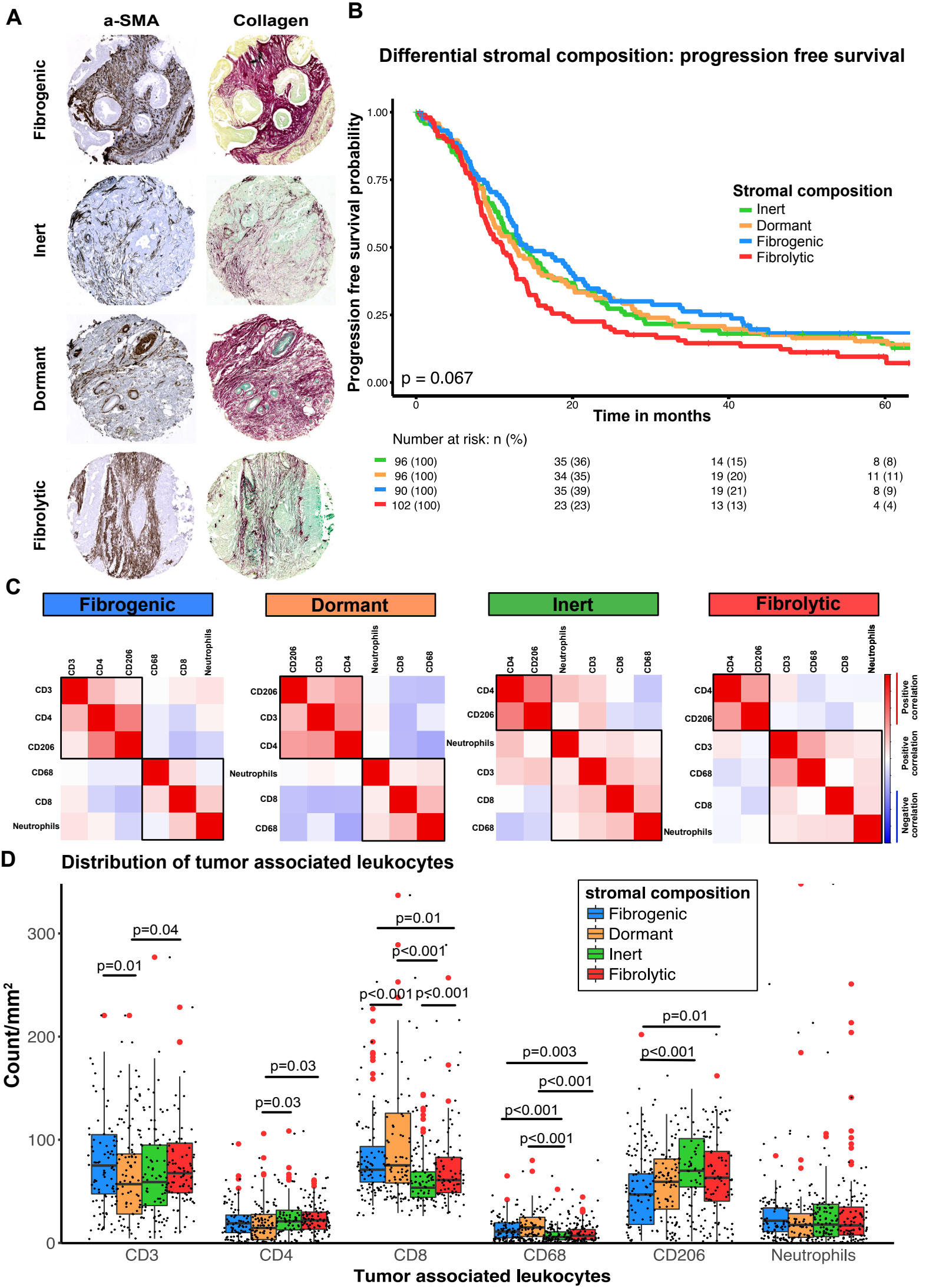
A
a-SMA
Collagen
Fibrogenic
Inert
Dormant
Fibrolytic
B
Differential stromal composition: progression free survival
Progression free survival probability
1.00
0.75
0.50
0.25
0.00
p = 0.067
0
20
40
60
Time in months
Stromal composition
Inert
Dormant
Fibrogenic
Fibrolytic
Number at risk: n (%)
96 (100) 35 (36) 14 (15) 8 (8)
96 (100) 34 (35) 19 (20) 11 (11)
90 (100) 35 (39) 19 (21) 8 (9)
102 (100) 23 (23) 13 (13) 4 (4)
C
Fibrogenic
Dormant
Inert
Fibrolytic
CD3
CD4
CD206
CD68
CD8
Neutrophils
Positive correlation
Positive correlation
Negative correlation
D
Distribution of tumor associated leukocytes
Count/mm²
300
200
100
0
stromal composition
Fibrogenic
Dormant
Inert
Fibrolytic
p=0.04
p=0.01
p=0.03
p=0.03
p=0.01
p<0.001
p<0.001
p<0.001
p=0.003
p<0.001
p<0.001
p<0.001
p=0.01
p<0.001
CD3
CD4
CD8
CD68
CD206
Neutrophils
Tumor associated leukocytes

Figure 3

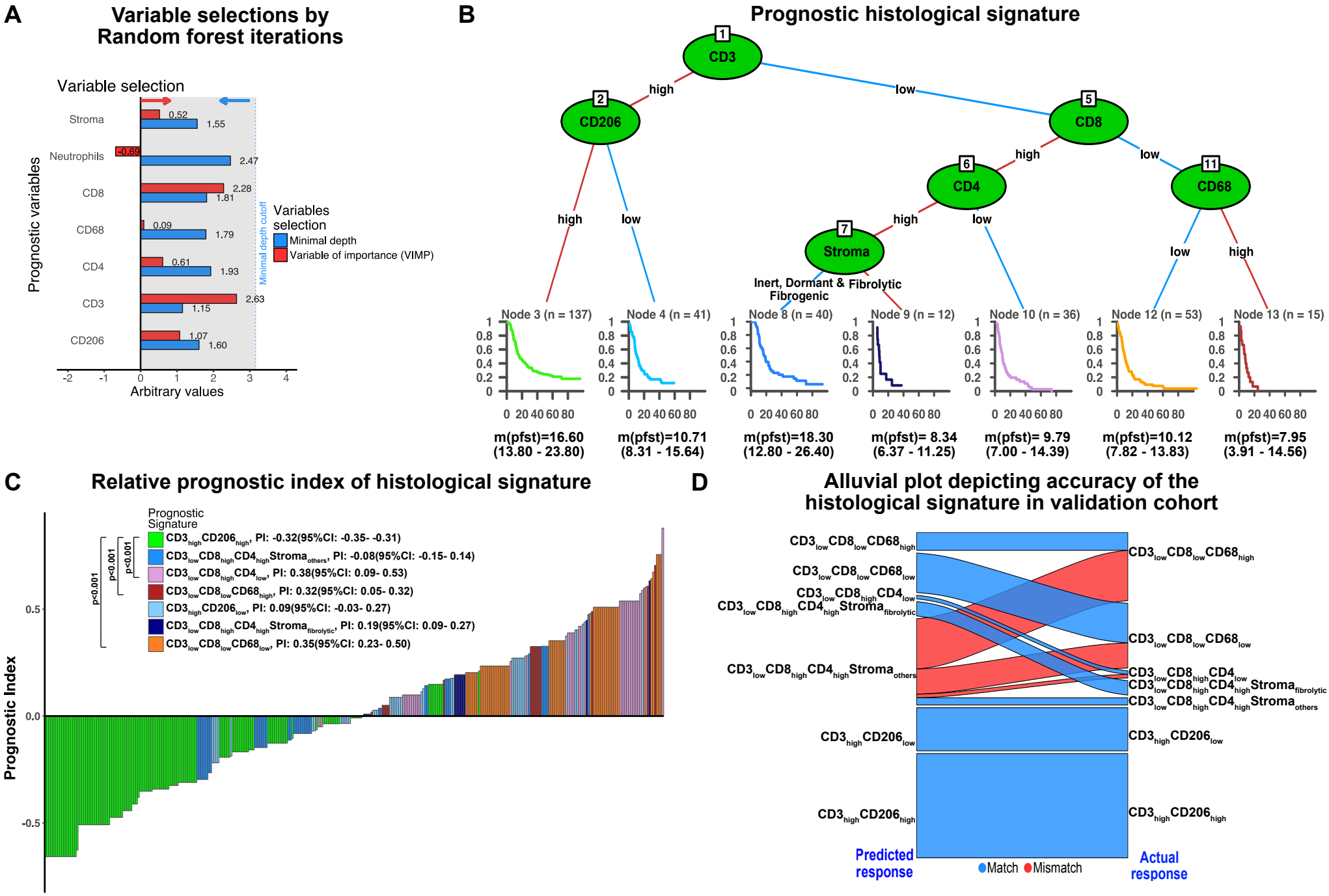
A
Variable selections by Random forest iterations
Variable selection
Stroma
Neutrophils
CD8
CD68
CD4
CD3
CD206
0.52
1.55
-0.69
2.47
2.28
1.81
0.09
1.79
0.61
1.93
2.63
1.15
1.07
1.60
Minimal depth cutoff
Variables selection
Minimal depth
Variable of importance (VIMP)
Prognostic variables
Arbitrary values
B
Prognostic histological signature
CD3
CD206
CD8
CD4
Stroma
CD68
high
low
Inert, Dormant & Fibrogenic
Fibrolytic
Node 3 (n = 137)
Node 4 (n = 41)
Node 8 (n = 40)
Node 9 (n = 12)
Node 10 (n = 36)
Node 12 (n = 53)
Node 13 (n = 15)
m(pfst)=16.60 (13.80 - 23.80)
m(pfst)=10.71 (8.31 - 15.64)
m(pfst)=18.30 (12.80 - 26.40)
m(pfst)= 8.34 (6.37 - 11.25)
m(pfst)= 9.79 (7.00 - 14.39)
m(pfst)=10.12 (7.82 - 13.83)
m(pfst)=7.95 (3.91 - 14.56)
C
Relative prognostic index of histological signature
Prognostic Signature
CD3high CD206high, PI: -0.32(95%CI: -0.35- -0.31)
CD3low CD8high CD4high Stromaothers, PI: -0.08(95%CI: -0.15- 0.14)
CD3low CD8high CD4low, PI: 0.38(95%CI: 0.09- 0.53)
CD3low CD8low CD68high, PI: 0.32(95%CI: 0.05- 0.32)
CD3high CD206low, PI: 0.09(95%CI: -0.03- 0.27)
CD3low CD8high CD4high Stromafibrolytic, PI: 0.19(95%CI: 0.09- 0.27)
CD3low CD8low CD68low, PI: 0.35(95%CI: 0.23- 0.50)
p<0.001
Prognostic Index
D
Alluvial plot depicting accuracy of the histological signature in validation cohort
CD3low CD8low CD68high
CD3low CD8low CD68low
CD3low CD8high CD4low
CD3low CD8high CD4high Stromafibrolytic
CD3low CD8high CD4high Stromaothers
CD3high CD206low
CD3high CD206high
Predicted response
Actual response
Match
Mismatch

WHAT YOU NEED TO KNOW

Background and context

Pancreatic ductal adenocarcinoma (PDAC) is accompanied by a high desmoplastic reaction and an immunosuppressive microenvironment. Differential stromal composition categorized by activated myofibroblasts and collagen expression is an independent prognostic marker in predicting outcome of PDAC patients. Though immunosuppressive PDAC presents with the inherent capacity to activate T-cell-mediated anti-tumour response, the exact nature of the complex interaction between desmoplastic stroma and leukocytes infiltration and its impact on PDAC patient prognosis remains unknown.

New Findings

This study demonstrates the clinical impact of leukocyte subpopulations and differential stromal compositions forming PDAC microenvironment. It provides a robust and independently validated leukocyte and stromal composition-based prognostic signature that correlates to progression free survival in patients with PDAC.

Limitations

This study has limitation including the retrospective design and the inability to study the predictive potential of the prognostic histological signature in correlation with a treatment response.

Impact

Tissue-typing the microenvironment of PDAC and using it as a prognostic signature may aid in stratifying the patients for immunomodulatory therapy as a step towards precision medicine.

LAY SUMMARY

The prognosis of pancreatic cancer is poor. To understand the influence of tissue composition (tumor cells, immune cells, stroma cells) of pancreatic cancer we developed a histological signature associated with a poorer outcome. Furthermore, we propose that the immune infiltrate determines tissue composition and not stromal cells.

Immune Cell and Stromal Signature Associated with Progression-free Survival of Patients with Resected Pancreatic Ductal Adenocarcinoma

U. M. Mahajan[1,2], E. Langhoff[2], E. Goni[1], E. Costello[3], W. Greenhalf[3], C. Halloran[3], S. Ormanns[4], S. Kruger[5], S. Böck[5], S. Ribback[6], G. Beyer[1,2], F. Dombroswki[6], F.-U. Weiss[2], J. P. Neoptolemos[3,7], J. Werner[8], J. G. D'Haese[8], A. Bazhin[8], J. Peterhansl[1], S. Pichlmeier[1], M. W. Büchler[7], J. Kleeff[9], P. Ganeh[3], M. Sendler[2], D. H. Palmer[3,10], T. Kohlmann[11], R. Rad[12], I. Regel[1], M.M. Lerch[2], J. Mayerle[1,2]

Supplementary materials and methods

Manufacturing of tissue microarrays (TMAs)

All TMAs were manufactured using standard operating procedures conducted to Good Laboratory Practice. Cores were taken from tumor regions identified by an experienced pancreatic pathologist using hematoxylin-eosin stained sections as reference. TMAs from the training cohort contained cores from patients of the chemotherapeutic arm of the ESPAC-1 trial and from patients of the ESPAC-3 trial randomized to either 5FU/folinic acid or to gemcitabine. TMAs were prepared with two cores from each block, with four to eight cores arrayed for each patient. For all arrays control cores, comprising 3 cores each of colon, kidney, liver, normal pancreas and chronic pancreatitis, were arranged in a fence around the test samples as described previously[1]. Although fixation protocols for formalin-fixed paraffin embedded tissue blocks varied across centers, they were standardized for each center with no evidence for the centre- or country-specific bias in immunostaining. TMAs used for the validation cohort consist of randomly selected PDAC cases resected between 2011 and 2017 at the Department of General, Visceral and Transplantation Surgery, University Hospital, LMU Munich, Germany. TMA construction was reported previously[2].

Single and multiplex immunostaining

Immunostaining of the TMAs from the training cohort was performed on 2µm sections for α-SMA (mouse anti-human α-SMA, Dako clone 1A4, 1:800), CD3 (mouse anti-human CD3, Dako clone F7.2.38, 1:100), CD4 (rabbit anti-human CD4, Cell Marque clone SP35, 1:100), CD8 (mouse anti-human CD8, Dako clone C8/144B, 1:100), CD68 (mouse anti-human

CD68, Dako clone PS-M1, 1:100) and CD206 (mouse anti-human CD206, R&D systems clone 685645, 1:40) as described earlier[3]. Briefly, after deparaffinization and rehydration of sections, antigens were retrieved by heat treatment in citrate buffer pH 6.0 (Dako Deutschland GmbH, Hamburg, Germany). After peroxidase block, slides were incubated with the primary antibodies at 4 °C overnight. Detection was performed after specific secondary antibody incubation using DAB complex conjugation reagent (vector Laboratories Ltd., Peterborough, UK). Negative controls were incubated with buffer alone, in place of primary antibody.

Chloracetate esterase staining for detection of neutrophils infiltration was performed using Naphthol AS-D chloroacetate (specific esterase) kit (Sigma-Aldrich) according manufacturer's instruction. Collagen staining was performed using Picrosirius red - Fast green staining solution (0.1% direct Red 80 and 0.1% Fast green FCF in aqueous picric acid). Briefly, after deparaffinization, tissue microarrays sections were incubated in Picrosirius red - Fast green staining solution for 60 minutes at room temperature, followed by dehydration and fixation.

For the validation cohort, multiplex immunostaining on TMAs was performed as described previously with some modifications[4]. The flow of multiplex immunostaining is delignated in **suppl fig. 11**, using one slide for multiple staining. Briefly, after deparaffinization, slides where stained with haematoxylin followed by 2 min incubation in 0.5 % ammonia solution. Slides were mounted using aqueous mounting media. Whole slides were scanned in Sysmex Panoramic MIDI II slide scanner (Sysmex Deutschland GmbH, Bornbarch, Germany). After scanning, coverslips were removed by immersing slide in PBS for 5 min. Slides were then subjected to antigen retrieval (Dako Antigen retrieval buffer, Dako Deutschland GmbH, Hamburg, Germany), blocking with 1% Aurion BSA-c™ (Aurion, Wageningen, The Netherlands) in PBS and first primary antibody incubation as described previously[5]. Next day, following secondary antibody incubation and washing, staining was performed using ImmPACT AMEC red (Vector Labs, Burlingame, USA) substrate. Slides were then mounted using aqueous mounting media and scanned in Sysmex Panoramic MIDI II slide scanner.

After removing coverslips, AMEC red destaining of the slides was performed as described[6] by dipping slides in 70 % ethanol for 2 min, followed by 95 % ethanol and 70 % ethanol and PBS for 2 min each. Next, antibody stripping was performed as described[7]. Here, slides were incubated with preheated solution of 25 mM Glycine, 1 % SDS, pH 2.0 for 30 min at 50 °C. After cooling, slides were proceeded for next primary antibody incubation. The flow was repeated for multiple antibodies used in following consecutive order: CD3, CD4, CD8, CD45, CD68, CD206, MPO and α-SMA (applied with the same dilutions as noted above). Lastly, the TMA slides were stained for Picrosirius red - Fast green as described above.

Image cytometry

All multiplex slides scans were processed as shown in **suppl fig.11.** Each core for each single staining (immune cell marker, α-SMA, collagen and hematoxylin; in total 10) was selected and matched for slide co-ordinates. All images were saved as TIFF files. Next, all the images were adjusted towards an intensity threshold and compensated using an in-house algorithm for NIH ImageJ software. For each staining, the images were sorted according their core ID and each of the 10 images per core were aligned pixel to pixel using in-house algorithm developed for NIH ImageJ software. Following alignment, images were subjected to colocalization analysis using algorithm developed for Cell Profiler software and described by Tsujikawa et al[4] with some modifications. The output files were then processed using FCS express 6 (DeNovo software, San Jose, USA) for image cytometric analysis similar to FACS analysis with appropriate gating. For all the markers, separate pseudo-color was assigned and colocalization were observed by merging all images per IDs. NIH ImageJ software algorithms can be provided upon request.

Primary cell isolation from tumor tissue

Isolation of intra-tumoral cells (ITCs) from freshly resected PDAC tumors (n=10) were performed as described previously[8]. Briefly, following resection, tumor samples were transferred in PBS including 1% Soybean trypsin inhibitor (ThermoFischer Scientific, Waltham, USA). Tumor samples were afterwards digested in 2 mg/ml Collagenase IV

(Serva, Heidelburg, Germany), 1 mg/ml hyaluronidase (Serva, Heidelburg, Germany), 1 % Soybean trypsin inhibitor and 0.1 mg/ml DNase I (ThermoFischer Scientific) solution. For an appropriate digestion, tumor tissue was minced into small pieces and incubated for 45 min at 37°C at 60 rpm in a water bath. Following incubation, suspension was filter through a 100 µm nylon mesh and centrifuged for 10 min at 400g at 4ºC. The obtained cell pellet was resuspended in PBS and $1x10^6$ cells were cryopreserved in 1 ml of freezing media (10% DMSO, 90 % FCS) at -150°C for flow cytometry analysis. $5x10^6$ cells were used for cytospins and cytoblock preparation, respectively.

Cytoblock and Cytospin slide preparation

After ITC isolation, cells were fixed in 4% buffered-PFA and processed in the Department of Pathology, University Hospital, LMU Munich, Germany for cytoblock preparation. Cytospins were prepared by pipetting 120µl (approx. $5x10^5$ cells) of the cell suspension in a funnel using Cytospin 4 (Thermo Scientific, Waltham, USA) and centrifuged at 800 rpm for 10 min and stained as described in Material and Methods section.

Peripheral blood derived monocytes cell (PBMC) isolation

PBMCs from 5 ml of intraoperative blood were isolated as described previously[9] using Ficoll gradient. $1x10^6$ cells were cryopreserved in 1 ml of freezing media (10% DMSO, 90% FCS) at -150°C for flow cytometry analysis.

Flow cytometry

Flow cytometry analysis of ITCs and PBMCs was performed as described previously[8,10]. Isolated ITCs and PBMCs were resuspended and washed with FACS buffer (PBS, 0.5% BSA, 2mM EDTA) at 700g for 5 min and subsequently incubated with 2 ml F_cR receptor blocking solution (Human BD Fc Block™, BD Biosciences, Heidelberg, Germany) for 15 min at 4 °C. After dilution to $2.5x10^5$ cells/ml and two more washing steps, leukocytes were labelled using the following fluorescence labelled anti-human antibodies: CD45 (BD Horizon™ BV650), CD3 (BD PerCP-Cy5.5), CD4 (BD Horizon™ BUV395), CD8 (BD APC-Cy7), CD68 (BD BV421) and CD206 (BD Pharmingen™ PE, all from BD Biosciences,

Heidelberg, Germany). After adding 3 µl of antibody solution, tubes were incubated at 4 °C for 30 min in the dark. Unbound antibodies were washed away at 700g for 5 min and cells were stored in 300µl FACS buffer at 4°C until analysis. Cells were analyzed using BD LSRFortessa (BD Biosciences, Heidelberg, Germany) and FCS express 6 (DeNovo software, San Jose, USA).

Addition notes

All the analysis R scripts will be provided on request**.**

References:

1. Greenhalf W, Ghaneh P, Neoptolemos JP, et al. Pancreatic Cancer hENT1 Expression and Survival From Gemcitabine in Patients From the ESPAC-3 Trial. JNCI J Natl Cancer Inst 2014;106:djt347–djt347.

2. Ormanns S, Assmann G, Reu S, et al. ALK expression is absent in pancreatic ductal adenocarcinoma. J Cancer Res Clin Oncol 2014;140:1625–1628.

3. Mahajan UM, Teller S, Sendler M, et al. Tumour-specific delivery of siRNA-coupled superparamagnetic iron oxide nanoparticles, targeted against PLK1, stops progression of pancreatic cancer. Gut 2016.

4. Tsujikawa T, Kumar S, Borkar RN, et al. Quantitative Multiplex Immunohistochemistry Reveals Myeloid-Inflamed Tumor-Immune Complexity Associated with Poor Prognosis. Cell Rep 2017;19:203–217.

5. Mahajan UM, Teller S, Sendler M, et al. Tumour-specific delivery of siRNA-coupled superparamagnetic iron oxide nanoparticles, targeted against PLK1, stops progression of pancreatic cancer. Gut 2016.

6. Glass G, Papin JA, Mandell JW. Simple: A Sequential Immunoperoxidase Labeling and Erasing Method. J Histochem Cytochem 2009;57:899–905.

7. Pirici D, Mogoanta L, Kumar-Singh S, et al. Antibody Elution Method for Multiple Immunohistochemistry on Primary Antibodies Raised in the Same Species and of the Same Subtype. J Histochem Cytochem 2009;57:567–575.

8. Gunderson AJ, Kaneda MM, Tsujikawa T, et al. Bruton Tyrosine Kinase-Dependent Immune Cell Cross-talk Drives Pancreas Cancer. Cancer Discov 2016;6:270–285.

9. Grievink HW, Luisman T, Kluft C, et al. Comparison of Three Isolation Techniques for Human Peripheral Blood Mononuclear Cells: Cell Recovery and Viability, Population Composition, and Cell Functionality. Biopreservation Biobanking 2016;14:410–415.

10. Albertsmeier M, Prix NJ, Winter H, et al. Monocyte-Dependent Suppression of T-Cell Function in Postoperative Patients and Abdominal Sepsis: SHOCK 2017;48:651–656.

Supplementary Table S1: Cut-off for low/high expression determined by cut-off finder

Sr. No	Marker	Low expression	High expression
1	α-SMA*	≤ 10.41	> 10.41
2	Collagen§	≤ 0.93	> 0.93
3	CD3†	≤ 63.25	> 63.25
4	CD4†	≤ 5.5	> 5.5
5	CD8†	≤ 60.75	> 60.75
6	CD68†	≤ 8.34	> 8.34
7	CD206†	≤ 30.25	> 30.25
8	CAE (Neutrophils) †	≤ 18.25	> 18.25

* H-score for intensity score and % stained area
§ H-score calculated based on intensity score and ratio of % stained area of Picrosirius red (Collagen) and Fast Green (all tissues)
† Median count of immune infiltrate per unit mm^3.

Supplementary Table 2: Relationship between Immune markers and patient or tumour characteristics.

Characteristics		CD3				
		Low CD3	High CD3	Total	*P Value*	Low CD4
WHO Performance Scale	0	53	75	128 (33.2%)	*0.051*	12
	1	104	106	210 (54.5%)		33
	2	29	18	47 (12.2%)		11
Maxium Tumour Diameter	<30mm	91	129	220 (60.8%)	*0.001*	31
	≥30mm	84	58	*142 (39.2%)*		20
Gender	Female	83	77	160 (41.6%)	*0.282*	28
	Male	103	122	225 (58.4%)		28
Chemotherapy	5FU	83	107	190 (49.4%)	*0.091*	48
	GEM	103	92	*195 (50.6%)*		8
Tumour Grade	Well	15	15	30 (7.9%)	*0.525*	2
	Moderate	114	132	246 (65.1%)		32
	Poor	54	48	102 (27.0%)		19
Tumour Stage	1	13	13	26 (6.8%)	*0.681*	5
	2	45	55	100 (26.3%)		13
	3	118	125	243 (63.9%)		36
	4	7	4	11 (2.9%)		1
Lymph Node Status	Negative	38	46	84 (21.8%)	*0.606*	9
	Positive	148	153	301 (78.2%)		47
Resection Margin	Negative	100	115	215 (55.8%)	*0.489*	29
	Positive	86	84	170 (44.2%)		27
Diabetes	No	142	149	291 (79.1%)	*0.830*	44
	IDDM	24	22	46 (12.5%)		9
	NIDDM	14	17	31 (8.4%)		2
Smoke	Never	74	75	149 (43.2%)	*0.442*	26
	Past	62	73	135 (39.1%)		21
	Present	34	27	61 (17.7%)		7
Local Invasion	NO	93	106	199 (53.5%)	*0.422*	27
	YES	89	84	173 (46.5%)		29
Age(Years)	<64	91	106	197 (51.2%)	*0.454*	30
	≥64	95	93	188 (48.8%)		26
Post Op CA19-9 (Units)	<27	69	71	140 (50.4%)	*0.718*	28
	≥27	72	66	138 (49.6%)		20
Surgery to Randomisation (Days)	<49	94	103	197 (51.2%)	*0.891*	28
	≥49	92	96	188 (48.8%)		28
CD3	Low					43
	High					13
CD4	Low	43	13	56 (16.3%)	*<0.0001*	
	High	118	169	287 (83.7%)		
CD8	Low	71	77	148 (41.1%)	*0.826*	10
	High	98	114	212 (58.9%)		46
CD68	Low	97	77	174 (45.5%)	*0.009*	11
	High	87	121	208 (54.5%)		45
CD206	Low	38	43	81 (23.3%)	*0.958*	27
	High	124	143	267 (76.7%)		28
Neutrophils	Low	87	90	177 (50.0%)	*0.670*	26
	High	82	95	177 (50.0%)		30
Stroma	Fibrolytic	43	57	100 (26.3%)	*0.046*	9
	Inert	52	43	95 (24.9%)		7
	Dormant	54	43	97 (25.4%)		25
	Fibrogenic	35	55	90 (23.6%)		15

CD4			CD8				
High CD4	**Total**	***P Value***	**Low CD8**	**High CD8**	**Total**	***P Value***	**Low CD68**
106	118 (34.5%)	*0.015*	53	73	126 (34.5%)	*0.607*	57
154	187 (54.7%)		84	114	198 (54.2%)		98
26	37 (10.8%)		14	27	41 (11.2%)		20
164	195 (60.7%)	*0.880*	79	130	209 (60.8%)	*0.166*	96
106	*126 (39.3%)*		62	73	*135 (39.2%)*		69
116	144 (42.1%)	*0.246*	59	93	152 (41.6%)	*0.466*	72
170	198 (57.9%)		92	121	213 (58.4%)		103
119	167 (48.8%)	*<0.0001*	26	157	183 (50.1%)	*<0.0001*	49
167	*175 (51.2%)*		125	57	*182 (49.9%)*		126
22	24 (7.2%)	*0.152*	9	16	25 (7.0%)	*0.661*	18
192	224 (66.9%)		100	134	234 (65.4%)		110
68	87 (26.0%)		38	61	99 (27.7%)		44
16	21 (6.2%)	*0.741*	8	16	24 (6.6%)	*0.243*	9
73	86 (25.4%)		30	57	87 (24.1%)		41
185	221 (65.4%)		108	132	240 (66.5%)		115
9	10 (3.0%)		3	7	10 (2.8%)		6
62	71 (20.8%)	*0.444*	27	48	75 (20.5%)	*0.354*	32
224	271 (79.2%)		124	166	290 (79.5%)		143
161	190 (55.6%)	*0.636*	88	115	203 (55.6%)	*0.252*	99
125	152 (44.4%)		63	99	162 (44.4%)		76
216	260 (78.5%)	*0.390*	113	165	278 (79.0%)	*0.584*	130
36	45 (13.6%)		22	24	46 (13.1%)		23
24	26 (7.9%)		13	15	28 (8.0%)		13
107	133 (42.8%)	*0.552*	63	80	143 (43.2%)	*0.108*	64
103	124 (39.9%)		58	72	130 (39.3%)		64
47	54 (17.4%)		17	41	58 (17.5%)		26
154	181 (53.9%)	*0.434*	73	122	195 (54.6%)	*0.113*	94
126	155 (46.1%)		75	87	162 (45.4%)		76
152	182 (53.2%)	*0.930*	85	104	189 (51.8%)	*0.180*	92
134	160 (46.8%)		66	110	176 (48.2%)		83
97	125 (50.0%)	*0.261*	61	71	132 (49.8%)	*0.121*	61
105	125 (50.0%)		48	85	133 (50.2%)		63
146	174 (50.9%)	*0.998*	76	112	188 (51.5%)	*0.786*	88
140	168 (49.1%)		75	102	177 (48.5%)		87
118	161 (46.9%)	*<0.0001*	71	98	169 (46.9%)	*0.826*	97
169	182 (53.1%)		77	114	191 (53.1%)		77
			10	46	56 (16.5%)	*0.000*	11
			131	153	284 (83.5%)		150
131	141 (41.5%)	*0.000*					86
153	199 (58.5%)						78
150	161 (46.9%)	*<0.0001*	86	78	164 (45.8%)	*0.000*	
137	182 (53.1%)		61	133	194 (54.2%)		
54	81 (23.8%)	*<0.0001*	12	68	80 (23.2%)	*<0.0001*	30
232	260 (76.2%)		131	134	265 (76.8%)		133
141	167 (49.1%)	*0.769*	86	84	170 (49.3%)	*0.000*	87
143	173 (50.9%)		55	120	175 (50.7%)		78
83	92 (26.5%)	*0.001*	46	50	96 (26.8%)	*<0.0001*	53
72	79 (23.1%)		51	35	86 (24.0%)		58
61	86 (25.1%)		26	64	90 (25.1%)		29
70	85 (24.8%)		23	63	86 (24.0%)		34

CD68			CD206				
High CD68	**Total**	***P Value***	**Low CD206**	**High CD206**	**Total**	***P Value***	**Low neutrophils**
71	128 (33.4%)	*0.839*	28	94	122 (34.9%)	*0.741*	56
111	209 (54.6%)		46	144	190 (54.3%)		101
26	46 (12.0%)		7	31	38 (10.9%)		23
123	219 (60.7%)	*0.437*	48	153	201 (61.1%)	*0.967*	105
73	*142 (39.3%)*		30	98	*128 (38.9%)*		66
88	160 (41.8%)	*0.900*	38	108	146 (41.7%)	*0.340*	74
120	223 (58.2%)		43	161	204 (58.3%)		106
138	187 (48.8%)	*<0.0001*	80	88	168 (48.0%)	*<0.0001*	66
70	*196 (51.2%)*		1	181	*182 (52.0%)*		114
11	29 (7.7%)	*0.182*	5	20	25 (7.3%)	*0.839*	17
136	246 (65.4%)		50	175	225 (65.6%)		117
57	101 (26.9%)		23	70	93 (27.1%)		42
16	25 (6.6%)	*0.479*	5	17	22 (6.4%)	*0.537*	9
59	100 (26.5%)		15	71	86 (24.9%)		39
127	242 (64.0%)		57	170	227 (65.6%)		126
5	11 (2.9%)		3	8	11 (3.2%)		3
51	83 (21.7%)	*0.177*	14	59	73 (20.9%)	*0.455*	34
157	300 (78.3%)		67	210	277 (79.1%)		146
114	213 (55.6%)	*0.808*	39	155	194 (55.4%)	*0.169*	105
94	170 (44.4%)		42	114	156 (44.6%)		75
161	291 (79.3%)	*0.778*	68	196	264 (78.6%)	*0.064*	140
23	46 (12.5%)		8	37	45 (13.4%)		24
17	30 (8.2%)		2	25	27 (8.0%)		10
84	148 (42.9%)	*0.764*	37	97	134 (42.4%)	*0.144*	68
72	136 (39.4%)		23	103	126 (39.9%)		70
35	61 (17.7%)		16	40	56 (17.7%)		28
105	199 (53.6%)	*0.629*	48	137	185 (54.3%)	*0.364*	82
96	172 (46.4%)		33	123	156 (45.7%)		95
106	198 (51.7%)	*0.833*	43	142	185 (52.9%)	*0.936*	85
102	185 (48.3%)		38	127	165 (47.1%)		95
80	141 (50.7%)	*0.737*	30	95	125 (49.2%)	*0.669*	63
74	137 (49.3%)		35	94	129 (50.8%)		63
108	196 (51.2%)	*0.828*	43	136	179 (51.1%)	*0.785*	89
100	187 (48.8%)		38	133	171 (48.9%)		91
87	184 (48.2%)	*0.009*	38	124	162 (46.6%)	*0.958*	87
121	198 (51.8%)		43	143	186 (53.4%)		90
45	56 (16.3%)	*<0.0001*	27	28	55 (16.1%)	*<0.0001*	26
137	287 (83.7%)		54	232	286 (83.9%)		141
61	147 (41.1%)	*0.000*	12	131	143 (41.4%)	*<0.0001*	86
133	211 (58.9%)		68	134	202 (58.6%)		84
			30	133	163 (46.8%)	*0.059*	87
			51	134	185 (53.2%)		90
51	81 (23.3%)	*0.059*					21
134	267 (76.7%)						148
90	177 (50.0%)	*0.394*	21	148	169 (49.3%)	*<0.0001*	
99	177 (50.0%)		59	115	174 (50.7%)		
46	99 (26.0%)	*<0.0001*	21	71	92 (26.4%)	*0.118*	50
36	94 (24.7%)		13	68	81 (23.2%)		40
68	97 (25.5%)		20	70	90 (25.8%)		49
56	90 (23.6%)		27	58	85 (24.4%)		37

Neutrophils		
High Neutrophils	**Total**	***P Value***
65	121 (33.7%)	*0.569*
94	195 (54.3%)	
20	43 (12.0%)	
103	208 (61.7%)	*0.992*
63	*129 (38.3%)*	
75	149 (41.5%)	*0.965*
104	210 (58.5%)	
109	175 (48.7%)	*<0.0001*
70	*184 (51.3%)*	
11	28 (8.0%)	*0.334*
114	231 (65.6%)	
51	93 (26.4%)	
12	21 (5.9%)	*0.194*
48	87 (24.5%)	
110	236 (66.5%)	
8	11 (3.1%)	
38	72 (20.1%)	*0.673*
141	287 (79.9%)	
95	200 (55.7%)	*0.370*
84	159 (44.3%)	
132	272 (78.6%)	*0.200*
21	45 (13.0%)	
19	29 (8.4%)	
71	139 (42.6%)	*0.690*
60	130 (39.9%)	
29	57 (17.5%)	
107	189 (53.8%)	*0.006*
67	162 (46.2%)	
103	188 (52.4%)	*0.064*
76	171 (47.6%)	
67	130 (49.8%)	*0.949*
68	131 (50.2%)	
94	183 (51.0%)	*0.634*
85	176 (49.0%)	
82	169 (47.7%)	*0.670*
95	185 (52.3%)	
30	56 (16.5%)	*0.769*
143	284 (83.5%)	
55	141 (40.9%)	*0.000*
120	204 (59.1%)	
78	165 (46.6%)	*0.394*
99	189 (53.4%)	
59	80 (23.3%)	*<0.0001*
115	263 (76.7%)	

46	96 (27.1%)	*0.604*
40	80 (22.6%)	
44	93 (26.2%)	
48	85 (24.0%)	

Supplementary Table S3: Univariate analysis of overall survival factors (ESPAC-Tplus cohort)

Characteristic		Univariate analysis	Multivariate analysis
Age		0.99 (0.98 to 1.01) χ^2=0.50 (P=0.48)	
Sex	Female	1(Referent)	
	Male	0.93 (0.75 to 1.16) χ^2=0.32 (P=0.36)	
Smoking	Never	1(Referent)	
	Past	1.17 (0.91 to 1.51) χ^2=3.87 (P=0.20)	
	Present	1.35 (0.98 to 1.85) χ^2=2.00 (P=0.05)	
Lymph Node Invasion	Negative	1(Referent)	
	Positive	2.00 (1.49 to 2.70) χ^2=21.34 **(P<0.0001)**	
Resection Margin	Negative	1(Referent)	
	Positive	1.54 (1.24 to 1.92) χ^2=15.16 **(P<0.0001)**	
Local Invasion	No	1(Referent)	
	Yes	1.29 (1.03 to 1.61) χ^2=5.29 **(P=0.02)**	
Tumor Stage	I	1(Referent)	
	II	1.63 (0.92 to 2.89) χ^2=14.68 (P=0.08)	
	III	2.30 (1.33 to 3.95) χ^2=3.00 **(P=0.002)**	
	IV	1.52 (0.63 to 3.64) χ^2=0.002 (P=0.34)	
Postoperative CA19.9		1.00 (1.00 to 1.01) χ^2=22.39 **(P<0.0001)**	
Maximum tumor size		1.00 (0.99 to 1.00) χ^2=2.70 (P=0.10)	
Differentiation status	well	1(Referent)	
	moderate	1.04 (0.69 to 1.56) χ^2=2.65 (P=0.84)	
	poor	1.27 (0.81 to 1.97) χ^2=2.00 (P=0.28)	
WHO Performance score	0	1(Referent)	
	1	1.29 (1.01 to 1.65) χ^2=4.44 **(P=0.02)**	
	2	1.18 (0.81 to 1.72) χ^2=2.00 (P=0.36)	
CD3	Low	1(Referent)	1(Referent)
	High	0.70 (0.56 to 0.87) χ^2=9.51 **(P=0.002)**	0.71 (0.56 to 0.92) z-stat=-2.61 **(P=0.008)**
CD4	Low	1(Referent)	
	High	0.79 (0.58 to 1.07) χ^2=2.30 (P=0.12)	
CD8	Low	1(Referent)	1(Referent)
	High	0.80 (0.64 to 1.01) χ^2=3.27 (P=0.07)	0.72 (0.54 to 0.96) z-stat=-2.24 **(P=0.02)**
CD68	Low	1(Referent)	1(Referent)
	High	0.78 (0.62 to 0.98) χ^2=4.49 **(P=0.03)**	0.85 (0.66 to 1.11) z-stat=-1.16 (P=0.24)
CD206	Low	1(Referent)	1(Referent)
	High	0.62 (0.47 to 0.82) χ^2=11.31 **(P=0.0007)**	0.55 (0.40 to 0.75) z-stat=-3.74 **(P=0.0001)**
Neutrophils	Low	1(Referent)	1(Referent)
	High	1.08 (0.86 to 1.36) χ^2=0.47 (P=0.49)	1.01 (0.78 to 1.30) z-stat=0.08 (P=0.93)
Stroma	Fibrolytic	1(Referent)	1(Referent)
	Inert	0.86 (0.63 to 1.18) χ^2=3.58 (P=0.36)	0.85 (0.60 to 1.20) z-stat=-0.91(P=0.36)
	Dormant	0.79 (0.58 to 1.08) χ^2=3.00 (P=0.14)	0.97 (0.69 to 1.37) z-stat=-0.13 (P=0.89)
	Fibrogenic	0.75 (0.55 to 1.03) χ^2=0.31 (P=0.08)	0.87 (0.62 to 1.23) z-stat=-0.75 (P=0.45)
Concordance			***0.60 ± 0.01***

Supplementary Table S4: LIFETEST procedure between survival factors stratified according to stromal composition for immune infiltrates (ESPAC-Tplus cohort)

		high_ dormant		high_ fibrogenic		high_ fibrolytic		high_ inert		low_ dormant		low_ fibrognic		low_ fibrolytic	
		PFS	***OS***	***PFS***	***OS***	***PFS***	***OS***	***PFS***	***OS***	***PFS***	***OS***	***PFS***	***OS***	***PFS***	***OS***
CD3	high_fibrogenic	0.74	0.79												
	high_fibrolytic	0.46	0.79	0.31	0.65										
	high_inert	0.74	0.83	0.56	0.69	0.74	0.96								
	low_dormant	0.25	0.65	0.11	0.48	0.74	0.79	0.53	0.79						
	low_fibrogenic	0.36	0.48	0.21	0.35	0.78	0.65	0.56	0.65	0.88	0.79				
	low_fibrolytic	0.04	0.35	0.01	0.21	0.15	0.48	0.11	0.48	0.31	0.65	0.34	0.88		
	low_inert	0.21	0.51	0.10	0.35	0.59	0.65	0.34	0.65	0.88	0.83	0.74	0.89	0.34	0.79
CD4	high_fibrogenic	0.64	0.90												
	high_fibrolytic	0.21	0.67	0.11	0.66										
	high_inert	0.48	0.70	0.19	0.66	0.73	0.99								
	low_dormant	0.24	0.71	0.12	0.66	0.83	0.90	0.64	0.90						
	low_fibrogenic	0.19	0.51	0.11	0.51	0.64	0.66	0.43	0.70	0.73	0.90				
	low_fibrolytic	0.48	0.66	0.33	0.66	0.83	0.90	0.73	0.90	0.89	0.90	0.73	0.90		
	low_inert	0.98	0.96	0.83	0.90	0.64	0.90	0.73	0.90	0.60	0.90	0.26	0.51	0.43	0.90
CD8	high_fibrogenic	0.84	0.97												
	high_fibrolytic	0.53	0.97	0.53	0.97										
	high_inert	0.84	0.97	0.80	0.97	0.80	0.97								
	low_dormant	0.53	0.97	0.53	0.97	0.84	0.97	0.61	0.97						
	low_fibrogenic	0.93	0.97	0.84	0.97	0.80	0.97	0.84	0.97	0.53	0.97				
	low_fibrolytic	0.50	0.97	0.50	0.97	0.77	0.97	0.53	0.97	0.84	0.97	0.53	0.97		
	low_inert	0.53	0.97	0.53	0.97	0.93	0.97	0.80	0.97	0.82	0.97	0.77	0.97	0.77	0.97
CD68	high_fibrogenic	0.90	0.94												
	high_fibrolytic	0.66	0.94	0.53	0.94										
	high_inert	0.99	0.94	0.99	0.94	0.66	0.94								
	low_dormant	0.66	0.94	0.51	0.94	0.99	0.94	0.60	0.94						
	low_fibrogenic	0.99	0.94	0.99	0.94	0.75	0.94	0.99	0.94	0.70	0.94				
	low_fibrolytic	0.41	0.94	0.41	0.94	0.66	0.94	0.41	0.94	0.82	0.94	0.51	0.94		
	low_inert	0.51	0.94	0.41	0.94	0.82	0.94	0.53	0.94	0.99	0.94	0.53	0.94	0.90	0.94
CD206	high_fibrogenic	0.82	0.99												
	high_fibrolytic	0.11	0.11	0.07	0.14										
	high_inert	0.31	0.22	0.22	0.26	0.75	0.95								
	low_dormant	0.01	0.00	0.00	0.00	0.25	0.01	0.09	0.01						
	low_fibrogenic	0.33	0.11	0.25	0.11	0.92	0.50	0.83	0.50	0.26	0.14				
	low_fibrolytic	0.36	0.39	0.28	0.39	0.96	0.99	0.83	0.92	0.39	0.11	0.92	0.79		
	low_inert	0.78	0.50	0.52	0.50	0.75	0.92	0.92	0.99	0.25	0.06	0.86	0.67	0.87	0.92
Neutrophils	high_fibrogenic	0.90	0.75												
	high_fibrolytic	0.37	0.75	0.37	0.75										
	high_inert	0.37	0.75	0.51	0.79	0.87	0.90								
	low_dormant	0.37	0.75	0.57	0.88	0.84	0.82	0.98	0.89						
	low_fibrogenic	0.90	0.92	0.80	0.75	0.37	0.75	0.37	0.75	0.37	0.75				
	low_fibrolytic	0.37	0.75	0.57	0.92	0.90	0.75	0.94	0.79	0.90	0.88	0.37	0.75		
	low_inert	0.68	0.82	0.90	0.88	0.57	0.75	0.68	0.75	0.75	0.82	0.68	0.79	0.57	0.88

Supplementary Table S5: LIFETEST procedure between survival factors stratified according resection margin (ESPAC-Tplus cohort)

		Neg_high		Neg_low		Pos_high	
		PFS	***OS***	***PFS***	***OS***	***PFS***	***OS***
CD3	Neg_low	0.00	0.01				
	Pos_high	0.00	0.00	0.67	0.38		
	Pos_low	0.00	0.00	0.15	0.17	0.26	0.38
CD4	Neg_low	0.14	0.29				
	Pos_high	0.00	0.00	0.38	0.29		
	Pos_low	0.00	0.01	0.08	0.19	0.23	0.29
CD8	Neg_low	0.08	0.26				
	Pos_high	0.01	0.05	0.34	0.26		
	Pos_low	0.01	0.05	0.16	0.14	0.26	0.29
CD68	Neg_low	0.00	0.00				
	Pos_high	0.00	0.00	0.20	0.16		
	Pos_low	0.00	0.00	0.46	0.86	0.39	0.16
CD206	Neg_low	0.36	0.34				
	Pos_high	0.00	0.01	0.31	0.57		
	Pos_low	0.00	0.00	0.04	0.01	0.05	0.00
Neutrophils	Neg_low	0.87	0.69				
	Pos_high	0.02	0.05	0.01	0.01		
	Pos_low	0.01	0.05	0.01	0.01	0.87	0.89

Supplementary Table S6: LIFETEST procedure between survival factors stratified according resection margin for stromal composition (ESPAC-Tplus cohort)

	Neg_ dormant		Neg_ fibrogenic		Neg_ fibrolytic		Neg_ inert		Pos_ dormant		Pos_ fibrogenic		Pos_ fibrolytic	
	PFS	***OS***	***PFS***	***OS***	***PFS***	***OS***	***PFS***	***OS***	***PFS***	***OS***	***PFS***	***OS***	***PFS***	***OS***
Neg_fibrogenic	0.83	0.83												
Neg_fibrolytic	0.09	0.14	0.07	0.19										
Neg_inert	0.39	0.33	0.35	0.50	0.46	0.62								
Pos_dormant	0.02	0.05	0.01	0.07	0.52	0.38	0.09	0.14						
Pos_fibrogenic	0.09	0.07	0.07	0.14	0.93	0.62	0.44	0.33	0.49	0.62				
Pos_fibrolytic	0.01	0.07	0.01	0.14	0.44	0.59	0.09	0.31	0.85	0.63	0.49	0.89		
Pos_inert	0.01	0.05	0.01	0.07	0.46	0.31	0.07	0.14	0.71	0.83	0.19	0.38	0.71	0.59

Supplementary table S7: LIFETEST procedure between survival factors stratified according to therapeutic arm (ESPAC-Tplus cohort)

		5FU_high		5FU_low		GEM_high	
		PFS	***OS***	***PFS***	***OS***	***PFS***	***OS***
CD3	5FU_low	0.30	0.35				
	GEM_high	0.42	0.57	0.12	0.14		
	GEM_low	0.01	0.14	0.12	0.55	0.00	0.05
CD4	5FU_low	0.02	0.25				
	GEM_high	0.17	0.43	0.17	0.43		
	GEM_low	0.87	0.91	0.19	0.43	0.78	0.78
CD8	5FU_low	0.00	0.10				
	GEM_high	0.06	0.49	0.17	0.25		
	GEM_low	0.02	0.16	0.17	0.39	0.90	0.39
CD68	5FU_low	0.29	0.38				
	GEM_high	0.97	0.91	0.29	0.38		
	GEM_low	0.29	0.41	0.88	0.43	0.29	0.41
CD206	5FU_low	0.02	0.00				
	GEM_high	0.11	0.08	0.20	0.08		
	GEM_low	0.14	0.31	0.20	0.66	0.19	0.51
Neutrophils	5FU_low	0.96	0.92				
	GEM_high	0.91	0.97	0.91	0.92		
	GEM_low	0.91	0.97	0.91	0.92	0.96	0.97

Supplementary Table S8: LIFETEST procedure between survival factors stratified according to therapeutic arm for stromal composition (ESPAC-Tplus cohort)

	5FU_ dormant		5FU_ fibrogenic		5FU _fibrolytic		5FU_ inert		GEM_ dormant		GEM_ fibrogenic		GEM_ fibrolytic	
	PFS	***OS***	***PFS***	***OS***	***PFS***	***OS***	***PFS***	***OS***	***PFS***	***OS***	***PFS***	***OS***	***PFS***	***OS***
5FU_fibrogenic	0.83	0.96												
5FU_fibrolytic	0.84	0.96	0.83	0.96										
5FU_inert	0.98	0.96	0.83	0.96	0.95	0.96								
GEM_dormant	0.83	0.96	0.95	0.96	0.83	0.96	0.84	0.96						
GEM_fibrogenic	0.83	0.96	0.95	0.96	0.83	0.96	0.83	0.96	0.95	0.96				
GEM_fibrolytic	0.83	0.96	0.83	0.96	0.83	0.96	0.83	0.96	0.83	0.96	0.83	0.96		
GEM_inert	0.95	0.96	0.83	0.96	0.95	0.96	0.95	0.96	0.83	0.96	0.83	0.96	0.83	0.96

Supplementary Table S9: Multivariate analysis of immune stromal markers with independent prognostic variables (ESPAC-Tplus cohort).

Covariate		PFS				OS			
		HR	***(95% CI)***	***z-stat***	***P***	***HR***	***(95% CI)***	***z-stat***	***P***
Stroma									
	Fibrolytic		1.00 (Referent)				1.00 (Referent)		
	Inert	0.89	0.64-1.25	-0.63	0.52	1.01	0.71-1.44	0.09	0.92
	Dormant	0.75	0.53-1.06	-1.90	0.10	0.88	0.62-1.27	-0.64	0.52
	Fibrogenic	0.72	0.51-1.00	-1.92	**0.05**	0.86	0.61-1.21	-0.81	0.41
CD3 expression									
	Low		1.00 (Referent)				1.00 (Referent)		
	High	0.71	0.55-0.92	-2.51	**0.01**	0.74	0.56-0.96	-2.21	**0.02**
CD4 expression									
	Low		1.00 (Referent)				1.00 (Referent)		
	High	0.75	0.52-1.06	-1.59	0.11	0.84	0.58-1.22	-0.87	0.38
CD8 expression									
	Low		1.00 (Referent)				1.00 (Referent)		
	High	0.77	0.58-1.01	-1.84	**0.05**	0.74	0.56-0.99	-2.00	**0.04**
CD68 expression									
	Low		1.00 (Referent)				1.00 (Referent)		
	High	0.87	0.66-1.13	-1.00	0.31	0.89	0.68-1.18	-0.76	0.44
CD206 expression									
	Low		1.00 (Referent)				1.00 (Referent)		
	High	0.66	0.48-0.90	-2.61	**0.008**	0.58	0.42-0.79	-3.45	**<0.001**
Lymph Node Invasion									
	Negative		1.00 (Referent)				1.00 (Referent)		
	Positive	2.18	1.38-3.46	3.35	**<0.001**	1.91	1.20-3.05	2.73	**0.006**
Resection Margin									
	Negative		1.00 (Referent)				1.00 (Referent)		
	Positive	1.55	1.21-1.99	3.51	**<0.001**	1.54	1.20-1.98	3.38	**<0.001**
Stage									
	I		1.00 (Referent)				1.00 (Referent)		
	II	0.95	0.50-1.80	-0.13	0.89	1.17	0.59-2.34	0.46	0.64
	III	0.80	0.38-1.66	-0.59	0.55	1.14	0.53-2.43	0.33	0.73
	IV	0.55	0.21-1.47	-1.17	0.29	0.87	0.31-2.42	-0.26	0.79
Concordance			***0.64 ± 0.01***				***0.63 ± 0.01***		
AIC			***2851.15***				***2704.17***		
AIC of stroma-TILs biomarkers model			***2792.91***				***2772.91***		

Supplementary Table S10: Demographics, surgery and pathology features of the patients scored in validation cohort.

Demographics Characteristics		Total N= 93
Age Median (IQR) years		67(40-83)
Sex	**Female**	42 (45.1%)
	Male	51 (54.8%)
ECOG		**N=66**
	0	39 (65.0%)
	1	18 (30.0%)
	2	3 (5.0%)
Diabetic status		**N=91**
	No	53 (80.3%)
	IDDM (Type 1)	5 (7.5%)
	NIDDM (Type 2)	6 (9.0%)
	Type 3 DM	2 (3.0%)
Post-Op. CA 19-9 Median (IQR) U/l		**N=60** 96 (0-7950)
Tumor grade		**N=87**
	Well	1 (1.0%)
	Moderate	26 (28.5%)
	Poor	64 (70.5%)
Lymph Node invasion		**N=91**
	Negative	30 (21.9%)
	Positive	61 (68.1%)
Resection margin		**N=91**
	Negative	70 (76.9%)
	Positive	21 (23.1%)
Local invasion		**N=87**
	No	52 (59.7%)
	Yes	35 (40.3%)
Tumor stage		**N=89**
	I	2 (2.1%)
	II	8 (8.6%)
	III	79 (85.8%)
	IV	3 (3.2%)
Perineural invasion		**N=87**
	No	24 (27.5%)
	Yes	63 (72.5%)
CD3 count		**N=92**
	Low	48 (52.1%)
	High	44 (47.9%)
CD4 count		**N=92**
	Low	26 (28.2%)
	High	66 (71.7%)
CD8 count		**N=92**
	Low	53 (57.6%)
	High	39 (42.3%)
CD68 count		**N=92**
	Low	37 (40.2%)
	High	55 (59.8%)
CD206 count		**N=92**
	Low	37 (40.2%)
	High	55 (54.7%)
MPO count		**N=92**
	Low	47 (51.0%)
	High	45 (49.8%)
$CD45^+$ cells	**Low**	45 (48.3%)
	High	48 (51.7%)
$CD45^+CD3^+$ cells	**Low**	40 (53.7%)
	High	43 (46.2%)
$CD45^+CD3^+CD4^+$ cells	**Low**	48 (51.6%)
	High	45 (48.3%)
$CD45^+CD3^+CD8^+$ cells	**Low**	39 (41.9%)
	High	54 (58.1%)
$CD45^+CD68^+$ cells	**Low**	56 (60.2%)
	High	37 (39.8%)
$CD45^+CD206^+$ cells	**Low**	55 (40.8%)
	High	38 (59.2%)
$CD45^+MPO^+$ cells	**Low**	46 (49.4%)
	High	47 (50.6%)
Stroma		**N=92**
	Inert	20 (21.7%)
	Dormant	26 (28.2%)
	Fibrogenic	20 (21.7%)
	Fibrolytic	26 (28.2%)

Supplementary Table S11: Univariate analysis of progression free survival and overall survival factors in validation cohort.

Univariate analysis: Validation cohort (Immunohistochemistry)			
Characteristics		**PFS**	**OS**
Sex	Female	1(Referent)	1(Referent)
	Male	0.93 (0.57 to 1.5) χ^2=0.08 (P=0.77)	1.09 (0.62 to 1.90) χ^2=0.09 (P=0.76)
Lymph node invasion	Negative	1(Referent)	1(Referent)
	Positive	1.46 (0.87 to 2.45) χ^2=2.06 (P=0.15)	1.07 (0.60 to 1.88) χ^2=0.05 (P=0.82)
Resection margin	Negative	1(Referent)	1(Referent)
	Positive	1.21 (0.67 to 2.20) χ^2=0.42 (P=0.51)	1.25 (0.60 to 2.60) χ^2=0.36 (P=0.55)
Tumor grade	Poor	1(Referent)	1(Referent)
	Moderate	5.13 (0.29 to 0.90) χ^2=2.0 **(P=0.02)**	7.38 (0.41-1.32) χ^2=2.0 **(P=0.30)**
	Well	2.8 (NA) χ^2=5.30 (P=0.99)	3.00 (NA) χ^2=1.03 (P=0.99)
Local invasion	No	1(Referent)	1(Referent)
	Yes	1.21 (0.73 to 2.01) χ^2=0.55 (P=0.45)	1.46 (0.83 to 2.56) χ^2=1.74 (P=0.18)
Tumor stage	I	1(Referent)	1(Referent)
	II	0.09 (0.01 to 0.75) χ^2=13.21 **(P=0.02)**	0.02 (0.00 to 0.40) χ^2=8.99 **(P=0.01)**
	III	0.04 (0.00 to 0.26) χ^2=3.00 **(P<0.01)**	0.01 (0.00 to 0.25) χ^2=3.00 **(P<0.01)**
	IV	0.02 (0.00 to 0.59) χ^2=0.01 **(P<0.01)**	0.01 (0.00 to 0.29) χ^2=0.02 **(P<0.01)**
Perineural invasion	Negative	1 (Referent)	1 (Referent)
	Positive	2.06 (1.10 to 3.84) χ^2=5.24 **(P=0.02)**	2.14 (1.07 to 4.28) χ^2=4.71 **(P=0.03)**
Post-operative CA19.9		1.00 (1.00 to 1.00) χ^2=12.09 **(P=0.005)**	1.01 (NA) χ^2= 0.14 **(P=0.70)**
CD3 count	Low	1(Referent)	1(Referent)
	High	0.5 (0.35 to 0.95) χ^2=4.62 **(P=0.03)**	0.54 (0.31 to 0.94) χ^2=4.65 **(P=0.03)**
CD4 count	Low	1(Referent)	1(Referent)
	High	0.82 (0.49 to 1.39) χ^2=0.5 **(P=0.48)**	0.72 (0.41 to 1.27) χ^2=1.25 **(P=0.26)**
CD8 count	Low	1(Referent)	1(Referent)
	High	0.58 (0.35 to 0.96) χ^2=4.43 **(P=0.03)**	0.81 (0.46 to 1.41) χ^2=0.52 **(P=0.47)**
CD68 count	Low	1(Referent)	1(Referent)
	High	0.80 (0.49 to 1.30) χ^2=0.79 **(P=0.37)**	1.26 (0.71 to 2.24) χ^2=0.66 **(P=0.41)**
CD206 count	Low	1(Referent)	1(Referent)
	High	1.86 (1.11 to 3.12) χ^2=5.62 **(P=0.01)**	1.68 (0.95 to 2.99) χ^2=3.24 **(P=0.07)**
MPO count	Low	1(Referent)	1(Referent)
	High	1.38 (0.84 to 2.26) χ^2= 1.66 **(P=0.19)**	1.46 (0.83 to 2.57) χ^2=1.73 **(P=0.18)**
Stroma	Fibrolytic	1(Referent)	1(Referent)
	Inert	0.69 (0.34 to 1.40) χ^2=13.84 **(P=0.31)**	0.55 (0.24 to 1.27) χ^2=4.74 **(P=0.16)**
	Dormant	1.04 (0.55 to 1.95) χ^2=3.00 **(P<0.88)**	1.02 (0.48 to 2.18) χ^2=3.00 **(P=0.94)**
	Fibrogenic	0.28 (0.13 to 0.59) χ^2=0.003 **(P<0.005)**	0.50 (0.25 to 1.06) χ^2=0.19 **(P=0.07)**

Supplementary Table S12: Multivariate analysis of individual immunohistochemistry markers in validation cohort

Covariate		PFS				OS			
		HR	***(95% CI)***	***z-stat***	***P***	***HR***	***(95% CI)***	***z-stat***	***P***
CD3 count	Low	1.00 (Referent)				1.00 (Referent)			
	High	0.22	0.10-0.46	-4.01	**<0.001**	0.26	0.11-0.58	-3.29	**<0.001**
CD4 count	Low	1.00 (Referent)				1.00 (Referent)			
	High	0.44	0.23-0.83	-2.51	**0.01**	0.62	0.33-1.16	-1.48	0.13
CD8 count	Low	1.00 (Referent)				1.00 (Referent)			
	High	1.04	0.55-1.95	0.12	0.89	1.15	0.70-3.22	1.06	0.28
CD68 count	Low	1.00 (Referent)				1.00 (Referent)			
	High	0.75	0.45-1.27	-1.03	0.29	1.10	0.60-2.03	0.33	0.74
CD206 count	Low	1.00 (Referent)				1.00 (Referent)			
	High	4.08	2.08-8.00	4.09	**<0.001**	2.39	1.25-4.57	2.63	**0.008**
Stroma	Fibrolytic	1.00 (Referent)				1.00 (Referent)			
	Inert	0.74	0.37-1.50	-0.06	0.94	0.67	0.28-1.06	-0.87	0.37
	Dormant	0.97	0.50-1.90	-0.82	0.40	1.13	0.50-2.57	0.31	0.75
	Fibrogenic	0.11	0.05-0.27	-4.87	**<0.001**	0.33	0.15-0.74	-2.67	**0.007**
Concordance		***0.76 ± 0.04***				***0.69 ± 0.04***			

Legends to supplementary figures:

Supplementary figure S1: Schematic representation of image analysis using Image J algorithm. (A) Schematic representation for the algorithm used for intensity calculation. **(B)** Schematic diagram for the algorithm used for immunostained cell count.

Supplementary figure S2: Inter-rater concordance in ESPAC cohort. (A) Plot depicting inter-rater reliability for H-Score for Picrosirius red/fast green staining with Inter-concordance coefficient (ICC), which is measure of concordance for continuous variables, as 0.84 (95%CI: 0.82-0.85). **(B)** Plot showing inter-rater reliability for H-Score for a-SMA staining with ICC, as 0.84 (95%CI: 0.82-0.85). ICC in the range of 0.75-1.00 is associated with excellent inter-rater concordance. **(C-D)** Plot depicting inter-rater reliability for Low/high stratification of for Picrosirius red/fast green staining with Cohen's Kappa, which is a measure for inter-rater concordance for categorical variables, as 0.75 (95%CI: 0.72-0-77) and for a-SMA as 0.79 (95%CI: 0.77-0.81). Cohen's kappa in the range of 0.61-0.80 depict good concordance.

Supplementary figure S3: Representative images of immunostaining illustrating low and high expression of α-SMA, picrosirius red/fast red staining for Collagen, CD3, CD4, CD8, CD68, CD206 and chloracetate estarase staining for neutrophils. Values in inserts depict respective H-score/counts per mm^3.

Supplementary figure 4 Correlation matrix depicting correlations of intratumoral cells FACS analysis with immunohistochemistry staining and stratification. Correlation matrix involved inter-methodological comparisons for immune markers stained for CD3, CD4, CD8, CD68 and CD206. The methods involved were classical immunohistochemistry on histological blocks, immunocytochemistry on tissue-blocks prepared from isolated intratumoral cells, immunostaining on cytospins slides prepared from isolated intratumoral cells and FACS analysis of isolated intratumoral cells. FACS analysis for same immune markers of peripheral blood derived monocytes (PBMCs) served as reference. Solid square (black) in correlogram depict correlation between immunohistochemistry staining on tissueblocks with intratumoral cells FACS. Scatter plots in insert represent the correlation

between individual immune markers. Each of the individual immune markers were stratified as low/high count. Dotted square (black) in correlogram depict correlation between immunohistochemistry staining on tissue-blocks with PBMCs FACS analysis. Number of stars in in correlograms are proportional to strength of agreement. P<0.05 considered statistical significant.

Supplementary figure S5: Influence of αSMA and collagen expression on progression free survival. (A) The Kaplan-Meier survival analysis shows that patients with low αSMA expression did not show deviation in progression free survival time in comparison to high αSMA expression. **(B)** The Kaplan-Meier survival analysis shows that patients with low collagen expression did not show deviation in progression free survival time in comparison to high collagen expression. **(C)** Tabular representation of LIFETEST procedure depicting combinations of stromal subtypes with respect to progression free survival.

Supplementary figure S6: Contribution of multifaceted stromal composition in defining overall survival. (A) Kaplan-Meier survival analysis of patients with resected PDAC in respect to stroma subtype. **(B)** The Kaplan-Meier survival analysis shows that patients with low αSMA expression did not show deviation in overall survival time in comparison to high αSMA expression. **(C)** The Kaplan-Meier survival analysis shows that patients with low collagen expression did not show deviation in overall survival time in comparison to high collagen expression. **(D)** Tabular representation of LIFETEST procedure depicting combinations of stromal subtypes with respect to overall survival.

Supplementary figure S7: Inferred leukocyte subtype frequencies associated with prognostic association in determining overall survival corresponding to stromal composition. (A) Random forest iterations illustrate variable of importance and minimal depth of the prognostic variables in determining progression free survival. Longer VIMP bars with shorter minimal depth bars indicate more important variables. Area shaded in grey depicts prognostic window for the prognostic variables. **(B)** Multivariate recursive partitioning for discrete-time survival tree for overall survival depicting prognostic signatures amalgating

two or more markers with median overall survival varying between 12.70 months to 29.20 months. The variable selection in multivariate recursive partitioning for discrete-time survival tree for the overall survival model is based on random forest iterations and is an unbiased selection. Also, the multivariate recursive partitioning for discrete-time survival tree model is based on prognostic strength of individual biomarkers taken into consideration. As the prognostic strength is different for PFS and OS, prognostic signature of OS differ significantly than PFS. **(C)** Waterfall representation of each prognostic signature as delineated from the terminal nodes illustrating the relative prognostic index of each signature calculated using Cox multivariate proportional hazards. **(D)** Box plot depicts the distribution of prognostic indices with respect to individual prognostic signatures. P<0.05 considered significant.

Supplementary figure S8: Prognostic associations of tumor stage, postOpCA19.9 and lymph node invasion and comparison of its composite signature with the histological signature. (A) By Random forest iterations we determined “variables of importance (VIMP)” and minimal depth of the prognostic variables in to predict progression free survival. Longer VIMP bars with shorter minimal depth bars indicate a higher effect/impact of the variable. Area shaded in grey depicts the prognostic window for the prognostic variables. **(B)** Multivariate recursive partitioning for discrete-time survival tree for progression free survival depicts the reference signature amalgating two or more markers with median progression free survival varying between 9.88 months to 19.71 months with a relative error of prediction given with 0.07 (X-error 0.01). **(C)** Survival ROC curve depicting comparison of histological signature with the reference signature.

Supplementary figure S9: CONSORT diagram of independent validation cohort.

Supplementary figure S10: Comparison of multiplex immunostaining with single immunohistochemistry staining in validation cohort. (A) Representative images of multiplex immunostaining with consecutive staining in order of haematoxylin (Nuclei), CD3, CD4, CD8,CD45, CD68,CD206, MPO, a-SMA and Collagen (Picrosirius red/ Fast green). Representative merged images of multiplex immunostaining for a PDAC TMA core. Images

in the insert depict enlarged images from white box. Tonsil multiplex immunostaining served as a control. **(B)** Scatter plots depicting correlation between classical immunohistochemistry and multiplex immunostaining followed by image cytometric analysis for markers, namely, CD3, CD4, CD8, CD68, CD206, MPO and a-SMA. **(C)** Tabular representation of the Kaplan-Meier survival analysis depicting influence of high and low expression of immune infiltrate markers from immunohistochemistry staining, CD3, CD4, CD8, CD68, CD206 and neutrophils in predicting PFS and OS in validation cohort. **(D)** Kaplan-Meier curve representative actual response and predicted response predicted from prognostic histological signature derived from ESPAC-Tplus cohort. Dotted lines depict the curves for predicted response whereas solid lines represent curves for actual response. The accuracy of prediction in validation cohort using prognostic histological signature is 0.75 (95%CI: 0.64-0.83, accuracy P>0.001). P<0.05 is considered as significant.

Supplementary figure S11: Work flow-chart for multiplexing immunostaining and quantification image cytometric analysis. Work flow highlighted in grey area depict multiple antibodies staining cycle (multiplexing).

Suppl Figure S1: Schematic representation of image analysis

(A)

Input

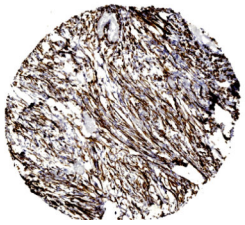

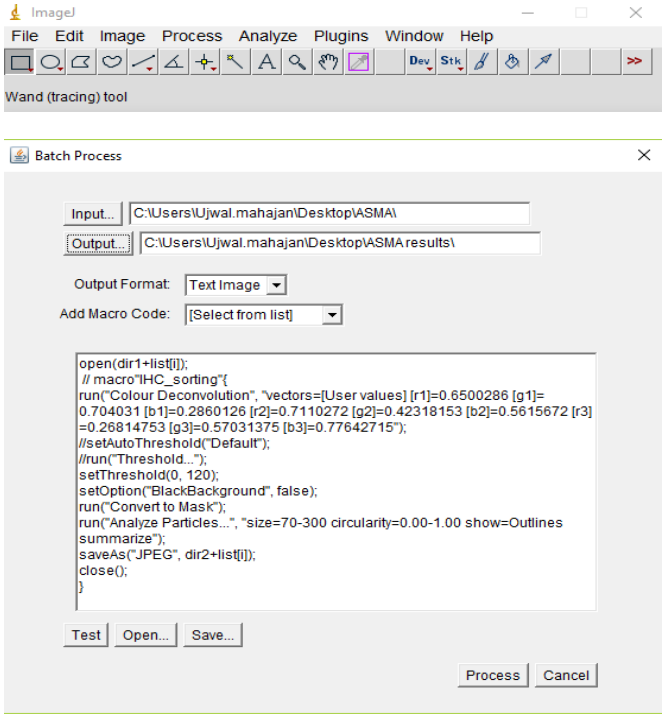

Output

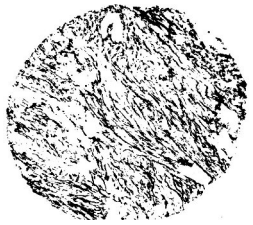

	Label	Area	Mean	StdDev	Min	Max	IntDen	%Area	RawIntDen
1	10B.jpg (Colour[3])	699300	0.92	15.3	0	255	644385	0.36	644385
2	10C.jpg (Colour[3])	699300	0.26	8.13	0	255	181560	0.1	181560
3	10D.jpg (Colour[3])	699300	0.45	10.74	0	255	316710	0.18	316710
4	10E.jpg (Colour[3])	699300	0.22	7.44	0	255	151725	0.09	151725
5	10I.jpg (Colour[3])	699300	4.64	34.09	0	255	3246405	1.82	3246405
6	10J.jpg (Colour[3])	699300	2.81	26.64	0	255	1967325	1.1	1967325
7	10K.jpg (Colour[3])	699300	1.27	17.96	0	255	888930	0.5	888930
8	10L.jpg (Colour[3])	699300	0.68	13.16	0	255	476085	0.27	476085
9	10M.jpg (Colour[3])	699300	3.15	28.15	0	255	2199630	1.23	2199630
10	10N.jpg (Colour[3])	699300	1.2	17.44	0	255	837675	0.47	837675
11	10O.jpg (Colour[3])	699300	1.93	22.12	0	255	1352010	0.76	1352010
12	11C.jpg (Colour[3])	699300	1.35	18.48	0	255	941460	0.53	941460
13	11D.jpg (Colour[3])	699300	0.49	11.14	0	255	340935	0.19	340935
14	11E.jpg (Colour[3])	699300	6.45	40.05	0	255	4512480	2.53	4512480
15	11F.jpg (Colour[3])	699300	4.11	32.13	0	255	2876910	1.61	2876910
16	11J.jpg (Colour[3])	699300	1.68	20.63	0	255	1174530	0.66	1174530
17	11M.jpg (Colour[3])	699300	1.29	18.09	0	255	902445	0.51	902445
18	11N.jpg (Colour[3])	699300	1.72	20.9	0	255	1205640	0.68	1205640
19	11P.jpg (Colour[3])	699300	0.15	6.26	0	255	107610	0.06	107610
20	12C.jpg (Colour[3])	699300	3.08	27.88	0	255	2157045	1.21	2157045
21	12D.jpg (Colour[3])	699300	1.29	18.08	0	255	901425	0.51	901425
22	12E.jpg (Colour[3])	699300	4.28	32.77	0	255	2994720	1.68	2994720
23	12F.jpg (Colour[3])	699300	2.07	22.89	0	255	1448910	0.81	1448910
24	12H.jpg (Colour[3])	699300	4.41	33.25	0	255	3085500	1.73	3085500

(B)

Input

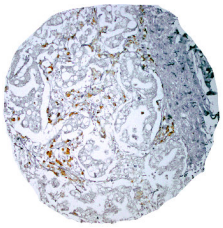

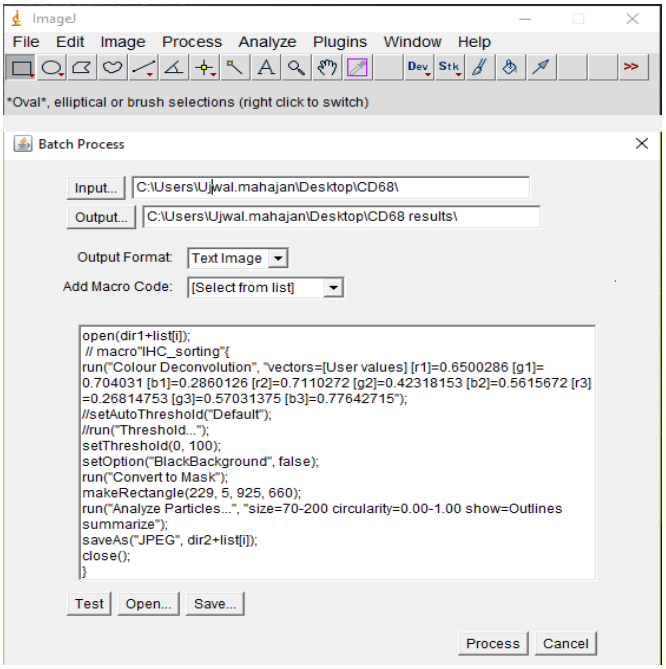

Output

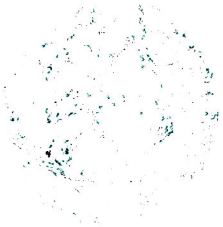

Slice	Count	Total Area	Average Size	%Area
10b.jpg (Colour[3])	11	760	69.09	0.12
10c.jpg (Colour[3])	4	326	81.5	0.05
10d.jpg (Colour[3])	3	193	64.33	0.03
10e.jpg (Colour[3])	33	3417	103.55	0.56
10f.jpg (Colour[3])	9	784	87.11	0.13
10i.jpg (Colour[3])	30	2828	94.27	0.46
10j.jpg (Colour[3])	32	3022	94.44	0.5
10k.jpg (Colour[3])	16	1247	77.94	0.2
10l.jpg (Colour[3])	32	2701	84.41	0.44
10m.jpg (Colour[3])	30	2904	96.8	0.48
10n.jpg (Colour[3])	29	2444	84.28	0.4
10o.jpg (Colour[3])	64	6028	94.19	0.99
11b.jpg (Colour[3])	26	2378	91.46	0.39
11c.jpg (Colour[3])	10	934	93.4	0.15
11d.jpg (Colour[3])	49	4179	85.29	0.68
11e.jpg (Colour[3])	3	269	89.67	0.04

Suppl Figure S2: Inter-rater concordance in ESPAC-Tplus cohort

(A)

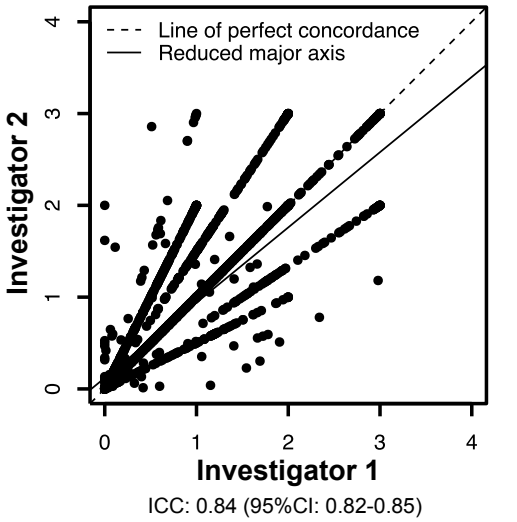

ICC: 0.84 (95%CI: 0.82-0.85)

(B)

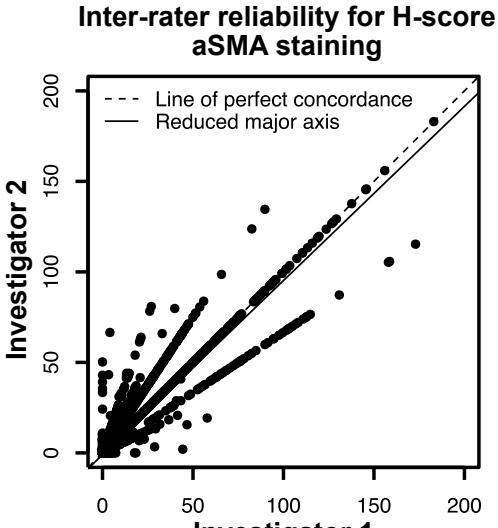

ICC: 0.92 (95%CI: 0.92-0.93-0.85)

(C)

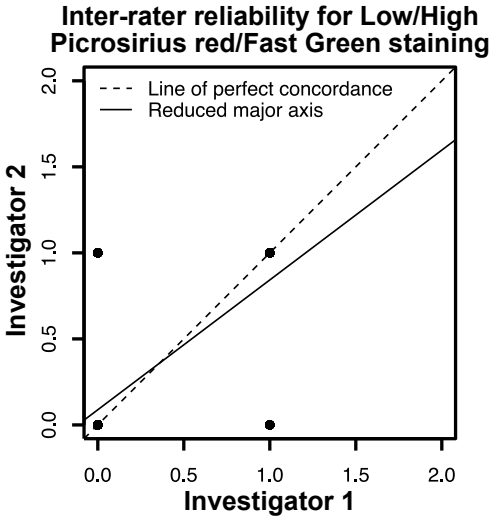

Cohen's Kappa: 0.75 (95%CI 0.72-0.77)

(D)

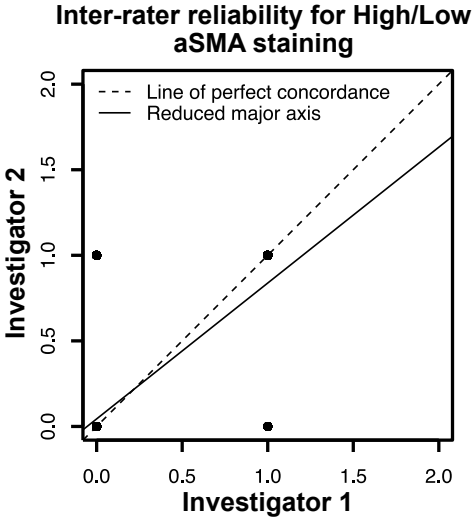

Cohen's Kappa: 0.79 (95%CI 0.77-0.81)

Suppl Figure S3: Representative IHC images with low/high categorization

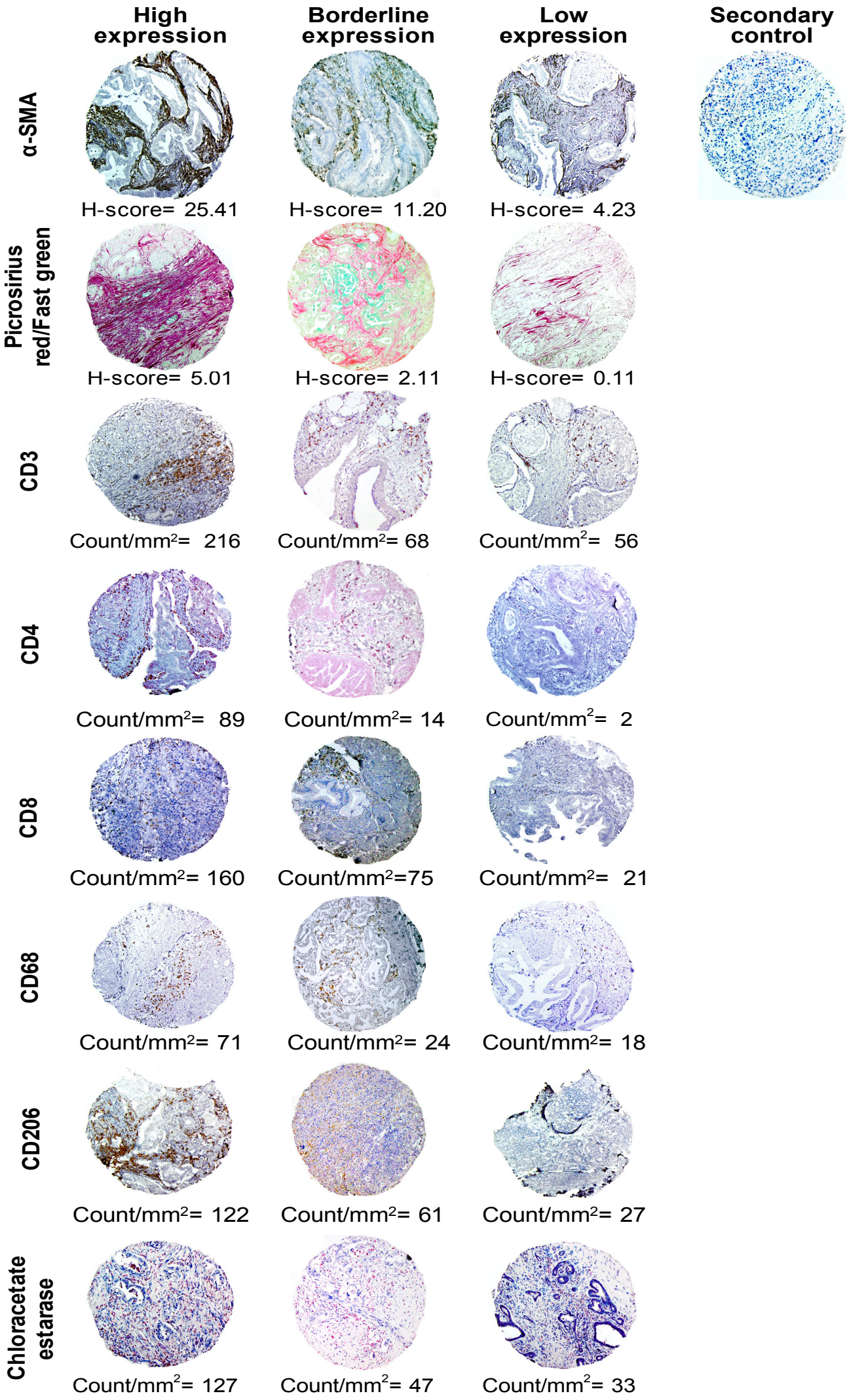

Suppl Figure S4: Correlation matrix depicting correlations of intra-tumoral cells comparing FACS with IHC staining

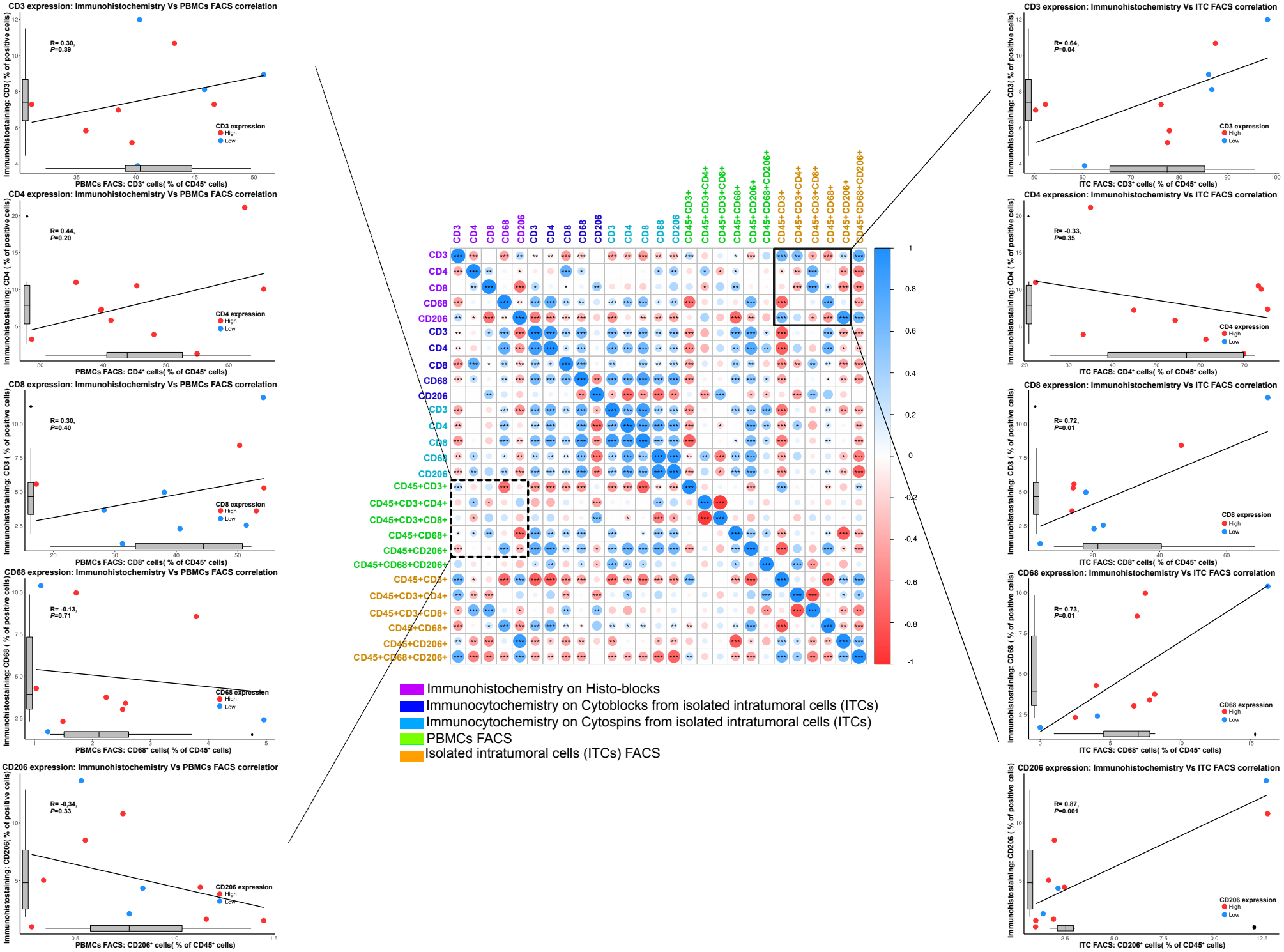

Suppl Figure S5: Influence of a-SMA and collagen expression on progression free survival.

(A)

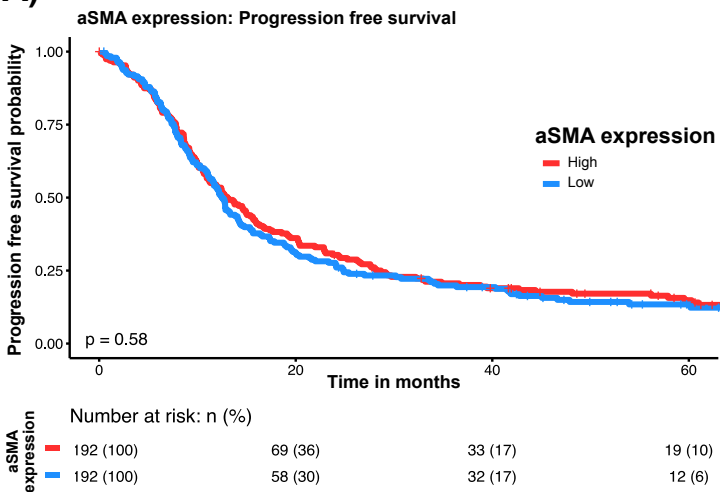

(B)

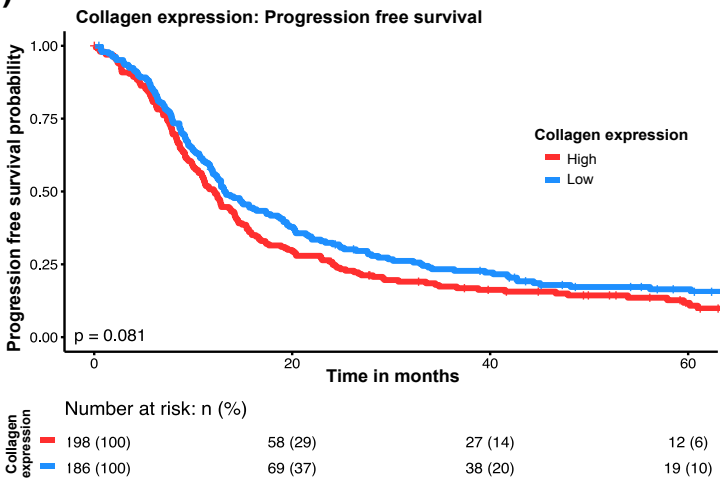

(C)

	Fibrolytic	Inert	Dormant
Inert	χ^2=2.25 (0.08)		
Dormant	χ^2=2.17 (0.08)	χ^2=0.003 (0.93)	
Fibrogenic	χ^2=5.45 (0.01)	χ^2=0.85 (0.38)	χ^2=0.94 (0.33)

Suppl Figure S6: Contribution of stromal subcompartments to overall survival

(A)

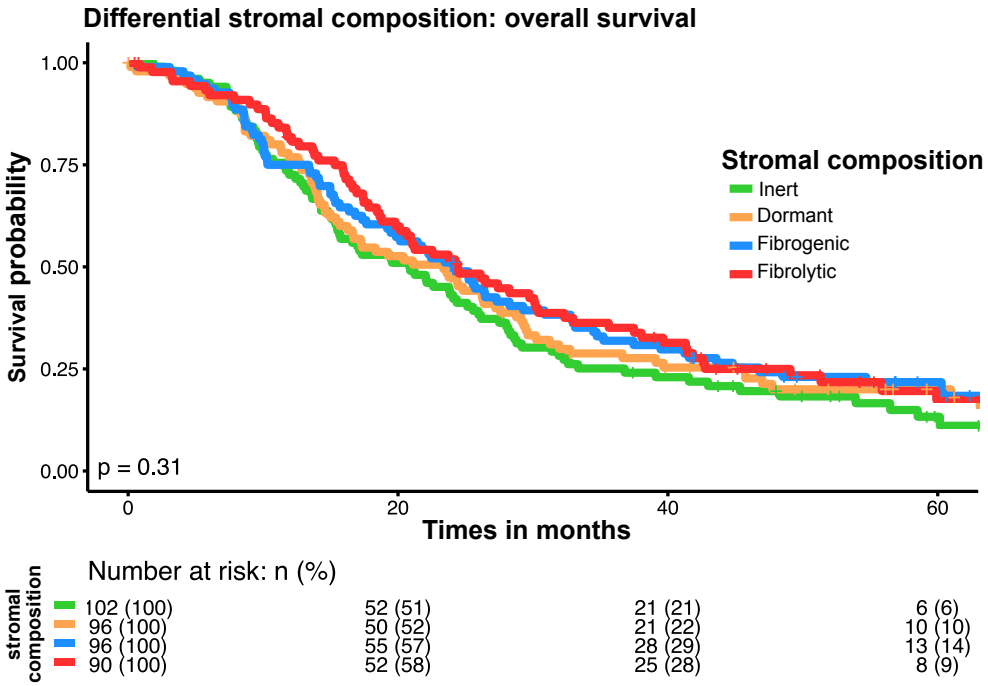

(B)

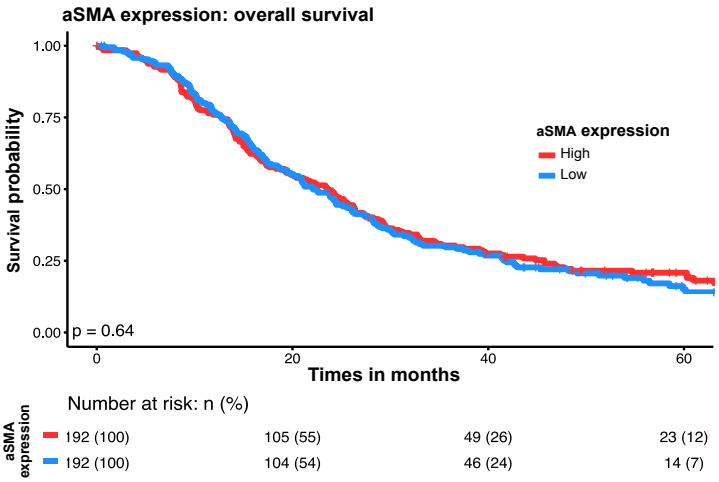

(C)

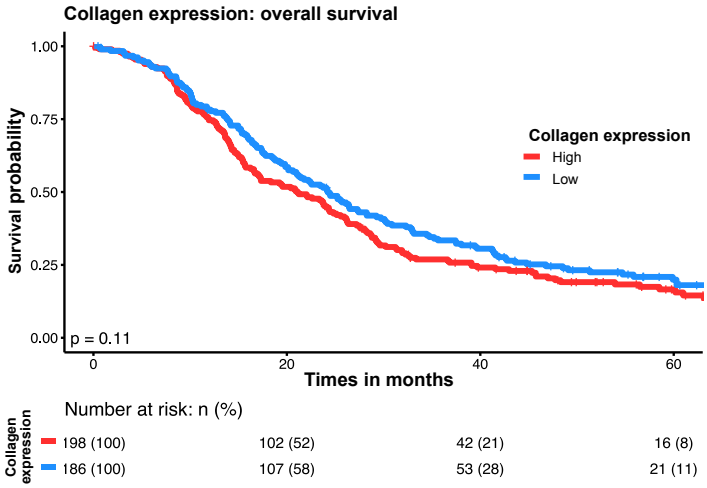

(D)

	Fibrolytic	Inert	Dormant
Inert	χ^2=0.32 (0.35)		
Dormant	χ^2=1.31 (0.13)	χ^2=0.29 (0.62)	
Fibrogenic	χ^2=3.08 (0.08)	χ^2=1.34 (0.41)	χ^2=0.34 (0.76)

Suppl Figure S7: Prognostic histological signature for overall survival

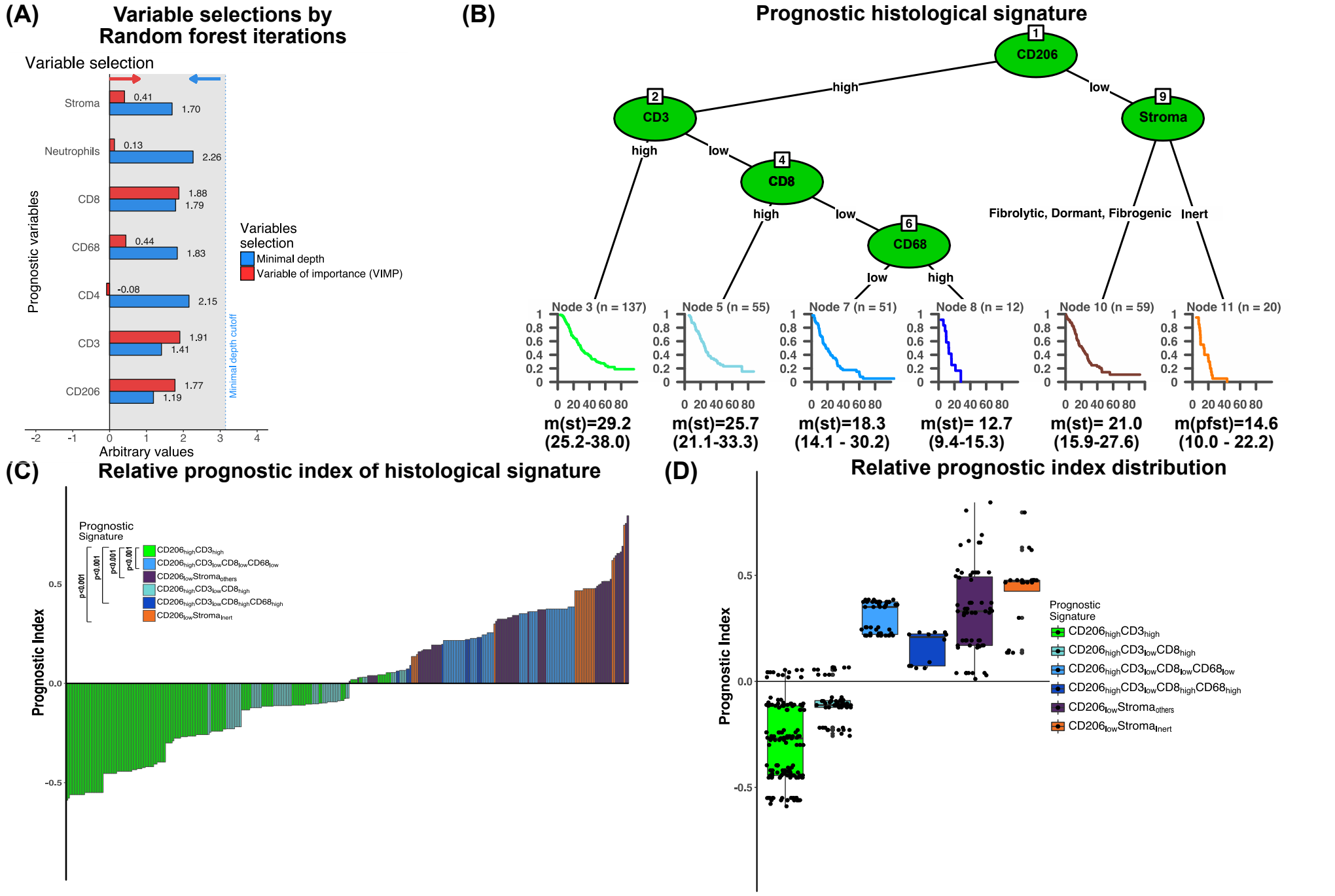

Suppl Figure S8

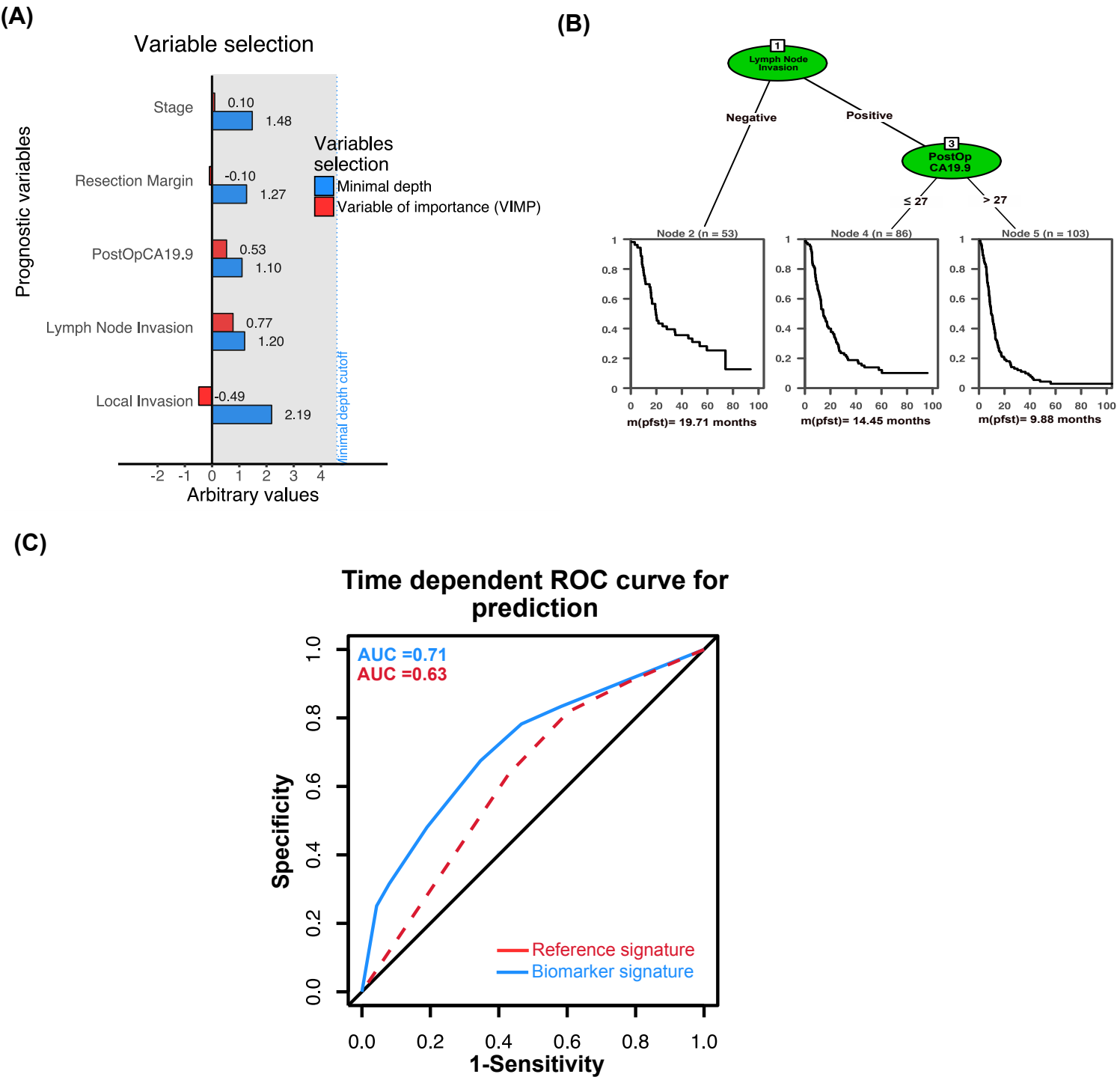

Suppl Figure S9: **CONSORT diagram of validation cohort**

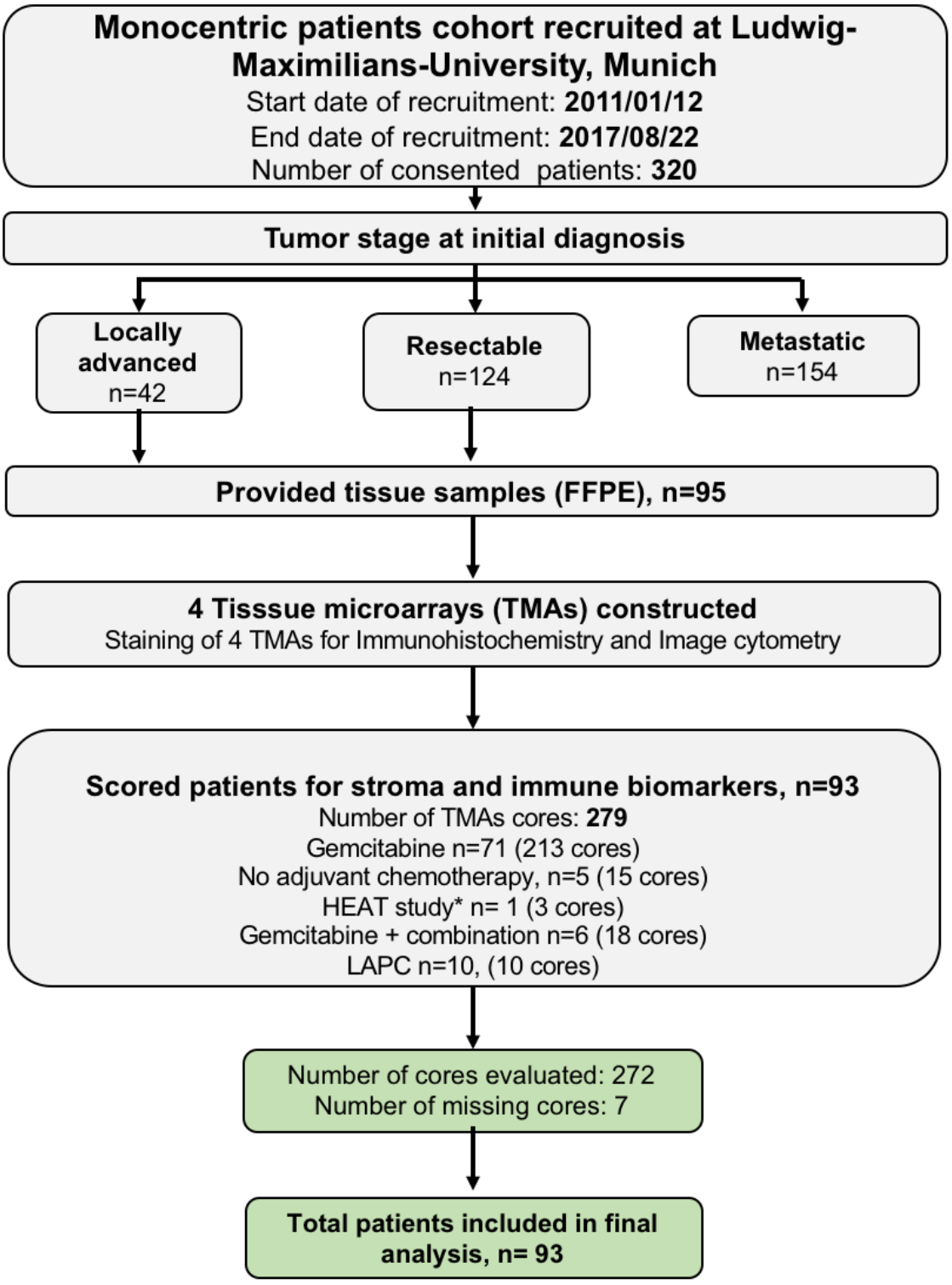

*HEAT Study = Gemcitabine (+/-) Capecitabine vs. Gemcitabine + Cisplatin in Combination with regional Hyperthermia

Suppl Figure S10: Comparison of multiplex immunostaining with single immunohistochemistry staining in validation cohort

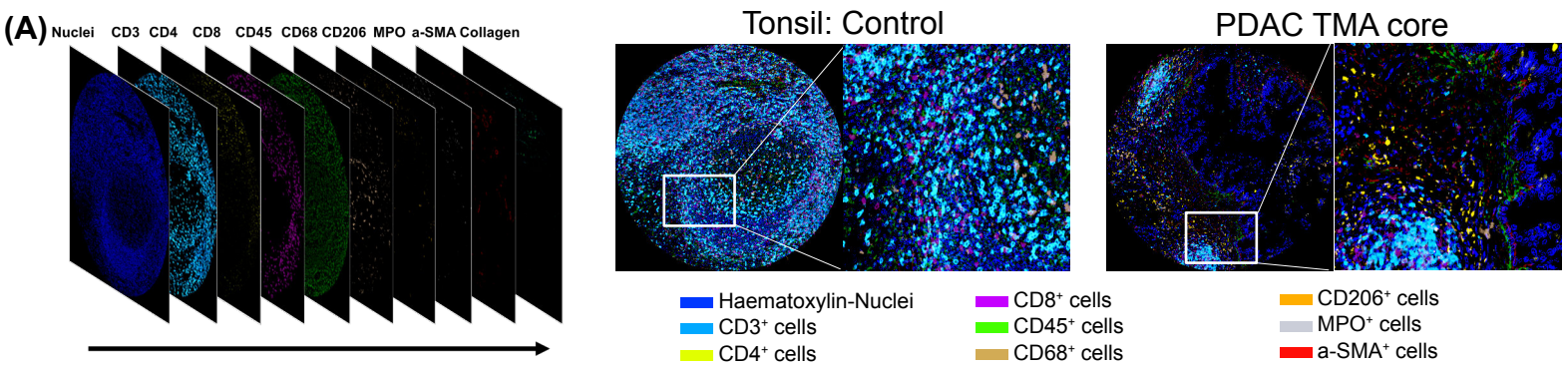

(B) Correlation between immunohistochemistry and multiplex immunostaining

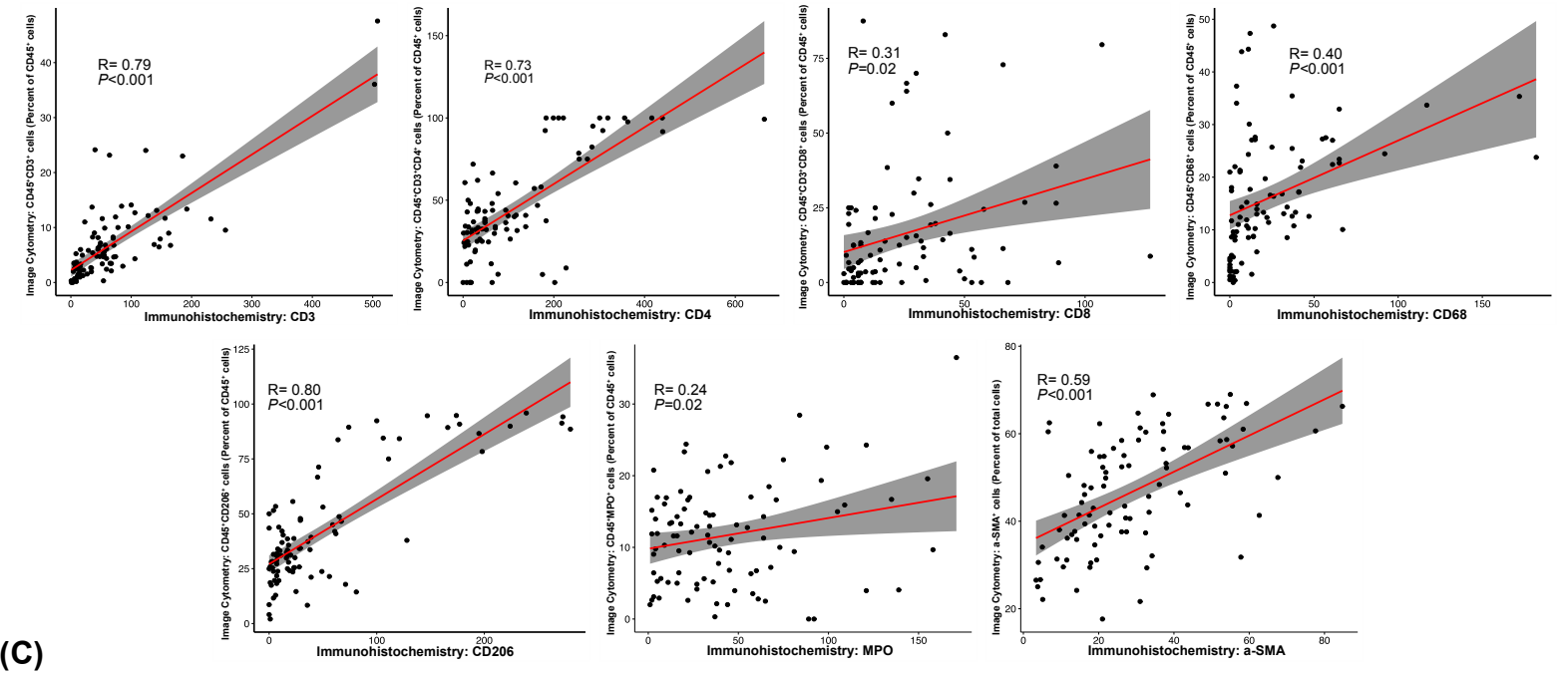

(C)

Immune marker	stratification	Progression free survival			Overall survival		
		m(pfst)	χ^2	*p*	m(st)	χ^2	*p*
CD3	Low	11.37 (95%CI: 8.87-15.84)	4.70	**0.03**	29.06 (95%CI: 19.33-32.87)	4.80	**0.03**
	High	20.71 (95%CI: 16.27-30.18)			37.41 (95%CI: 33.53-47.76)		
CD4	Low	13.38 (95%CI: 8.44-18.77)	0.50	0.48	24.59 (95%CI: 19.06-18.77)	1.30	0.26
	High	17.19 (95%CI: 11.99-21.17)			36.42 (95%CI:30.57-41.19)		
CD8	Low	12.55 (95%CI: 9.17-17.09)	4.50	**0.03**	31.95 (95%CI: 23.47-39.81)	0.50	0.50
	High	21.17 (95%CI: 14.03-34.78)			37.31 (95%CI: 27.38-41.19)		
CD68	Low	13.11 (95%CI: 8.87-20.35)	0.80	0.40	39.81 (95%CI: 23.96-48.92)	0.70	0.40
	High	17.19 (95%CI: 12.55-24.92)			30.57 (95%CI: 24.59-37.31)		
CD206	Low	21.74 (95%CI: 11.73-30.18)	5.80	**0.02**	39.81 (95%CI: 29.06-48.92)	3.30	0.07
	High	13.38 (95%CI: 10.02-17.09)			30.57 (95%CI: 23.37-36.42)		
Neutrophils	Low	17.22 (95%CI: 13.38-22.09)	1.70	0.20	33.89 (95%CI: 25.08-37.41)	1.70	0.20
	High	12.55 (95%CI: 9.20-20.35)			33.53 (95%CI: 24.59-47.76)		
Stroma	Fibrogenic	29.85 (95%CI: 17.19-45.48)	15.30	**0.002**	41.19 (95%CI: 23.47-55.65)	4.90	0.20
	Inert	16.27 (95%CI: 7.55-29.39)			39.81 (95%CI: 23.96-47.61)		
	Dormant	13.11 (95%CI: 8.44-17.22)			26.10 (95%CI: 20.97-46.65)		
	Fibrolytic	11.55 (95%CI: 6.47-20.35)			30.57 (95%CI: 14.43-37.41)		

(D) Accuracy of prediction of prognostic histological signature in the validation cohort

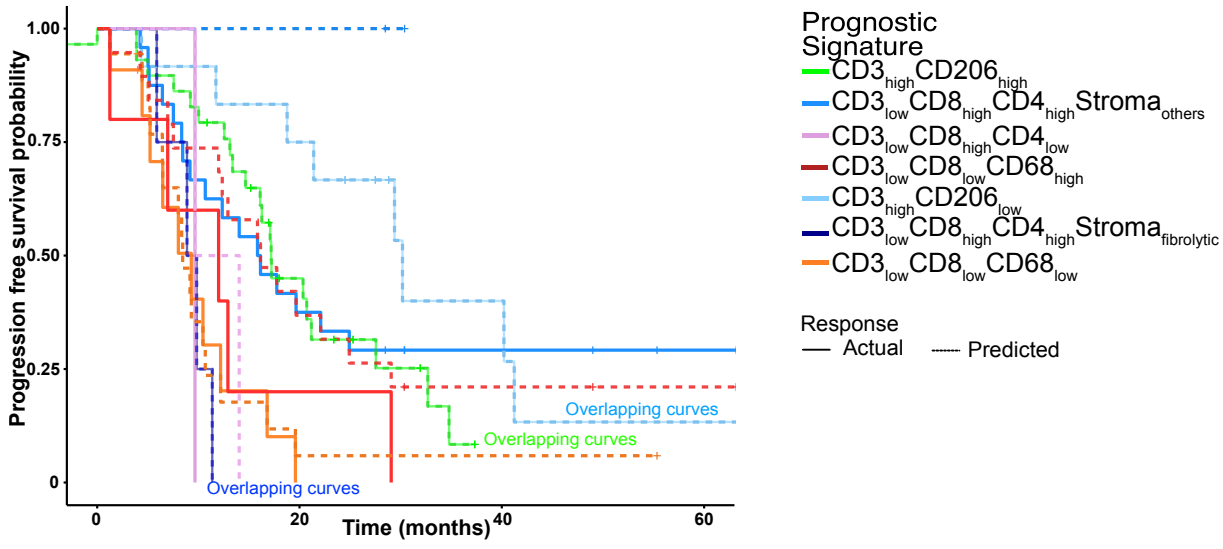

Suppl Figure S11: work-flow for the multiplex immunostaining and quantification